Exploring an alternative approach for deriving NDVI-based forage scarcity in the framework of index-based livestock insurance in East Africa

LUCAS HERNÁN DE OTO
February, 2017

SUPERVISORS:
Dr. A. Vrieling
Dr. C.A.J.M. de Bie

Exploring an alternative approach for deriving NDVI-based forage scarcity in the framework of index-based livestock insurance in East Africa

LUCAS HERNÁN DE OTO
Enschede, The Netherlands, February, 2017

Thesis submitted to the Faculty of Geo-Information Science and Earth Observation of the University of Twente in partial fulfilment of the requirements for the degree of Master of Science in Geo-information Science and Earth Observation.
Specialization: Natural Resources Management

SUPERVISORS:
Dr. A. Vrieling
Dr. C.A.J.M. de Bie

THESIS ASSESSMENT BOARD:
Prof. Dr. A.D. Nelson (Chair)
Dr. Francesco Fava (External Examiner, International Livestock Research Institute)

ABSTRACT

Recurrent drought represents a major threat in arid and semi-arid regions of East Africa. Prolonged lack of water availability may trigger widespread livestock mortality due to forage scarcity and disease outbreaks. Pastoralists in these regions depend entirely on their herds for subsistence and therefore, they are severely affected by this events. To protect them against this peril, index-based insurance products constitute an innovative intervention. Under this scheme, indemnities are payed based on objectively measured variables which are highly correlated with the loss being insured. A satellite-derived product that is frequently used as a proxy in this framework is the normalized difference vegetation index (NDVI).

The Index Based Insurance for Livestock (IBLI), developed by the International Livestock Research Institute (ILRI) uses area-aggregated NDVI values from Enhanced Moderate Resolution Imaging Spectroradiometer (eMODIS) to calculate a seasonal forage scarcity index based on which indemnities are determined per administrative unit. Although the index has been tested and proved to be correlated with the actual livestock losses experienced by pastoralists, the early spatial aggregation of NDVI values hides spatial variability within the units which may negatively impact the performance of the product. In Ethiopia, the Geodata for Innovative Agricultural Credit Insurance Schemes (GIACIS) project uses a different insurance scheme that first groups pixels based on a similar NDVI temporal behaviour and then pools the pixel-level data within the clusters to generate statistics and derive indemnities.

The present research integrates the index design logic of GIACIS into IBLI and proposes an alternative design for IBLI which accounts for ecological variability within the administrative units. First, an unsupervised classification has been performed on NDVI series of the study area using the Iterative Self-Organized Unsupervised Clustering Algorithm (ISODATA). Then, the resulting classes have been evaluated in terms of significance for forage production in order to discard those that are irrelevant from further analysis. Trigger and exit points have been set for the retained classes, then used to calculate payouts per pixel. Finally, the indemnities were aggregated per spatial unit. The results have been contrasted against spatially-aggregated monthly household survey data on drought outcome parameters from different sample sites within the study area. The proposed design has a slightly stronger correspondence to available livestock mortality data for selected areas. Although further validation is required, the integration of two existing methods may provide a sound basis for an insurance product with lower basis risk.

ACKNOWLEDGEMENTS

I would like to thank the ITC Directorate for giving me the opportunity to complete this MSc through the UTS-ITC Excellence Scholarship programme and also express my profound gratitude to all those who have contributed to this research. Thanks for sharing your time and knowledge with me, thanks for your support and kindness, thanks for your patience and dedication, thanks for your advice and your willingness to collaborate:

Dr. Anton Vrieling
Dr. Kees de Bie
Dr. Francesco Fava
Mr. Willem Nieuwenhuis
Dr. Munenobu Ikebami
Mr. Oscar Niaibei

TABLE OF CONTENTS

LIST OF FIGURES

LIST OF TABLES

ABBREVIATIONS

ASAL: Arid and Semi-Arid Lands

eMODIS: Enhanced Moderate Resolution Imaging Spectroradiometer

EOS: End of Season

GIACIS: Geodata for Innovative Agricultural Credit Insurance Schemes

GBI: GIACIS-Based IBLI

IBLI: Index Based Livestock Insurance

ILRI: International Livestock Research Institute

ISODATA: Iterative Self-Organized Unsupervised Clustering Algorithm

LRLD (or LR): Long Rain-Long Dry season

NDMA: National Drought Management Authority

NDVI: Normalized Difference Vegetation Index

SOS: Start Of Season

SPOT VGT: Satellite Pour l'Observation de la Terre –Vegetation

SRSD (or SR): Short Rain-Short Dry season

1. INTRODUCTION

1.1. Background

Recurrent drought represents a major hazard in arid and semi-arid regions of East Africa (Nkedianye et al., 2011). This can severely affect pastoralist communities residing in these areas (Homewood, Trench, & Brockington, 2012). Prolonged lack of water availability may lead to forage scarcity and disease outbreaks which can result in widespread livestock mortality, especially if adverse conditions prevail for more than one season (Vrieling et al., 2016). Pastoralists are then forced to sell what remained of their livestock for little money, losing their sole source of income. As a result, they are prone to fall into chronic poverty traps (Dror, Maheshwari, & Mude, 2014).

The frequency and severity of recurrent droughts seems to be increasing in the region (The Presidency of the Republic of Kenya, 2015). In effect, during the last 30 years, the Horn of Africa has witnessed a persistent decrease in rainfall during the "long rains" season (March-May) (Tierney, Ummenhofer, & DeMenocal, 2015). This has had grave consequences for regional food security which largely depends on local agriculture and livestock production (Tierney et al., 2015). In 2010-11, a large part of East Africa has been struck by the most severe drought in the region in the last 60 years, triggering a major humanitarian crisis (Yang, Seager, Cane, & Lyon, 2014). In order to control such catastrophic events and minimize its impacts, efficient mitigation strategies need to be implemented (Vrieling et al., 2016).

A promising innovative intervention against episodic droughts is the development of index-based insurance products (Mude et al., 2010). Unlike traditional agricultural insurances that require expensive and time-consuming verification of individual losses by the insurer, the index-based model constitutes a more cost-effective approach (Barnett, Barrett, & Skees, 2008). Payouts under this scheme are based on objectively measured variables which are highly correlated with the loss being insured (Carter, de Janvry, Sadoulet, & Sarris, 2014). The insurance indemnifies the policyholder based on readings of an index in relation to pre-specified thresholds (de Leeuw et al., 2014). Often-used indices comprise rainfall (gauge measurements or satellite-derived estimates) and satellite-based measures of vegetation greenness (Turvey & Mclaurin, 2012). A satellite-derived product that is frequently used as a proxy to calculate these indices is the normalized difference vegetation index (NDVI) (Gommes & Kayitakire, 2013).

A crucial step in the process of developing index-based insurance is the selection and design of the index, i.e., the proxy variable that should be correlated with the peril being insured (Chantarat, Mude, Barrett, & Carter, 2013). As the index will be constructed around readings of that proxy, this decision will largely determine the effectiveness of the product in terms of basis risk (i.e. inconsistencies between the index-triggered indemnity payments and the insured's actual losses). Index design hence does not stop at selecting a data source for deriving the proxy, but also the process of transforming that data source into the proxy, which implies various design options (Brown, Osgood, & Carriquiry, 2011 ; de Leeuw et al., 2014).

During the last decade, many index-based insurance schemes have been designed and implemented in developing countries in Africa, Asia and Latin America (Miranda & Farrin, 2012). In East Africa, the International Livestock Research Institute (ILRI) together with several partners in the public, private and non-profit sectors have designed the Index Based Insurance for Livestock (IBLI), aimed to protect pastoralists residing in the Arid and Semi-Arid Lands (ASALs) from drought related asset losses

(International Livestock Research Institute (ILRI), 2016). The product was commercially launched in the Marsabit District in Kenya in January 2010 and extended to the Borana Zone, in southern Ethiopia in July 2012 (Woodard, Shee, & Mude, 2013).

IBLI aimed at finding a variable that was highly correlated with livestock mortality (Chantarat et al, 2013). In the ASALs region livestock depends entirely on forage for nutrition, and thus an indicator of greenness levels such as NDVI was used as a livestock mortality predictor (Dror et al., 2014). In order to test to what extent the index was accurately reflecting the risk of the insured, community and household surveys have been conducted between 2007 and 2009 in the Marsabit district. The studies confirmed a reasonably good correlation between the index predictions and the actual livestock losses experienced by pastoralists in the area[1] (Chantarat et al, 2013).

The original method conceived for IBLI to transform NDVI values into an insurance index has changed through the years in a constant effort to reduce basis risk (Vrieling et al., 2014). In the current design, 10-daily NDVI composites from Moderate Resolution Imaging Spectroradiometer (MODIS) at 250 m resolution are averaged and aggregated first spatially per administrative unit, then temporally per season, and finally compared between years to estimate the relative condition of forage per unit for a particular season (Vrieling et al., 2016). While originally spatially-constant time periods were used for integration (i.e., March-September and October-February) phenological analysis of NDVI time series allowed to provide more accurate spatially-variant seasonal definitions while removing always dry periods in the year when NDVI provides little information (Vrieling et al, 2016). However, further gains to IBLI's accuracy could be achieved through more careful consideration of the spatial aggregation step (Vrieling et al, 2014).

Different reasons justify spatial aggregation based on administrative units in the context of index construction for insuring livestock drought-related losses. Firstly, drought is a spatially extended natural hazard which tends to affect vast neighbouring zones at the same time (Vrieling et al., 2014) Secondly, additional data that could be used for comparison or validation (such as official statistics) are often only available at an aggregated scale (Food and Agriculture Organization of the United Nations (FAO) E-learning Centre, 2014). Finally, sticking to political boundaries may result convenient to manage other commercial operations related to the product (i.e. sales, payments, advertising, etc.).

An early direct aggregation of NDVI values may however hide spatial variability within the units. This loss of information may negatively impact the performance of the product. Although IBLI units have been adjusted in coordination with local stakeholders considering particular ecological characteristics (Vrieling et al., 2016), differential responses to drought within the same spatial unit may not be captured by the model. This could lead to over- or underestimations of actual losses in certain areas which may result in an increase of the product's basis risk. A more detailed assessment of spatial variability before aggregation could potentially positively affect the performance of the product.

In combination with existing land cover maps, crop calendars and high resolution data, image temporal series can be used to define different ecological strata based on similar behaviour of NDVI values through time (de Bie et al., 2011). In Ethiopia, the Geodata for Innovative Agricultural Credit Insurance Schemes (GIACIS) project is currently using NDVI-based stratification in the framework of an insurance scheme aimed to protect small farmers in the rainfed cropping areas of the highlands (Netherlands Space Office,

[1] Overall adjusted R^2 between 52 and 61%

2016). Although this product has been conceived to insure crops, some elements of its spatial logic could be tested for IBLI as an alternative scheme for spatial aggregation. Identifying ecological strata would provide an interesting base to reinstate spatial variability within administrative units. Even if the latter are eventually maintained as the reference entity for indemnity payouts, accounting for ecological subunits could improve the accuracy of IBLI estimations by rising the signal to noise ratio.

The present research attempts to integrate the index design logic of GIACIS into IBLI and consequently to propose an alternative design for IBLI with the overall goal to further reduce the basis risk of the insurance product.

1.2. Research objectives

The main objective is ***to explore and evaluate an alternative approach for deriving NDVI-based forage scarcity in the framework of index-based livestock insurance in East Africa***

1.2.1. Specific objectives

- To perform an ecological stratification of the study area based on NDVI time series, and assess each strata's likelihood of forage provision based on NDVI profiles and high resolution data.
- To incorporate the ecological stratification into an alternative design to calculate forage scarcity index for IBLI by modifying the spatial aggregation logic presently used for the product.
- To compare outcomes from both the current and the proposed alternative method and estimate to what extent applying the new design affects the indemnity payments.
- To evaluate the performance of both methods against spatially-aggregated monthly household survey data on drought outcome parameters.

1.3. Research questions

- Which number of NDVI-based strata maximize the separability in terms of temporal behavior between them?
- Which of the classes are more likely to be used as grazing areas? Which are less significant in terms of forage provision?
- How can the strata-based drought index design of the existing GIACIS-product be modified to match the logic and needs of IBLI's current forage scarcity index product?
- To what extent are insurance payouts affected by the new approach?
- Where do the results differ the most?
- How do the outcomes of both calculation methods correlate with monthly household survey data on livestock mortality and forage availability?
- To what extent does the spatial aggregation of indemnities affect the strength of the correlation?

2. STUDY AREA AND DATA

2.1. Study area

The study area is located in Eastern Africa between 5°40'N and 3°04'S, and between 33°59'E and 41°54'E. It encompasses nine Kenyan counties (Baringo, Garissa, Isiolo, Mandera, Marsabit, Samburu, Tana River, Turkana, and Wajir) and the Borana zone in southern Ethiopia. The area comprises a total of 129 divisions, which constitute the current insurance units used in the framework of the IBLI project (Vrieling et al., 2016). These spatial units correspond to administrative divisions whose boundaries have been in some cases adjusted in collaboration with local stakeholders in order to better reflect the use of rangelands by pastoralists in the area. The size of the units varies between 104 km2 to 14,000 km2. The smaller divisions are mainly located in Borana and Baringo and the bigger ones in Isiolo, Turkana and Tana River. A map of the study area can be seen in Figure 1.

The nine Kenyan counties are referred to as the Arid Counties (The Presidency of the Republic of Kenya, 2015) and cover 60% of the total area of the country. According to the last national census 9.6% of the country total population lives in the arid counties (3.7 million inhabitants) (Kenya National Bureau of Statistics (KNBS), 2009). The Borana district has an area of 43,000 km2 which represents around 4% of the total area of Ethiopia. Borana is home to 962,489 inhabitants (about 1.3% of the population of the entire country) (Central Statistical Agency (CSA), 2007).

Based on 1998–2012 data of the Tropical Rainfall Measurement Mission (TRMM 3B43 product), average annual rainfall tends to increase from the centre to the boundaries of the study area, ranging from less than 300 mm in the dry parts of Isiolo, Marsabit, Turkana, and Wajir, to more than 1000 mm in the south-western part of Baringo. Two rainfall seasons can be differentiated: the long rains from March to–May and the short rains from October to December. Clear dry seasons separate both periods in most parts of the area (Vrieling et al., 2014).

The economic spine of the arid lands is livestock production. The livestock population includes beef and dairy cattle, camels, goats, sheeps and chickens (Johnson & Wambile, 2011). In wetter areas of the region, crop cultivation is gaining increasing importance as an economic diversification strategy (Rufino et al., 2013).

The arid lands of Kenya have the highest incidences of poverty and the lowest level of access to basic services of the country. Infant mortality rates are high while school enrolment rates are low. Disease outbreaks are frequent and affect both human and animal populations. Drought is a major factor contributing to poverty in these regions (Johnson & Wambile, 2011).

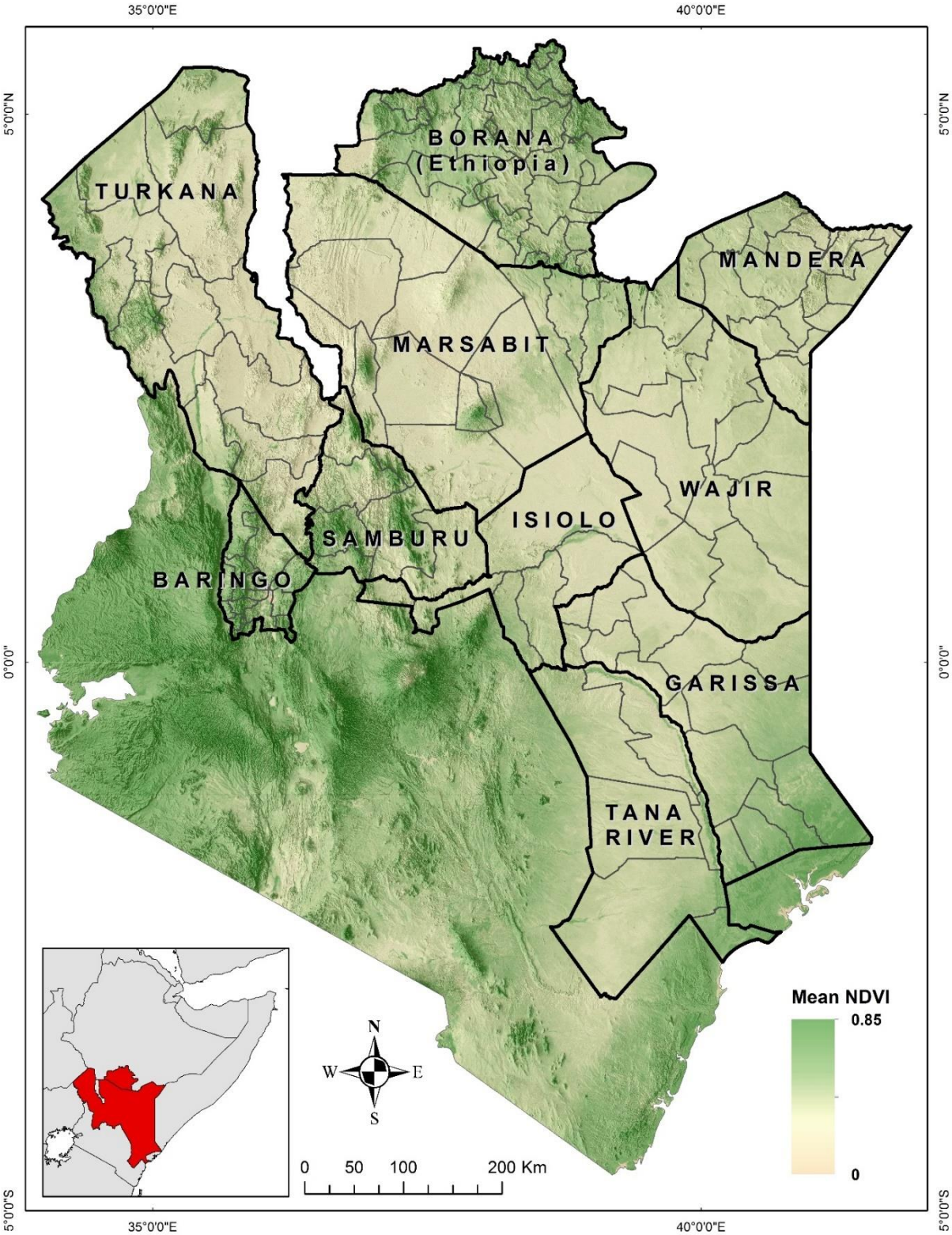

Figure 1. Map of the study area. The main divisions are the nine Kenyan counties and Borana in Ethiopia. The secondary division correspond to the current insurance units used in the framework of the IBLI project. The background shows mean NDVI values from eMODIS time series

2.2. Data

2.2.1. eMODIS

The NDVI product that has been used in this research is the Enhanced Moderate Resolution Imaging Spectroradiometer (eMODIS) time series. This product is generated by the United States Geological Survey (USGS) based on MODIS data acquired by the Terra satellite. This is the dataset that IBLI is currently using. The eMODIS product consists of 10-day (dekadal) maximum value NDVI composites at 250m resolution (U.S. Geological Survey, 2015). Aiming to minimize atmospheric effects that degrade the NDVI signal, a temporal smoothing is applied to the product. The smoothing is based on the Swets algorithm which applies a weighted least-squares regression to a moving temporal window for each pixel time series assigning largest weights to local peaks in the NDVI profile (Swets, Reed, Rowland, & Marko, 1999). The smoothed product is available for free download from January 2001 onwards. The composites are generated every 5 days which results in 6 overlapping composites per month (Famine Early Warning System Network (FEWSNET), 2016; Vrieling et at., 2016). A set of 72 images per year for the period 2001-2016 was downloaded for East Africa. Overlapping composites were deleted, retaining only the composites for day 1-10, 11-20, and 21-end of each month.

2.2.2. Ancillary data

To aid interpreting and assessing the results of the stratification, two sources of high resolution imagery were used, i.e.:

- Google Earth integrates high and medium resolution satellite imagery, aerial photography and digital map data to create and enhance a three-dimensional interactive virtual template of the Earth (Google Inc., 2015). The software provides toponymical information and picture layers which are particularly useful when performing visual interpretation.

- ArcGIS World Imagery was last updated in August 2016. This layer combines high resolution imagery from different sources. Within the area under study it integrates 15 m TerraColor imagery at small and mid-scales, 2.5m SPOT Imagery and 1 m DigitalGlobe imagery (ESRI, 2016).

2.3. Validation data

For validating results, three existing datasets have been used. At the moment of conducting this research, these datasets compiles all the information available on different drought parameters for the study area.

2.3.1. National Drought Management Authority (NDMA)

Since 1996 the Government of Kenya's Arid Land Resource Management Project (ALRMP) is collecting monthly data at household level in various representative locations referred to as sentinel sites. The survey is organized by the National Drought Management Authority (NDMA) and there are around 350 sentinel sites across the ASAL's. The sites have been purposively selected to account for population density across the district. For each community site, 30 households are randomly selected by the enumerators to conduct the survey (Mude, Barrett, McPeak, Kaitho, & Kristjanson, 2009a). The data have been collected for 10 different districts (Dror et al., 2014). Unfortunately, poor data organization and storage have resulted in

substantial losses rendering some areas too fragmented for any rigorous analysis. Furthermore, collection procedures and sampling methodologies employed have not been properly documented (Mude et al., 2009a).

The survey consists of two main questionnaires. The Household Monthly Questionnaire (HH-A) focuses on herd size and mortality, income sources, and coping strategies. The Key Informants Interview Questionnaire (KI-A) is longer than the previous one and contains questions about rainfall, food availability, human and livestock diseases among others. Of particular relevance is the fact that this survey contains a few questions related to forage condition and accessibility.

For this study, all the sentinel sites situated within the study area have been scrutinized in order to identify those presenting at least three years of consecutive monthly data and mortality reaching 1% at least once during that period. A total of 18 sites met this criteria, all of them located in the north-west of the study area in the districts of Turkana, Samburu and Baringo.

2.3.2. IBLI Marsabit household survey

The IBLI Marsabit household survey was conducted as a collaborative effort of ILRI and American universities (i.e Cornell University, the BASIS Research Program at the University of California at Davis, and Syracuse University) in the framework of the project *Index based livestock insurance (IBLI) for northern Kenya's arid and semi-arid lands: the Marsabit Pilot*. The survey gathers seasonal[2] information corresponding to 16 sites purposively selected within the Marsabit district (Ikegami & Sheahan, 2016). The sites are defined as smaller polygons within the units[3]. The size of the polygons ranges from 27 km^2 to 4617 km^2. For this research, all the sites have been analysed.

2.3.3. Borana recall exercise

A recall exercise focused on livestock mortality was conducted in 2011 in Borana by ILRI. Eight communities have been selected in order to sample both the woredas and agro-ecological zones where IBLI is implemented (ILRI, 2011). Focus group discussions have been arranged in every community with the aim of comparing recall mortality from both Long Rain-Long Dry (LRLD) and Short Rain-Short Dry (SRSD) seasons from 1998 to 2011 against mortality predictions based on NDVI response functions from Marsabit. Each focus group discussion was integrated by 6-8 elders including at least one female (ILRI, 2011). In this research, mortality rates from all the sites as reconstructed by the enumerators have been analysed.

2.4. Software

The following software was used in this thesis:

- Erdas Imagine 2016 (Hexagon Geospatial, 2016): Image classification.
- ArcGIS 10.4.1 (ESRI, 2015): Index and indemnities calculation; cartography.
- IDL Version 8.5.1 (Exelis Visual Information Solutions Inc., 2015): data reduction, percentiles calculation, phenological analysis.
- Microsoft Excel 2010: minor calculations; plots.

[2] The larger definition of seasons is used in the survey: LRLD from March to September and SRSD from October to February
[3] A map of the sample sites is presented in Section 7, Appendix II, p. 52.

3. METHODS

3.1. Ecological stratification

3.1.1. Pre-processing and ISODATA clustering

Many ecological studies have highlighted the relevance of NDVI as an index linking vegetation performance to different biotic and abiotic agents (Pettorelli et al., 2005). Direct effects of climatic conditions on biomass and phenological patterns of vegetation as assessed by the use of the NDVI have been reported for many ecosystems (Wang, Rich, & Price, 2003). The NDVI has also been used to improve predictions and impact assessments of disturbances such as drought (Singh, Roy, & Kogan, 2003) or fire (Maselli, Romanelli, Bottai, & Zipoli, 2003). Although NDVI does not directly reflect drought, vegetation stress due to water scarceness can be properly identified as abnormal deviations of the index with respect to long-term means (Pettorelli, 2013). Classifying land surfaces according to long-term NDVI behaviour serves then to describe the climatological features of the region and constitutes an appropriate base to detect and analyse anomalies based on weather events (Udelhoven, van der Linden, Waske, Stellmes, & Hoffmann, 2009). For this reason, ecological strata based on NDVI have been used in this study as pillars for the calculation of forage scarcity index[4].

Median, 10th and the 90th percentiles have been retrieved from the distribution of values per pixel for each dekad over all the years in order to speed up the classification runs by reducing the amount of data to be processed and at the same time base the stratification on relevant information (i.e. 10th and 90th percentiles are the tails of the distribution curve, where anomalies are situated). This resulted in 36 (dekads) times 3 (parameters) equalling 108 data layers. Only pixels located within the study area have been processed. To make sure that the pixels belonging to the area of interest were fully included a buffer of five kilometres around the study area has been considered. All NDVI values below 0 have been masked out since they mostly correspond to water bodies. The ecological stratification of the area was performed on the resulting stack of 108 layers, following the method proposed by de Bie et al. (2011) and using the ISODATA algorithm as implemented by Erdas Imagine (Hexagon Geospatial, 2016).

The ISODATA algorithm is one of the most common unsupervised satellite image classification methods (Abburu & Babu Golla, 2015). This approach is particularly useful when training data is not available for the study area (Mount, Netanyahu, & Le Moigne, 2007). Based on the minimum spectral distance formula this algorithm aim at identifying spectral clusters in the data. It begins with either arbitrary cluster means or the means of an existing signature set, and each time the clustering repeats, the means of these clusters are shifted. The new cluster means are used for the next iteration. The clustering is repeated for the image until either a maximum number of iterations has been performed, or a maximum percentage of unchanged pixels has been reached between two iterations. The method is iterative because it repeatedly performs an entire classification and recalculates statistics. It is self-organizing in terms of the way in which it locates the clusters that are inherent in the data (Hexagon Geospatial, 2017).

To achieve a maximum separability of classes, a series of runs have been carried out with a predefined minimum of 10 and maximum of 100 classes, increasing one class every run. The maximum number of

[4] In this study, the terms *class, zone* and *stratum* are used interchangeably to refer to these ecological areas. In contrast, the terms *unit* and *division* are used to make reference to territorial spaces defined by political or administrative boundaries.

iterations has been set to 50. In order to identify the run with the best separability, the distance between classes has been evaluated for each of the resulting classified images. For this purpose, the divergence statistical measure of distance (Swain & Davis, 1978) as implemented by Erdas Imagine (Hexagon Geospatial, 2016) has been used to determine both the minimum and mean separability between cluster signatures. The higher the distance, the more distinct the clusters are. The optimal number of classes to stratify the study area is the one presenting a distinguishable peak in mean separability (de Bie et al., 2011).

With the aim of checking to what extent the data reduction performed at the beginning was affecting the results, an ISODATA classification was also run on the original stack of 540 data layers with the retained number of classes and identical parameters.

3.1.2. Vegetation seasonality per class

Phenological analysis from NDVI time series allows to obtain a spatio-temporal representation of vegetation seasonality (Vrieling, de Beurs, & Brown, 2011). Following the definition of classes, in this study we used a pre-existing phenological analysis based on eMODIS data (Vrieling et al., 2016) to estimate strata-specific start-of-season (SOS) and end-of-season (EOS) with the aim to identify the key period when forage biomass develops. The phenological analysis approach used is first described by Meroni, Verstraete, Rembold, Urbano, & Kayitakire (2014) with modifications specified by Vrieling et al. (2016). First, the Lomb method (Scargle, 1982) is used to estimate per-pixel seasonality based on the distribution of the signal power throughout the time series. Then for each dekad, median values are retrieved for the whole series. The resulting median profile is used to identify the NDVI minima which are regarded as breakpoints between seasons. Finally, a parametric double hyperbolic tangent model is fitted to the data. The per-pixel SOS (EOS) is estimated for each year as the moment when the model surpasses (falls below) 20% (80%) of the total amplitude between the minimum NDVI before (after) the vegetation green-up (decay) and the maximum NDVI of that season.

The NDVI phenological analysis resulted per pixel in a 15-year time series of season-specific SOS and EOS values. For each stratum the spatial average of these measures has been then computed. This gave per stratum the average SOS and EOS estimate as well as its (temporal) standard deviation. With the aim of setting a fixed temporal window for which the index is to be calculated, the temporal range defined by the average SOS and EOS estimate has been widened to account for possible earlier (later) than average start (end) of seasons. The information provided by the temporal standard deviation of the two events has been used for each unit as a measure of the inter-annual variability of the seasonality. Finally, the resulting dates has been translated into a number from 1 to 36, reflecting the dekad that the date represents, i.e. 1 being 1–10 January.

3.1.3. Evaluating classes' importance for forage

Each stratum has been assessed in terms of relevance for forage production on the basis of the following elements:

- NDVI annual profile analysis: different indicators have been calculated, plotted and visually inspected, namely: mean, maximum and minimum annual NDVI and standard deviation; median, 10th and 90th percentiles for each dekad over all the years.

- Class phenology: for each class the pixels have been classified according to its seasonality (i.e. unimodal, bimodal or no defined seasonality) and the percentage of the seasonality types within each stratum has been calculated.

- Class location and spatial distribution: each class has been mapped and spatial indicators have been calculated for each of them, namely: area, perimeter, mean and maximum distance between pixels within the class (i.e. these last measures give an indication of how spread in space the classes are).

- High resolution images: freely available imagery from Google Earth (Google Inc., 2015) and World Imagery (ESRI, 2016) has been examined. The inspection focused on visual variables like color, pattern and shape, and was oriented towards the identification of areas that are particularly relevant for grazing (e.g. natural pastures, notably those that are close to human settlements), and areas that are poor forage producers (e.g. sparse shrublands on sandy or rocky soils). Of notable utility for this step has been the integration of pictures made, georeferenced and uploaded to the platform by users.

  Based on the results of this analysis, the following criteria and thresholds have been set according to which some of the classes were discarded as they are considered irrelevant as forage producers.

  - Mean annual NDVI: at least 0.15.
  - Pixels with undefined seasonality: no more than 40%.
  - Per pixel overall variability[5]: at least 0.10 for all the pixels within the class.

3.2. Forage index calculation

3.2.1. Current IBLI-design and implementation

For this study, two different versions of IBLI have been considered. The first one will be referred to as ***IBLI 1*** and it corresponds to the way the method is being presently implemented by ILRI (see Figure 2a). According to this scheme, 10-day NDVI composites from MODIS at 250 m resolution are first spatially averaged per administrative unit (Figure 2a1), then temporally averaged using two time windows: 1st of March to 30th of June for the LRLD and 1st of October to 31st of December for the SRSD (Figure 2a2). This results in a seasonal average NDVI per administrative unit. To assess relative forage condition for that particular season with respect to historical conditions, this average is transformed into a z-score using the seasonal average and its standard deviation calculated using the complete time series. Finally, percentiles are calculated based on the z-scores of the whole time series (Figure 2a3). The trigger point is set at the 20th percentile and the exit point at the 1st percentile[6]. This means that all the pastoralists within an administrative unit will start receiving a payment every time the percentile ranking of the index for a particular season falls below 20%. The indemnity increases following a linear function and reaches 100% for the first percentile. LRLD and SRSD are treated independently throughout the process.

The second version will be referred to as ***IBLI 2*** and corresponds to the method proposed in Vrieling et al (2016). It only differs from IBLI 1 in the temporal aggregation step (Figure 2a2). While in IBLI 1 the same

[5] As in Vrieling et al (2016), per pixel overall variability has been defined here as the difference between the 95th and the 5th percentiles for all the values of the time series

[6] Given that the eMODIS archive contains only 16 years of data, in practice this implies that a value very close to the minimum is selected.

time window is applied to all the administrative units, in IBLI 2 unit-specific start and end of season dates are calculated based on the phenological model described in Section 3.1.2.

3.2.2. New approach based on GIACIS

The GIACIS approach clusters pixels based on their similar temporal behaviour and pools the pixel-level data within the clusters to generate statistics and derive indemnities (de Bie, 2016). Under this scheme, 16-year of time series of Satellite Pour l'Observation de la Terre – Vegetation (SPOT VGT)[7] images at 1km resolution are classified using the ISODATA algorithm to generate agro-ecological zones defined according to the similarity in long-term NDVI behaviour. Trigger and exit values are derived by using the 15 and 5% percentiles respectively. In order to properly determine these percentiles, pixel values are pooled from the same zone for each individual dekad. For each zone and dekad, the NDVI readings of all pixels and years are used to extract NDVI values corresponding to the trigger and exit percentile values. Then for a particular dekad and year, the NDVI value of each individual pixel is compared against these thresholds. If the pixel value triggers payment, the indemnity is decided using a linear function connecting trigger level (0% indemnity) to exit level (100% indemnity).

In this study a similar ecological stratification logic is used in the framework of IBLI. This new approach will be referred to as ***GIACIS-Based IBLI (GBI)*** (Figure 2b). First, strata have been defined and then assessed in terms of their relevance for forage provision and possibly discarded based on this criterion (Figure 2b1). While the GIACIS design considers individual dekads as temporal analysis units, IBLI analyses seasonal forage scarcity with the rationale that total primary productivity during a season is what affects forage availability, irrespective of the precise timing of this forage formation. This original IBLI logic has been maintained in the new design. Using the phenological model described in Section 3.1.2, average start and end of season dekads have been calculated for each strata. These dekads will be henceforth referred to as $\boldsymbol{SOS_s}$ and $\boldsymbol{EOS_s}$. Per pixel dekadal values of NDVI have been first aggregated in time according to these stratum-specific $\boldsymbol{SOS_s}$ and $\boldsymbol{EOS_s}$. This step can be expressed as:

$$\boldsymbol{CumNDVI_p^s} = \sum_{t=SOS_s}^{t=EOS_s} \boldsymbol{NDVI_p^t}$$

where $\boldsymbol{CumNDVI_p^s}$ is the cumulative NDVI value per season (s) for a pixel (p) and $\boldsymbol{NDVI_p^t}$ is the value of that pixel in one of the dekads (t) belonging to the season using the seasonality defined by the stratum (c) to which the pixel belongs (Figure 2b2).

For each stratum and season (i.e., separate for long and short rains), the distribution of all contained $\boldsymbol{CumNDVI_p^s}$ values over the whole time series has been used as the basis to calculate percentiles (Figure 2.b2). Following the traditional IBLI scheme, the 20th and the 1st percentiles have been set to be the trigger and the exit points respectively. The $\boldsymbol{CumNDVI_p^s}$ values corresponding to both thresholds for each zone will be referred to as $\boldsymbol{20P_c}$ and $\boldsymbol{1P_c}$.

For every season of the whole time series, the value of each pixel has been contrasted against the trigger and exit points of the class where it belongs to and an indemnity amount per pixel ($\boldsymbol{I_p}$) has been calculated according to the following model:

[7] From January 2014, the program is using Project for On-Board Autonomy (PROBA-V) the successor of SPOT VGT

If $\boldsymbol{CumNDVI_p^s > 20P_c \rightarrow I_p = 0}$
If $\boldsymbol{1P_c < CumNDVI_p^s < 20P_c \rightarrow I_p = (20P_c - CumNDVI_p^s \ / \ 20P_c - 1P_c) * 100}$
If $\boldsymbol{CumNDVI_p^s < 1P_c \rightarrow I_p = 100}$

The indemnity is expressed as percentage of the total insured amount (Figure 2b3).

In the final step, per pixel indemnities have been aggregated per administrative unit. This step can be expressed as:

$$\boldsymbol{I_U = \sum_{p=1}^{p=N} I_p \ / \ \mathrm{N}}$$

Where $\boldsymbol{I_U}$ is the average indemnity payout for a certain season for a unit ($\boldsymbol{U}$) and $\boldsymbol{p}$ is one of the **N** pixel locations within that unit (Figure 2b4).

Although this final aggregation step still provides a single indemnity measure for a specific season/unit combination, the logic of calculating that indemnity measure is now accounting for the internal ecological variability within the unit.

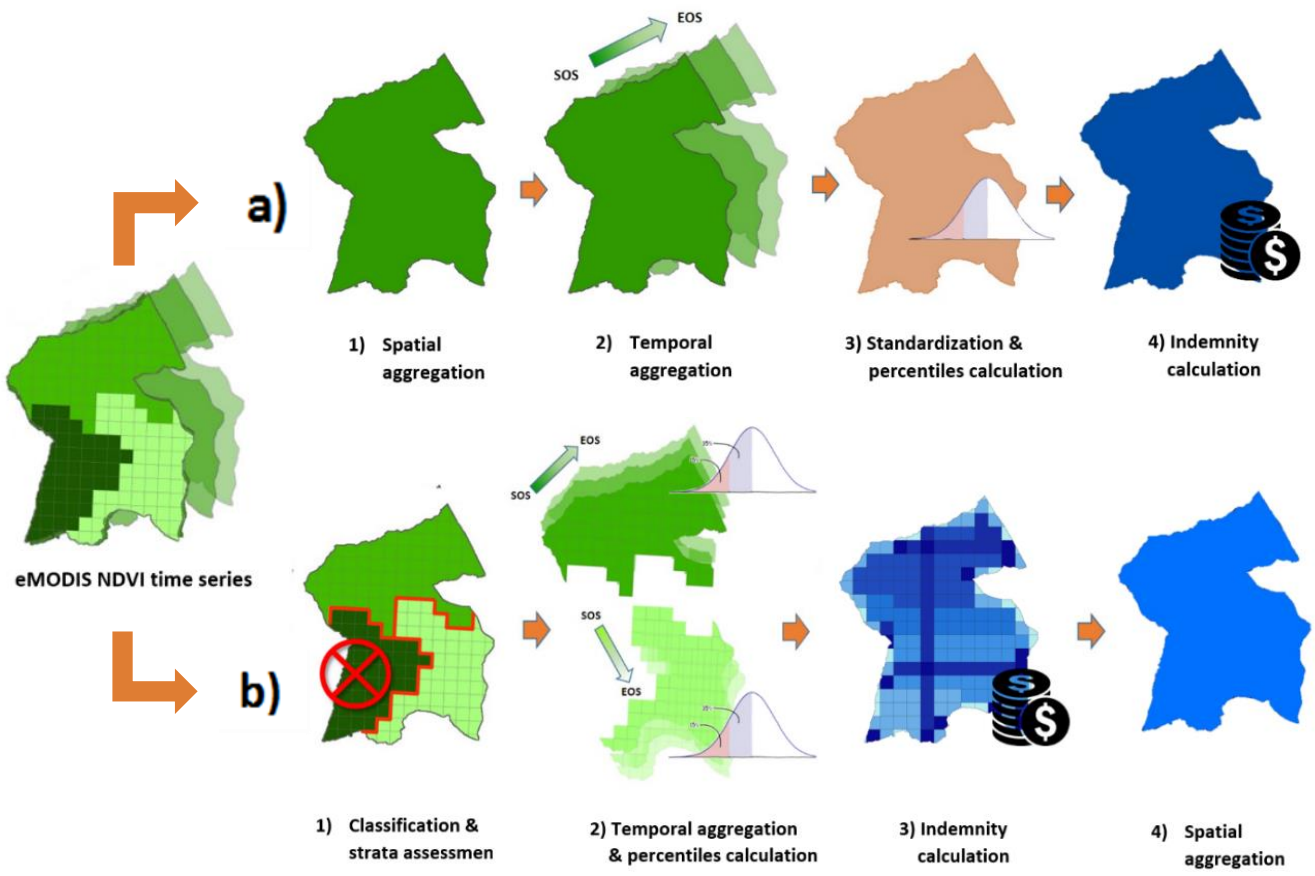

Figure 2. Schematic representation of index and indemnities calculation process according to the different methods a) IBLI 1 and IBLI 2. They only differ from each other in the second step (temporal aggregation) b) GBI

3.3. Comparison of indemnity payouts from the two approaches

Indemnity payouts have been calculated for all the seasons of the time series (15 LRLD and 15 SRSD) for IBLI 1, IBLI 2, and GBI. In order to harmonize the calculation of indemnities for the three methods, the standardization step has been omitted for IBLI 1 and 2 and the percentiles logic as implemented in GBI has been applied instead.

Per unit outcomes for the whole time series have been compared in terms of:

- Mean payment: Per unit average of indemnity payments considering all seasons from LRLD 2001 to SRSD 2015
- Payment decision: Percentage of mismatching seasons per unit. A mismatch means that according to one method the payment has been triggered for in a unit for a particular season while according to the other not. For GBI, unit-level indemnities lower than 1% have been considered as no payment for this comparison.
- Payment amount: per unit average difference in indemnity amount considering only matching seasons (i.e. payment has been triggered according to both method) from LRLD 2001 to SRSD 2015.
- Correlation between indemnity amounts: Pearson's correlation coefficient calculated per unit considering all the indemnities (matching and mismatching seasons) from LRLD 2001 to SRSD 2015.

The results have been mapped and visually analysed.

3.4. Performance evaluation

In order to validate the outcomes of GBI and compare its performance with respect to IBLI 1 and 2, index readings as calculated by the three methods have been contrasted against survey data on different drought indicators retrieved from the following sources:

- NDMA survey
- IBLI Marsabit household survey
- Borana recall exercise

3.4.1. NDMA

For every selected site, three variables have been plotted together for visual analysis:

- Livestock mortality rate per month. The rate has been estimated based on herd size and number of dead animals per species (i.e. camels, cattle, sheeps and goats). The variable is expressed in tropical livestock units (TLUs), a standard measure used to aggregate different species based on similar average metabolic weight (Chantarat et al, 2013). The rate represents the number of dead animals as a percentage of the total herd size for a particular month.
- Forage availability (i.e. expressed as a binary variable: normal / low availability)
- Indemnity payout as estimated by the three methods.

Livestock mortality have been plotted using bars while the indemnities have been depicted as overlapping areas covering periods marked by the corresponding SOS and EOS. As a background, monthly information

on the state of forage has been added. The plots are useful to study the way the variables interact: how livestock mortality relates to forage availability, how the payments are triggered for the different methods in relation to the state of forage and whether the indemnities correspond to herd mortality rates.

For each of the sample sites, the number of dead animals per month in TLUs has been summed to obtain cumulative values for each season[8]. Then all these values from all the sample sites together have been correlated with the corresponding indemnities as calculated by the three methods.

3.4.2. IBLI Marsabit Household Survey

For this research, seasonal mortality rates from 2008 to 2013 have been correlated with indemnity payouts as calculated by the three methods. For GBI, an alternative spatial aggregation of indemnities was also performed whereby pixel-level indemnities were aggregated within each sample site. First a correlation coefficient has been calculated for each site, then for all the sites together.

Similar to what was described in Section 3.4.1, plots have been generated that integrate mortality rate and indemnity payouts as calculated by the three methods with information on forage availability retrieved from the NDMA survey.

3.4.3. Borana recall exercise

Mortality rates from all the sample sites have been plotted together with the indemnities as calculated by the three methods aiming at visual analysis. In this case, information on forage state was not available. The data have also been correlated with corresponding payouts as calculated by the 3 methods considering all the seasons and all the sites together.

[8] The larger definition of seasons is used: LRLD from March to September and SRSD from October to February

4. RESULTS

4.1. Ecological stratification

4.1.1. Divergence statistics

Figure 3 shows that the average divergence separability peaks at three points: 35, 76 and 93 classes. The three peaks have similar values with the peak at 35 being slightly higher than the others. This means that classifying the study area into either 35, 76 or 93 classes will result in clusters that among them have a good separability based on their temporal behavior of NDVI. Of the three, the first one corresponds also with a peak in the minimum separability. This means that using 35 classes to classify the image will ensure both a large average divergence between clusters and also a large minimum separability between them. Considering this study's objectives and the available time, it was deemed better to keep the number of classes low in order to make the processing and interpretation of results more manageable. Therefore, 35 have been retained as the optimal number of clusters to classify the study area.

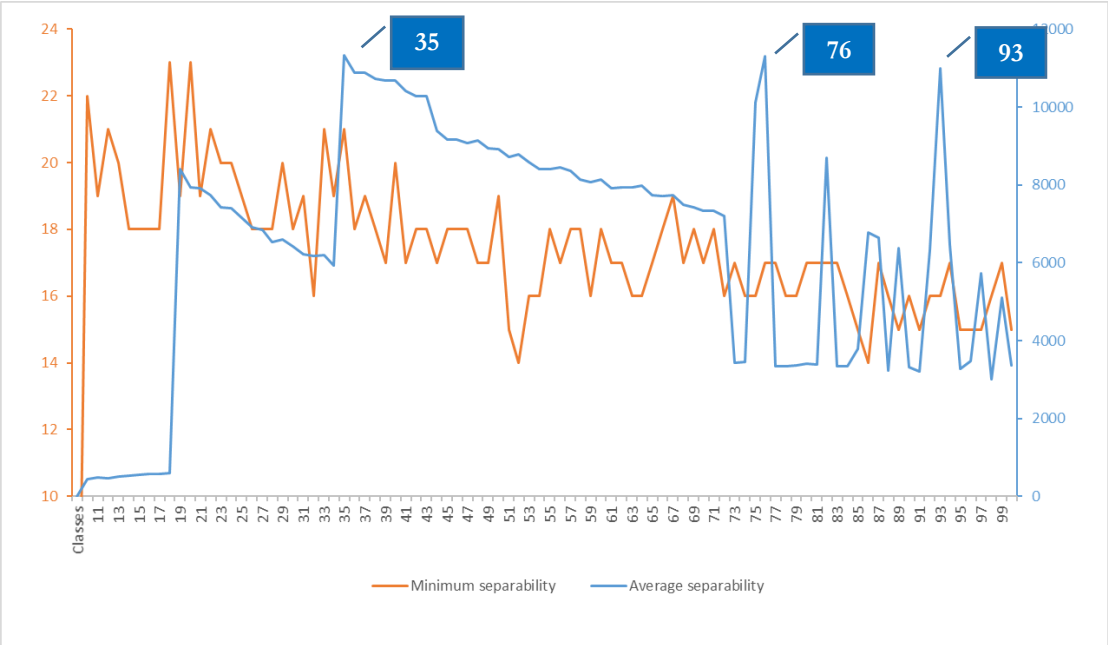

Figure 3. Divergence statistics analysis. Three peaks in average separability are identifiable. The first one coincides also with a peak in minimum separability

4.1.2. Classified image

Figure 4 shows the result of the ISODATA classification using 35 classes on the 108 data layers that comprise the median, 10th, and 90th percentile values for each of the 36 dekads of the year. Classes are arranged in increasing order according to their mean NDVI. Violets and purples correspond to bare soil or very sparsely vegetated areas, including salty or rocky deserts. Turquoises and greens correspond mostly to bimodal seasonal areas with two clearly-separated green-up and decay periods in a year. Yellows, oranges and reds correspond to more densely forested areas with a predominance of evergreen species.

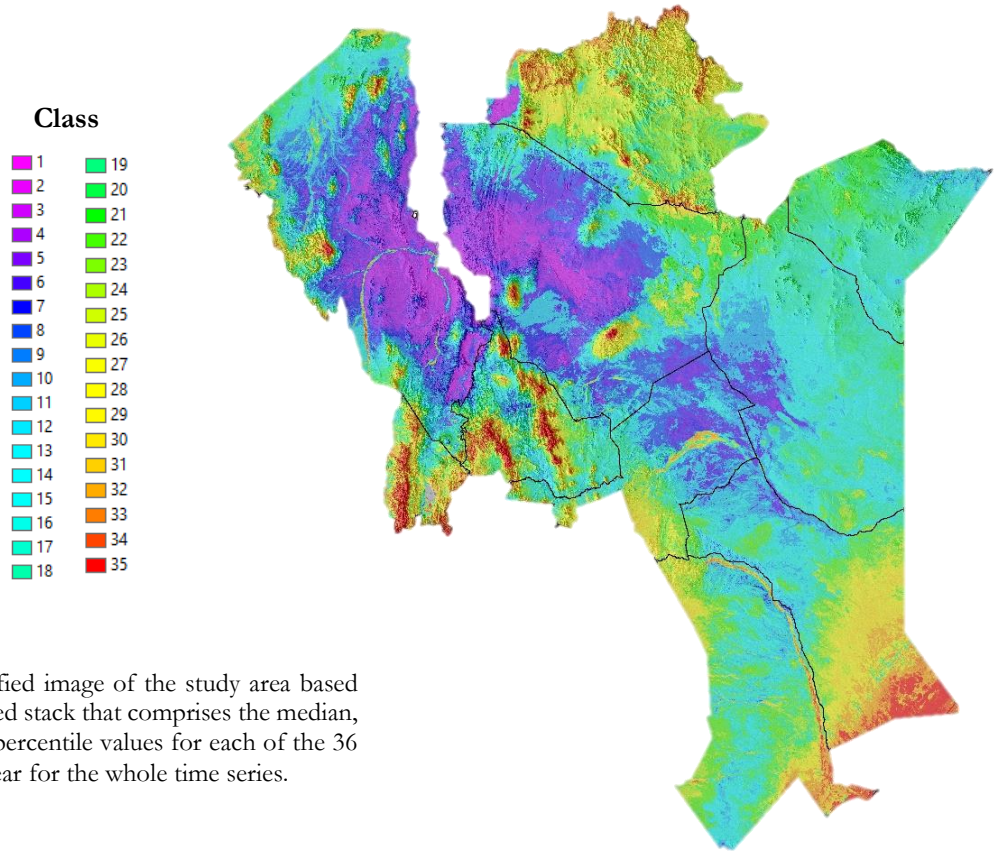

Figure 4: Classified image of the study area based on a data-reduced stack that comprises the median, 10th, and 90th percentile values for each of the 36 dekads of the year for the whole time series.

When running the ISODATA clustering on the complete NDVI stack (i.e. 36 dekads * 15 years = 540 layers) setting 35 classes, very similar results were obtained. Figure 5 shows captures of the same area as classified using the complete (5a) and the reduced (5b) stack. The spatial distribution of the different classes looks overall very similar and therefore it was decided to continue the study with the image as classified using the data reduced stack. However, small differences have been noticed. As it can be seen in the figure, some transitional classes that can be found in (5a) (i.e. oranges between bright red and yellow) are less extended or even disappear in (5b).

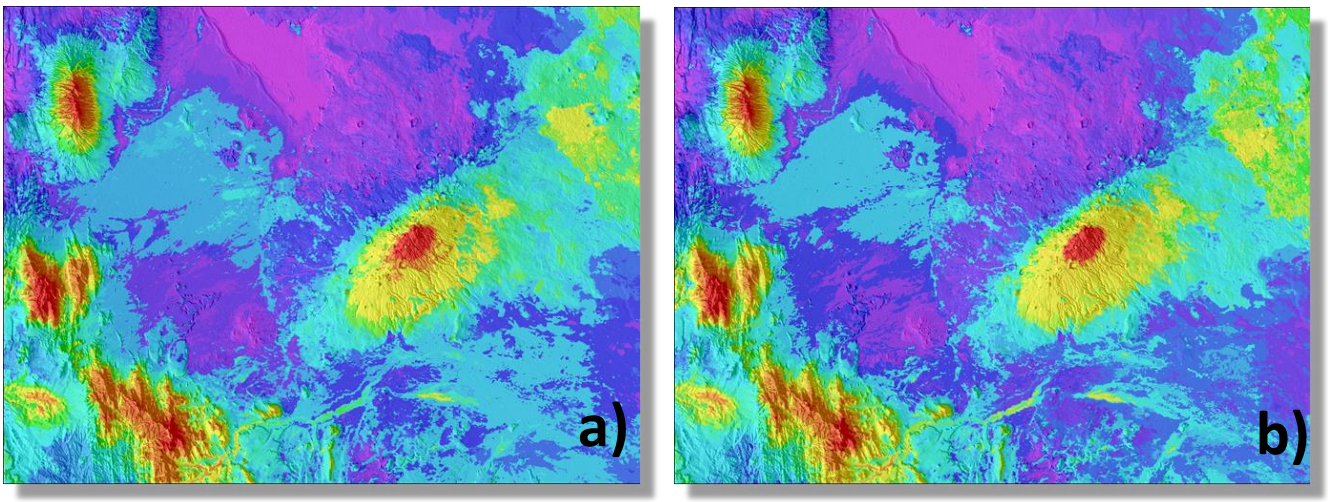

Figure 5. Captures of the same area showing the result of the classification as performed using a) the complete stack (540 layers) and b) the data-reduced one (108 layers)

4.1.3. Main strata types

The 35 classes obtained can be grouped in four major types. Figure 6 shows typical profiles of each type and their location and Figure 7 characterizes each class in terms of four variables: annual mean NDVI, percentage of pixels presenting bimodal seasonality, total season duration (calculated as the sum of long rains and short rains) and NDVI dynamic range (calculated as the average difference between the maximum and the minimum NDVI value registered during the same year).

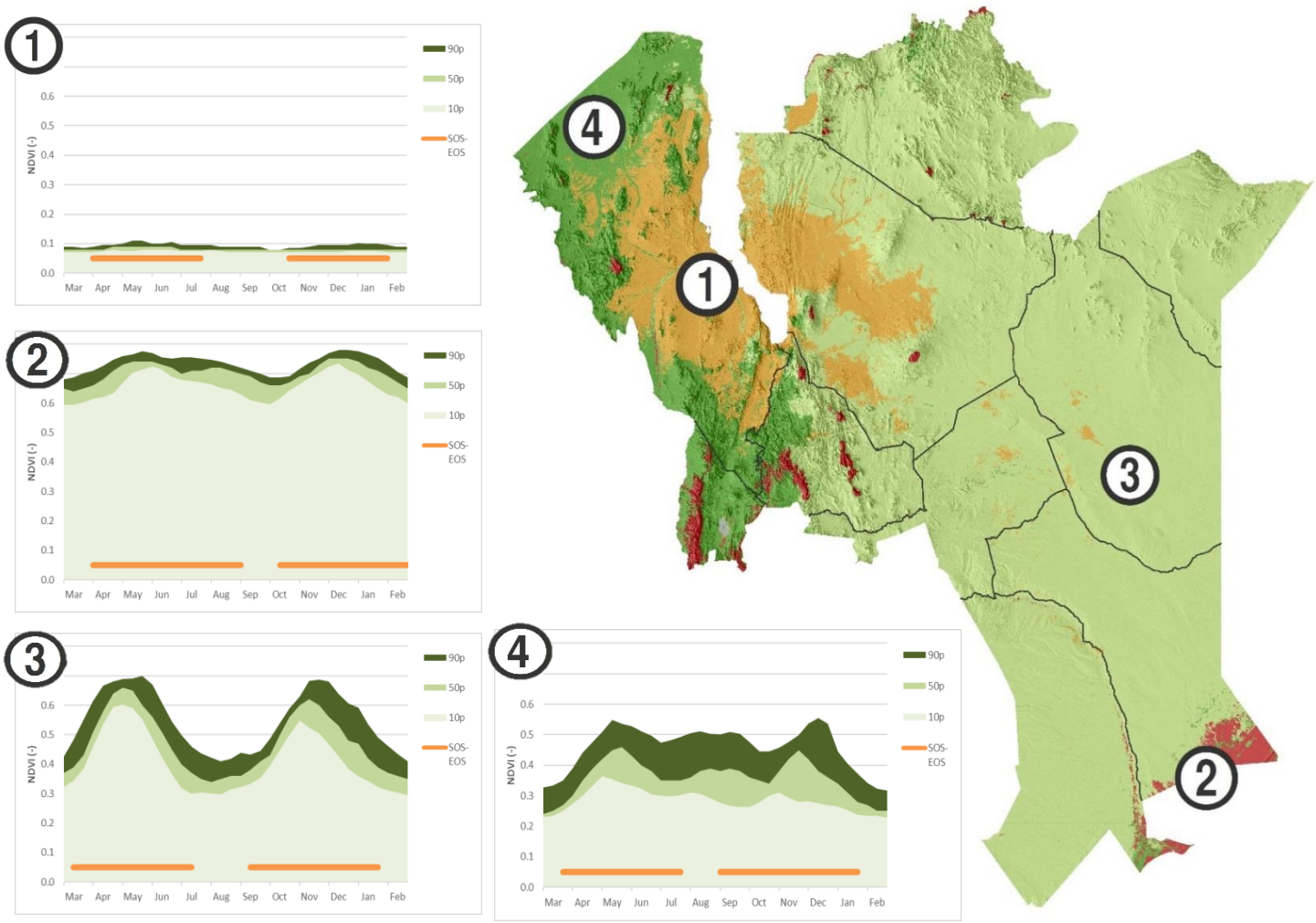

Figure 6. Main strata types. The map indicates the location of the different types in the study area. The graphs represent a typical annual profile of the classes grouped in each type. The multi-annual median is depicted in medium green, the 10th percentile in light green and the 90th percentile in dark green. The orange bars represent average season duration

Type 1 occupies around 13% of the study area. It include classes presenting constant small NDVI values during the whole year. This is the type with the lowest mean NDVI and the lowest dynamic range. Vegetation in these areas is sparse and bare soil predominates. These classes are mainly located in desert zones in the north west of the study area, in the surroundings of Lakes Turkana and Chew Bahir, including the Chalbi desert and the northern part of the Rift Valley. These classes can also be found as small isolated patches spread throughout the center of the study area corresponding to unvegetated sandy or clay terrains, rocky outcrops or dry riverbeds. According to the phenological analysis performed on the data as detailed in Section 3.1.2., about 60% of pixels belonging to this type present either unimodal (14%) or non-defined (46%) seasonality.

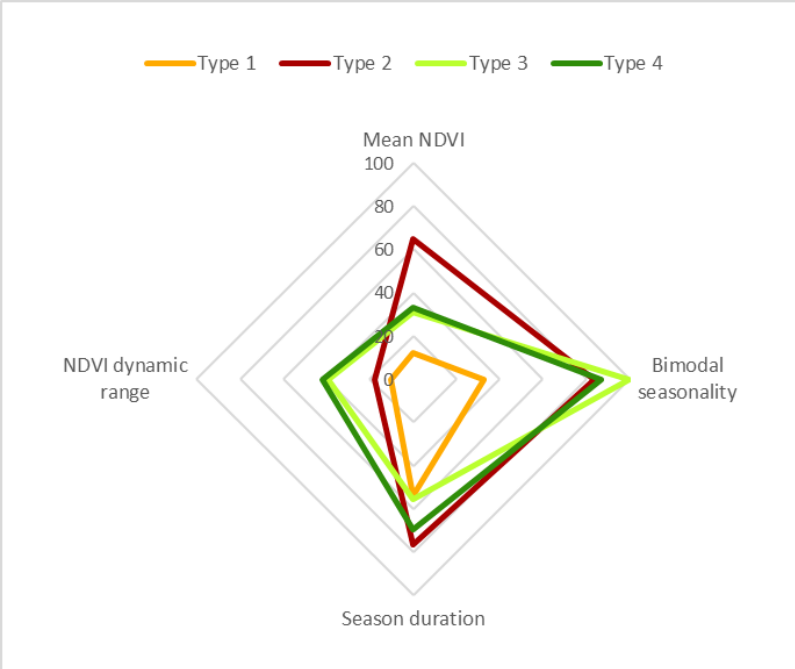

Figure 7. Star plots of the different types based on four variables: mean NDVI, annual NDVI dynamic range, percentage of pixels presenting bimodal seasonality and average duration of season

On the opposite extreme, type 2 gathers classes presenting persistent high NDVI values throughout the year. It corresponds to densely forested areas located in highlands in the north and northwest of the study area, coastal zones in the southeast and banks of the main rivers. Around 83% of pixels present bimodal seasonality. The dynamic range remains however low for this type due to the presence of evergreen vegetation which keeps NDVI values high during the senescence of deciduous species. Type 2 classes occupy around 2% of the study area, and as such have the smallest spatial extension.

On the contrary, type 3 is the most spatially extended, occupying 72% of the area and grouping all classes that present a very clear bimodal seasonality. This type dominates the north, center and eastern parts of the study area. Of all pixels contained in this class, 99.9% are classified as bimodal in the phenological analysis. As a result of this bimodality, the average annual NDVI for these classes is situated halfway between types 1 and 2, although the average maximum NDVI approaches the levels of type 2 classes due to a high dynamic range.. These classes tend to present a relatively stable timing of green-up and decay between years (Figure 8a). This makes that average seasonal definitions (season start and end) provide a stable basis to analyze seasonal drought anomalies.

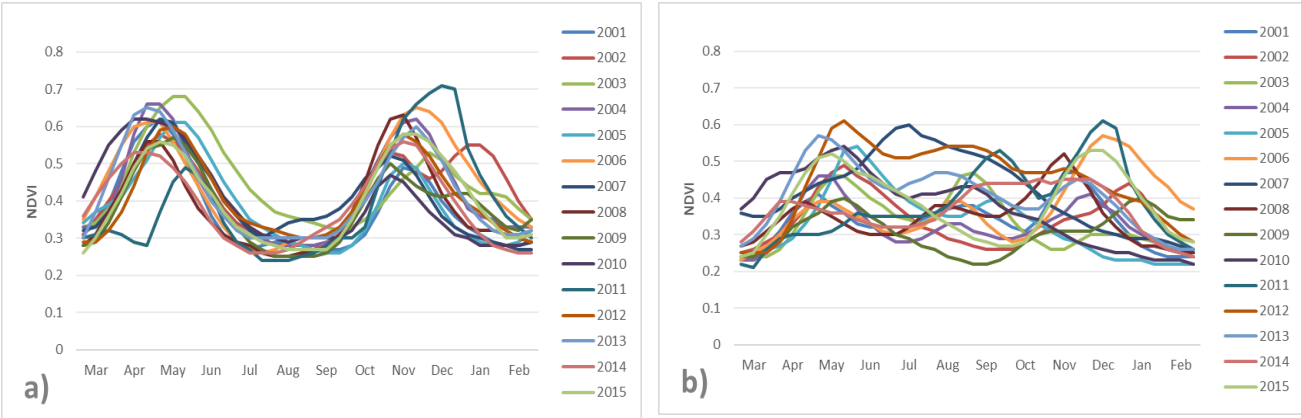

Figure 8. Annual NDVI profiles 2001-2015 corresponding to a class belonging to a) type 3 and b) type 4

In contrast, type 4 classes present a more chaotic phenological behaviour (Figure 8b). From year to year the temporal NDVI behaviour tends to differ making it problematic to accurately estimate seasonal drought anomalies based on fixed seasonal definitions. In some years the vegetation shows a clear bi-seasonal behavior, whereas in others only one green-up and senescence can be identified. This results in a third in-between "hump" on the average yearly NDVI profile plots (Figure 6). Considering those years when two seasons are identifiable, the start and end of seasons are shifted from year to year. As a result, this type presents longer average season duration than the previous one although the dynamic range and annual average NDVI remains very similar. This type of classes are located in the west of the study area occupying large areas in the districts of Turkana, Baringo and Samburu.

4.1.4. Discarded classes

The 35 classes were evaluated using the criteria described in Section 3.1.3 to identify areas that are not relevant for forage production. Those classes where at least one of these criteria were not met, have been discarded. Figure 9 shows the profiles and location of the classes that have been excluded.

Classes 1 and 2 both comprise a small number of pixels located on the land/water boundary of the Lakes Turkana, Logipi and Baringo. These areas are seasonally flooded and since the water bodies have been masked out from the original eMODIS stack, valid NDVI values for these pixels are only present in certain layers. Classes 3 and 4 correspond mainly to both rocky and salty desert areas in the surroundings of Lake Turkana (i.e. Chalbi Desert) and the Chew Bahir in southwest Borana. These four classes belong to type 1.

In addition to these four classes that did not meet the criteria of Section 3.1.3, also class 35 was discarded. This type 2 class meets all the criteria to be considered in the calculation, but experienced professionals at ILRI who know the area suggested to exclude it. This is because class 35 areas are dominated by dense forests that are not usable for grazing either because they are situated at high altitudes or because they are part of preserved zones and the access to them is therefore restricted.

In total, about 6% of the study area has been found to be irrelevant in terms of forage production and therefore discarded from further analysis.

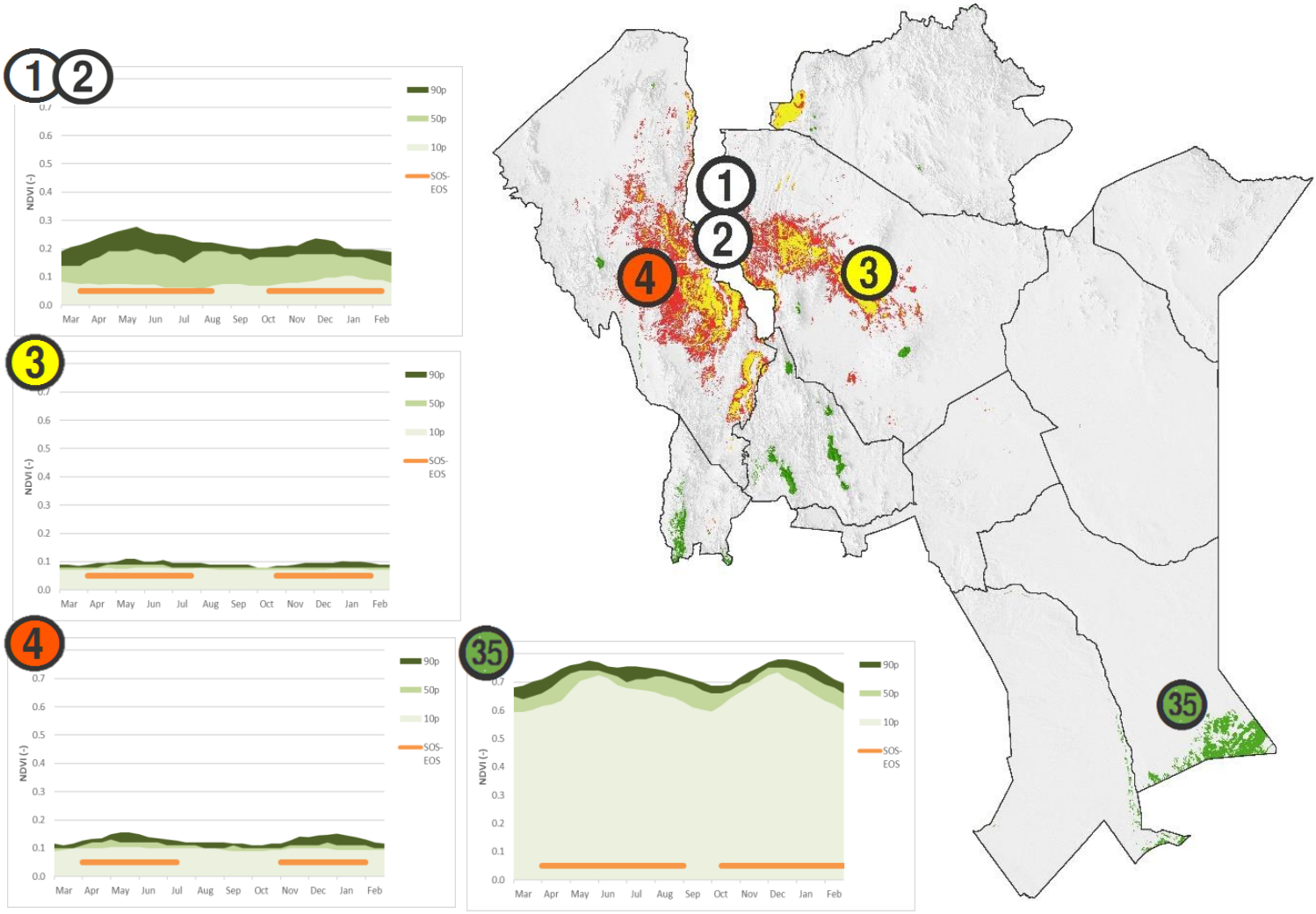

Figure 9. Discarded classes. The map indicates the location of the classes in the study area. The graphs represent the annual NDVI profiles of the classes. The multi-annual median is depicted in medium green, the 10th percentile in light green and the 90th percentile in dark green. The orange bars represent average season duration. Classes 1 and 2 have very similar profiles and have been both represented using Class 1 profile.

4.2. Indemnities calculation using the GBI approach

Figure 10 shows the evolution of indemnities throughout the whole time series as calculated by GBI for four units: the one with the lowest mean payout (Lafey, Mandera), the one with the highest (Golbo Dire, Borana) and two with average payouts (Gurar, Wajir and Sankuri, Garissa). The plots show that payouts are triggered almost every seasons, even if sometimes the amounts are very low. Conversely, indemnities higher than 50% are rather rare and the exit threshold is never attained.

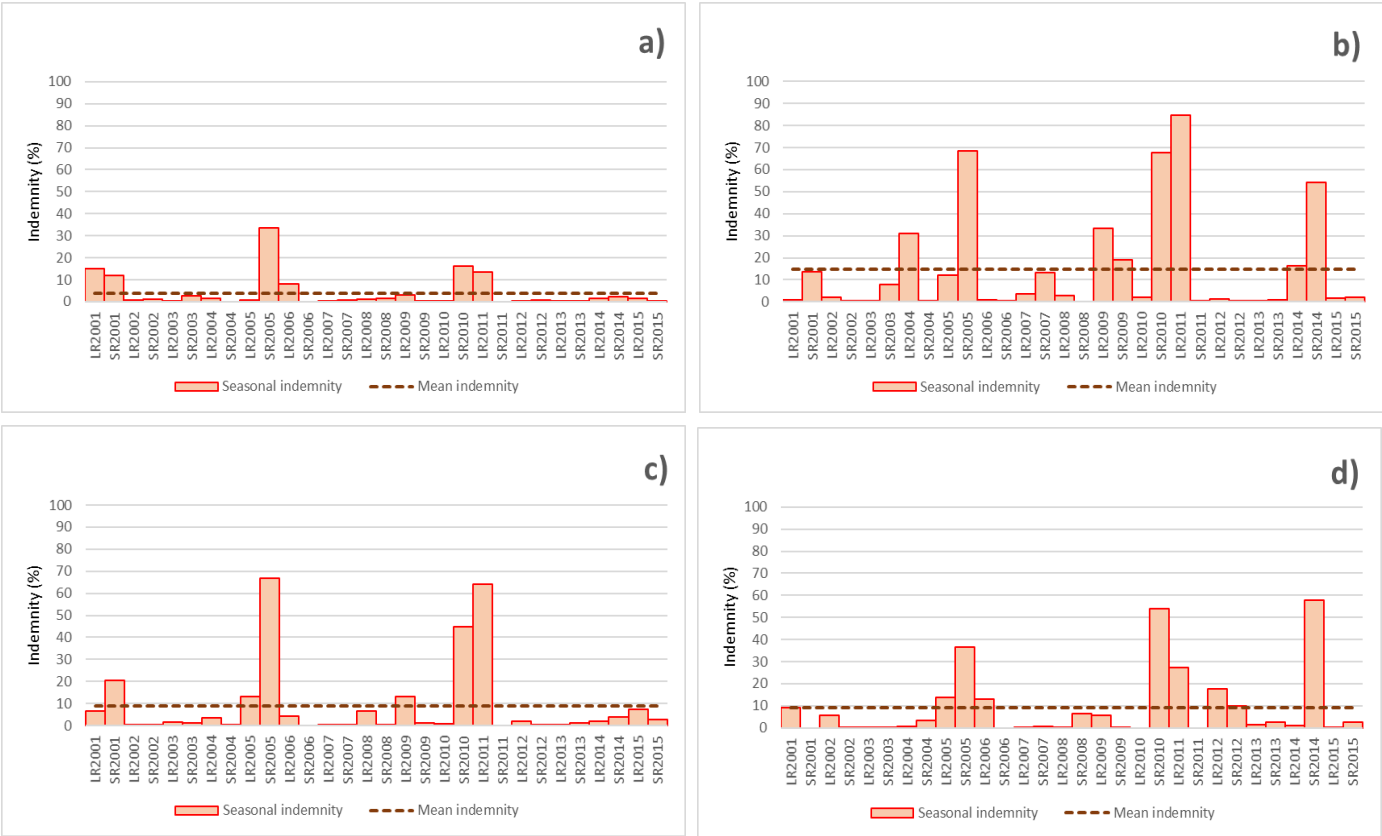

Figure 10. Indemnities as calculated with GBI for four different units a. Lafey, Mandera; b. Golbo Dire, Borana; c. Gurar, Wajir and d. Sankuri, Garissa The dotted line represents the mean indemnity for the considered period (LRLD 2001 – SRSD 2015)

Figure 11 shows per pixel indemnities and the corresponding spatial average for two different seasons purposely selected to represent a very dry period (i.e. LR 2011 is the season with the highest average payout for the study area) and an average one. As a result of the spatial aggregation, the maximum payouts per season at unit level are on average 55% lower than the maximums at pixel level. While across the study area the exit threshold is reached at least in one pixel every season, none of the units attaints full payout during the whole time series (the maximum payout at unit level is 97% in Moyale, Borana, during the long rains 2011).

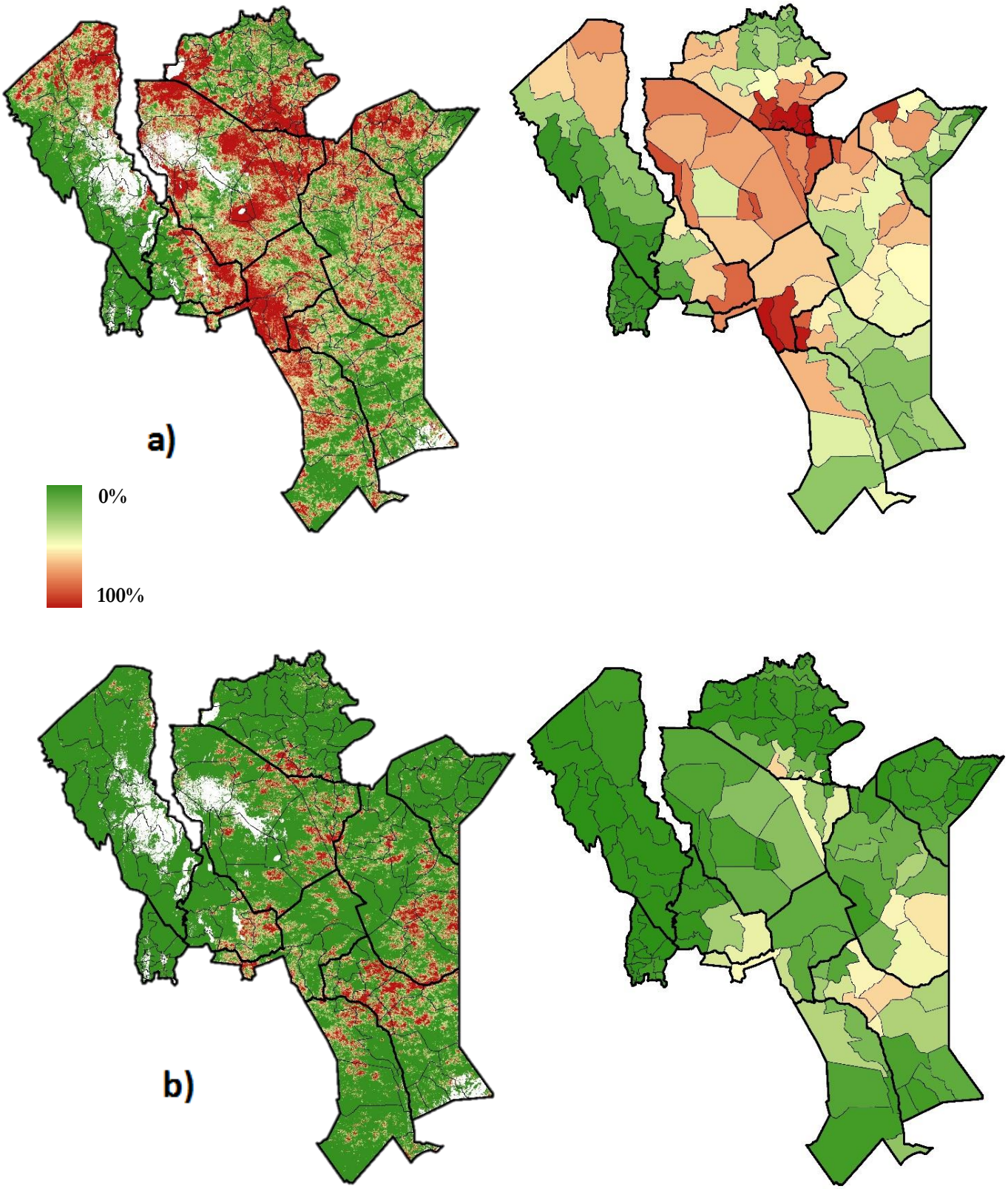

Figure 11. Indemnities at pixel and unit level as calculated with GBI for two different seasons a. LRLD 2011 and b. SRSD 2014

Figure 12 shows mean payouts per pixel for the whole time series and mean payouts per unit for the same period. When considering pixel level, the mean indemnity is 8.96% with a standard deviation of 7%. When considering averaged payouts at unit level, the mean remains the same, but the standard deviation drops down to 2.8%. The spatial aggregation serves to correct for intra-unit variability in average payout.

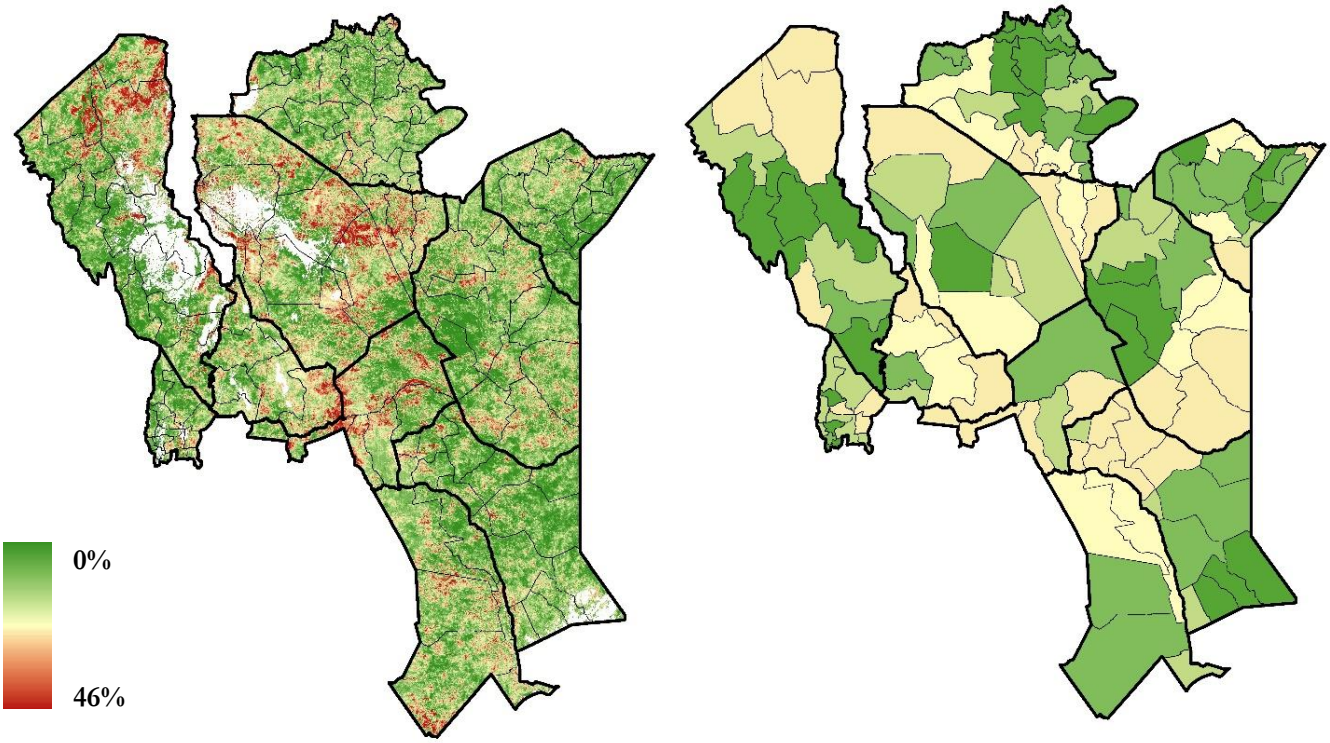

Figure 12. Mean indemnity per pixel and per unit level as calculated with GBI over the complete time series (LRLD 2001 – SRSD 2015)

4.3. Outcomes comparison

GBI results in smoother indemnity amounts than IBLI 1 and 2. Table 1 shows that payments are much more often triggered when applying GBI. In contrast, the exit level is never reached. In terms of mean payout per unit, GBI presents the lowest value. This indicates that the payout is triggered more often, but the indemnities are lower.

Method	Average number of seasons with partial payment	Average number of seasons with full payment	Average indemnity (%)
IBLI 1	5.95	2.08	12.24
IBLI 2	5.94	2.03	12.34
GBI	28.5	0	8.96

Table 1: Average number of seasons with partial and full payment and average indemnity per unit considering all the seasons of the whole time series (LRLD 2001 – SRSD 2015)

As an example, Figure 13 illustrates the chronology of payments for Tarbaj, in the district of Wajir. Under the scheme of GBI, payments are triggered in 28 of the 30 seasons considered. Under the other two methods, it happens only 6 times. On the other hand, whilst IBLI 1 and 2 reached both the exit level twice, the highest indemnity according to GBI is 47% (S2010-11). Overall, the mean payout for GBI is around 35% lower than for the other two.

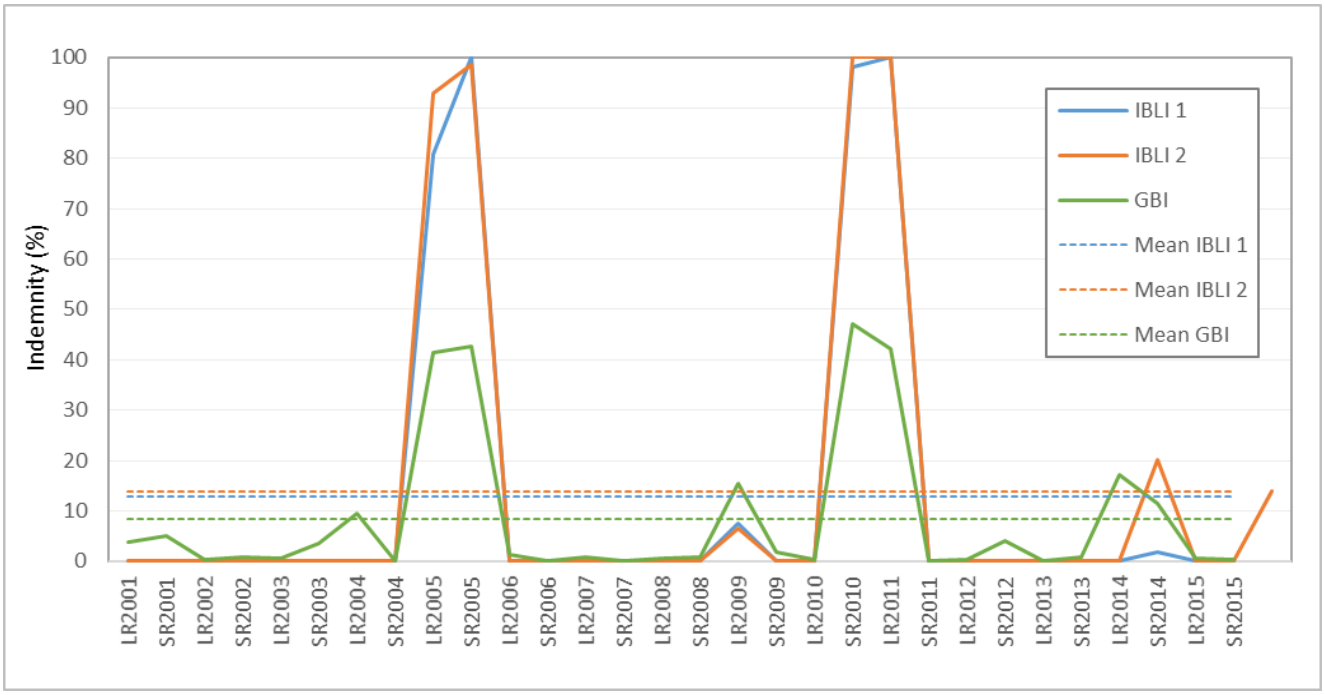

Figure 13. Chronology of payments as calculated with the 3 methods for the district of Tarbaj, in Wajir.

Figure 14 illustrates the spatial distribution of mean payouts per unit across the whole study area. The maps reveal not only that GBI results in lower values in the majority of the units, but also that the spatial pattern differs significantly.

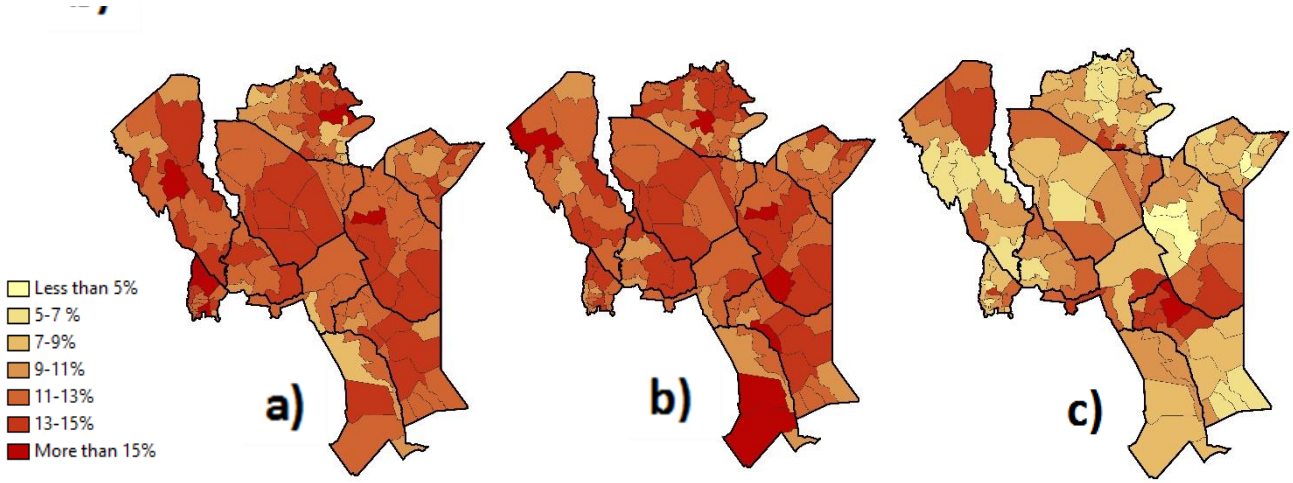

Figure 14. Mean payout per unit as calculated by the three methods considering all the seasons of the whole time series (LRLD 2001 – SRSD 2015) a) IBLI 1; b) IBLI 2; c) GBI

Figure 15 exhibits spatial outcomes of a comparison of the three methods in terms of mean absolute difference in indemnity paid per unit across the 15 years. Again IBLI 1 and 2 show closer results, with discrepancies in amounts lower than 1% for the majority of the units and maximums ranging from 4 to 6% in a few units in Turkana and Borana. In the comparisons with GBI however, the variable raises up to 10% peaking in western Wajir in both cases.

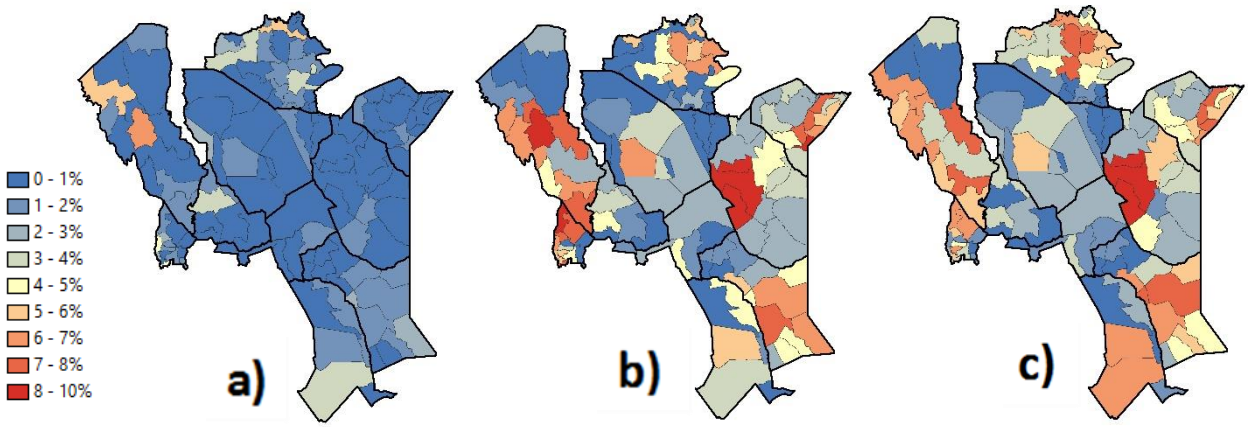

Figure 15. Mean absolute difference in indemnity amount per unit. For each unit, the absolute difference between indemnities as estimated by each method has been calculated for each season, then averaged over the whole time series (LRLD 2001 – SRSD 2015) a) IBLI 1 vs IBLI 2; b) IBLI 1 vs GBI; c) IBLI 2 vs GBI

Figure 16 provides a spatial overview of a comparison between the three methods in terms of payment decision. The results are expressed in percentage of mismatching seasons (i.e. a season when a payment is triggered for a unit according to one method, but not according to the other method). While between IBLI 1 and 2 there is a maximum of 20% mismatching seasons, for GBI versus the IBLI approaches there is up to a 60% mismatch[9].

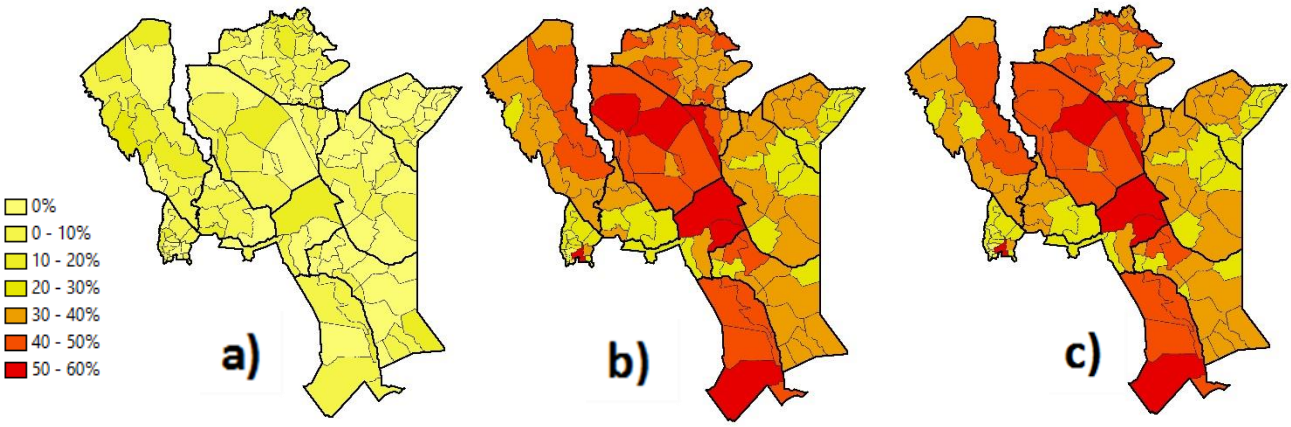

Figure 16. Disagreement in payment decision per unit. For each unit the number of seasons where the payment is triggered according to one method but not according to the other is expressed as a percentage of the total number of seasons of the time series (LRLD 2001 – SRSD 2015: 30 seasons). For GBI, indemnities lower than 1% have been considered as no payment. a) IBLI 1 vs IBLI 2; b) IBLI 1 vs GBI; c) IBLI 2 vs GBI

Although notable differences exist between the three methods in terms of both payment decision and indemnity amounts, the temporal correlation between outcomes remains strong for the majority of the units. Figure 17 exhibit the spatial distribution of Pearson correlation coefficient across the study area. In the three cases, more than 85% of the units present high coefficients ($r > 0.8$). In addition, the weakest correlations tend to be grouped in the same districts in the three cases (i.e., Borana, Turkana, Baringo).

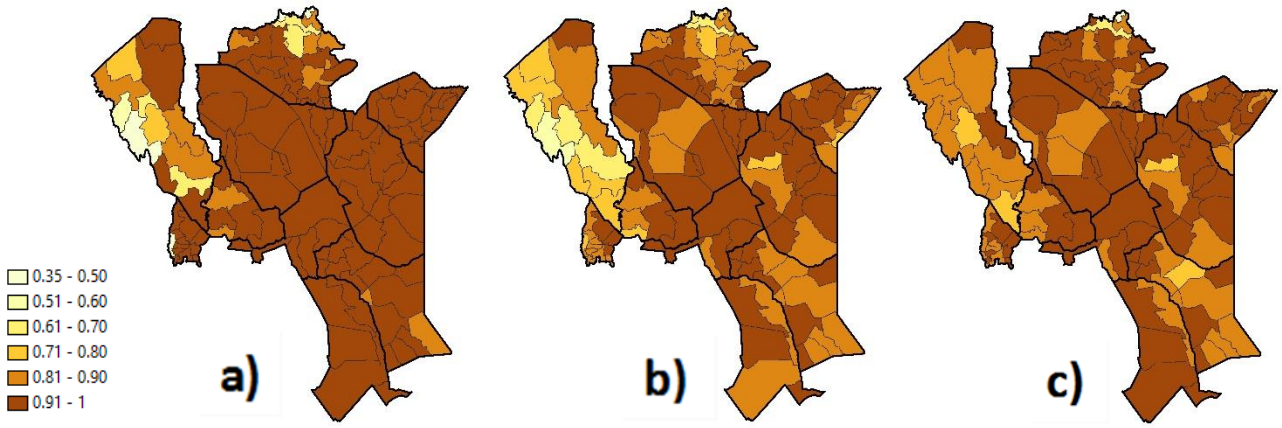

Figure 17. Pearson correlation coefficient that expresses the agreement between methods in terms of indemnity amount paid per unit considering all the seasons of the whole time series (LRLD 2001 – SRSD 2015). a) IBLI 1 vs IBLI 2; b) IBLI 1 vs GBI; c) IBLI 2 vs GBI

[9] As explained in Section 3.3, for method 3, indemnities lower than 1% have been considered as no payment

4.4. Performance evaluation

4.4.1. NDMA survey

Figure 18 shows validation results for three of the sample sites, one representative for each of the three counties: Samburu, Baringo and Turkana.[10] The major mortality outbreaks correspond in the three cases to periods presenting low forage availability (e.g. Figure 18a, March-November 2009; Figure 18b, June-July 2014). However, the dataset also indicates minor mortality events during periods perceived as good in terms of forage (e.g. Figure 18b, March-May 2011; Figure 18c, May 2006-September 2006). For the three samples, payouts are correctly triggered by the three methods to cover the main mortality events. For some cases IBLI 1 and 2 result in high indemnity payments (e.g. Figure 18b, September 2009-January 2010: Figure 18c, March-August 2009), whereas GBI has lower payouts but also covers smaller isolated mortality events (e.g. Figure 18a, July – November 2008; Figure 18b, March-September 2008).

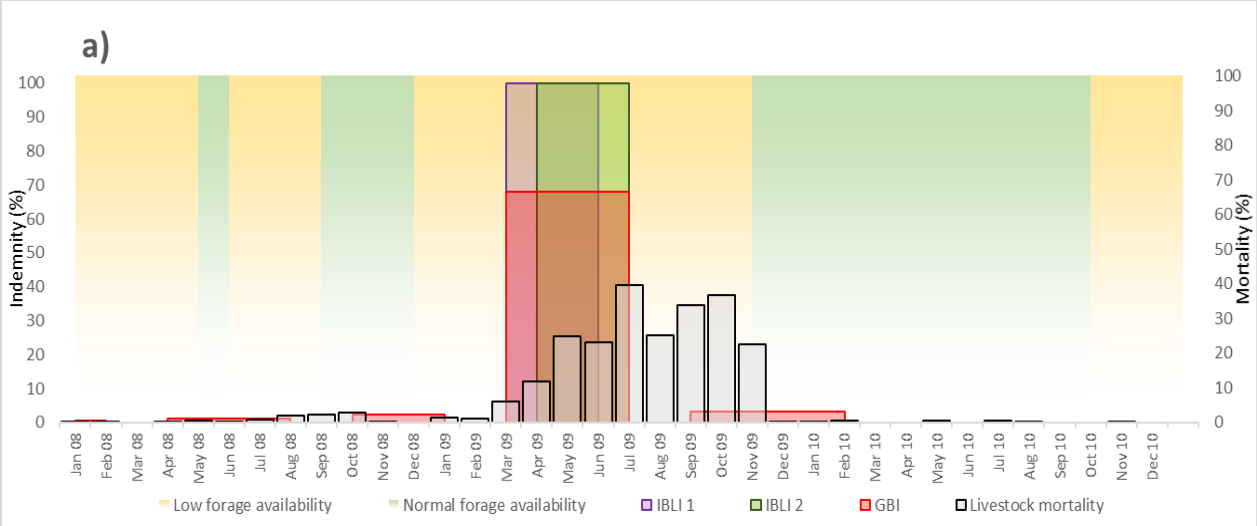

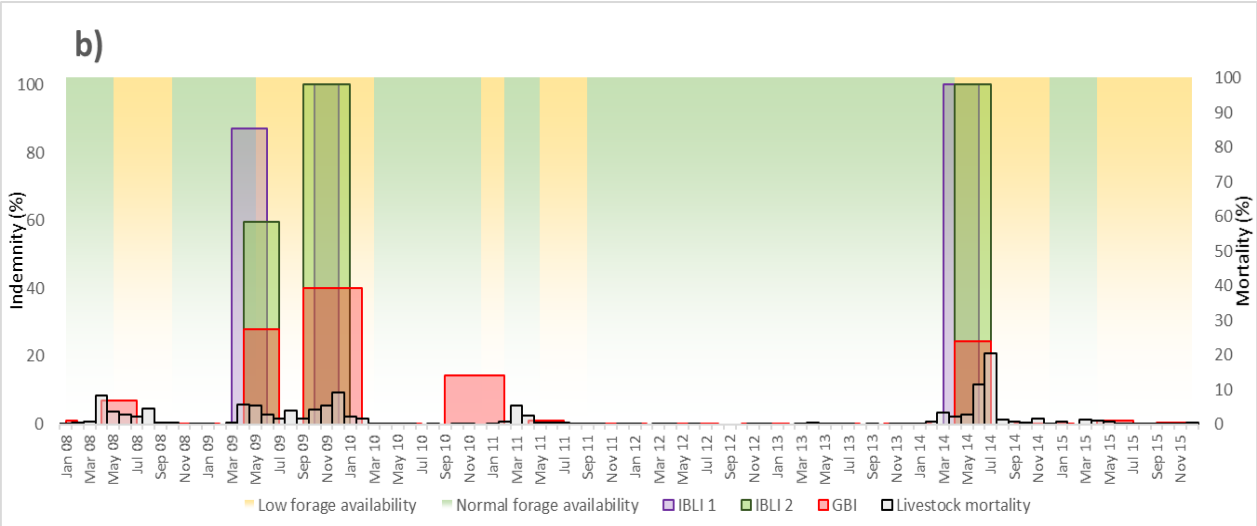

[10] The complete set of graphs and plots can be seen in Section 7., Appendix I, p. 47

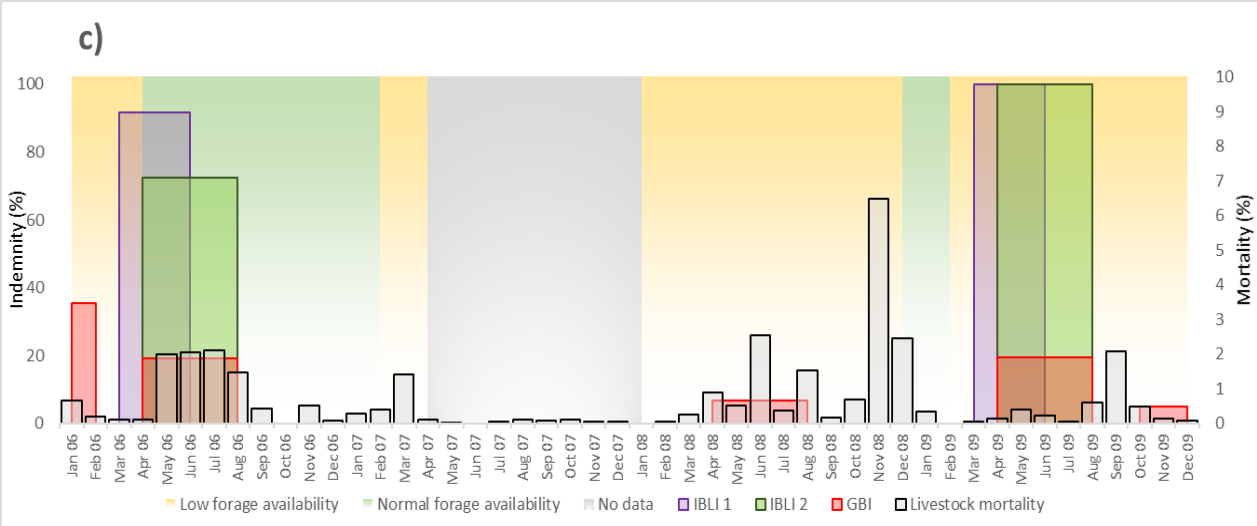

Figure 18. Timelines integrating livestock mortality, forage availability and indemnities as calculated by IBLI 1, IBLI 2 and GBI for three sample sites: a) Lodungokwe, Samburu; b) Maron, Baringo and c) Lokapel, Turkana

Figure 19 shows the plots corresponding to the correlation between livestock mortality and indemnities as calculated for each of the three methods for all the sites and all the seasons together. The correlation is significant for the three methods at the 90% confidence level. GBI present the highest coefficient.

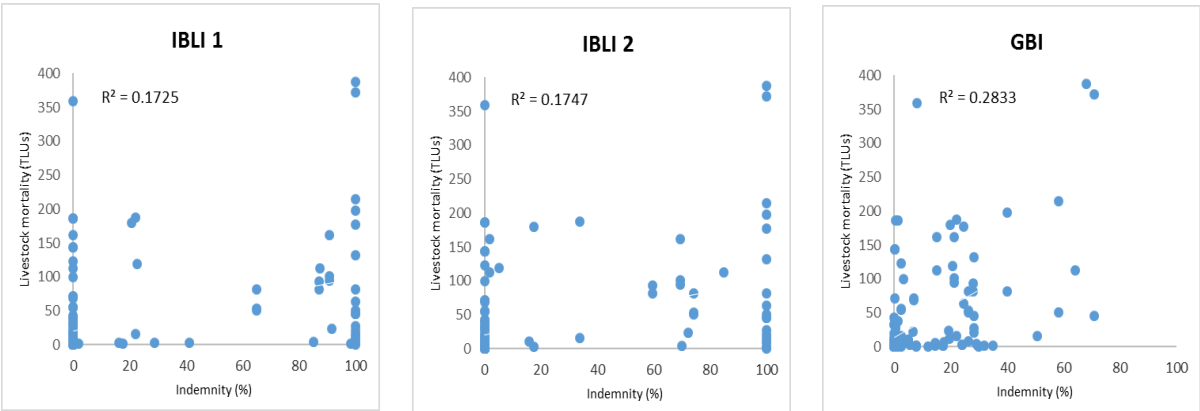

Figure 19. Scatterplots showing the correlation between livestock mortality and indemnity as calculated for each of the three methods considering all the sample sites and seasons together (177 observations)

4.4.2. IBLI Marsabit Household Survey

For the 16 sample sites considered in the IBLI Marsabit household survey, the Pearson correlation coefficient between livestock mortality rate and indemnities was determined and it significance evaluated at 90% confidence level. Table 2 compiles the results of the correlation performed on every site separately. The number of sites presenting significant correlations remains very similar for the three methods. The two versions of GBI (aggregation at unit and sample site level) present also similar results.

IBLI 1	IBLI 2	GBI	
		Unit level	Sample site level
11	10	12	12

Table 2: Number of sample sites presenting significant correlations between mortality rate and indemnities as calculated by the three methods for the period SRSD 2008 – LRLD 2013 (10 seasons)

Figure 20 show scatterplots corresponding to the correlation between livestock mortality rate and indemnities as calculated for each of the three methods for all the sites and all the seasons together. The correlation is significant for the three methods at the 90% confidence level. GBI present the highest coefficient. The correlation becomes slightly stronger when considering per pixel indemnities as aggregated at sample site level.

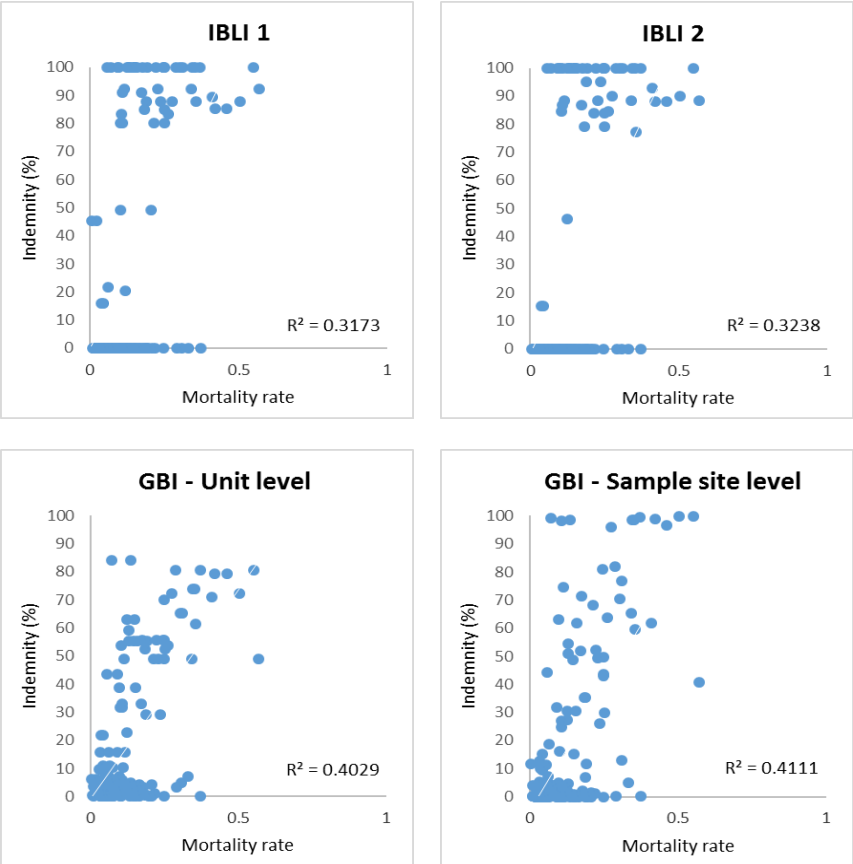

Figure 20. Scatterplots showing the correlation between mortality rate and indemnity as calculated for each of the three methods considering all the sample sites and seasons together (160 observations). For GBI, indemnities have been calculated at unit and at sample site level

Figure 21 exhibit validation graphs for three sites purposely selected to show examples of strong, medium and weak correspondence between livestock mortality and indemnity amount (i.e. Figures 20. a; 20.b and 20.c respectively)[11]. In two of them (Figure 20.b and 20.c) the main mortality events correspond to periods of low forage availability. For Karare (Figure 20.a) the information on forage is not available for the periods presenting the highest mortality but as it can be seen, payouts are correctly triggered by the three methods, covering the events. In Dirig Gombo (Figure 20.b), the first event is properly covered by the three methods, but there seems to be an overpayment during SRSD 2010. The smaller events of 2012 and 2013 are only partially covered by GBI. In Loiyangalani the two mortality peaks seems to be properly covered by the three methods, but from SRSD 2011 on, none of them is triggered (with the exception of a very low amount by GBI during LRLD 2013) even if the forage is perceived as scarce and the mortality remain quite high.

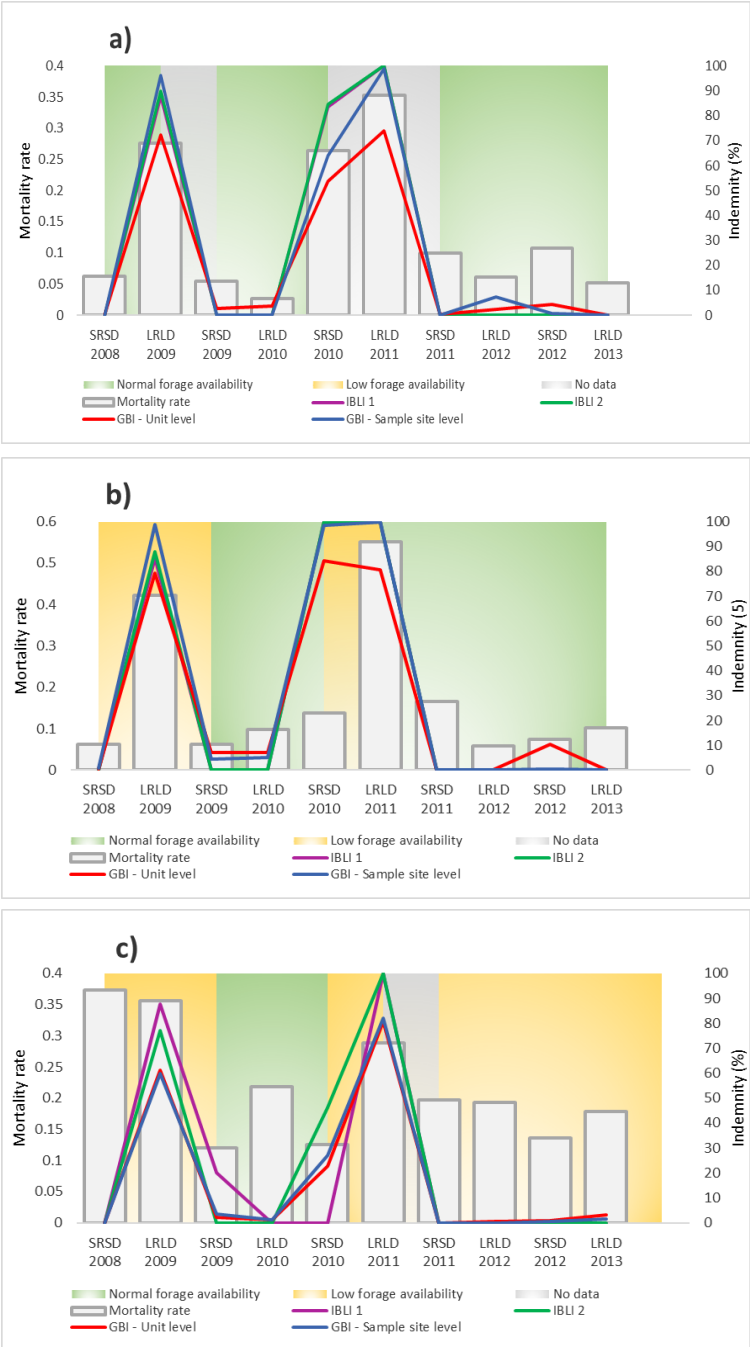

Figure 21. Timelines integrating livestock mortality rate, forage availability and indemnities as calculated by IBLI 1, IBLI 2 and GBI (aggregated at unit level and at sample site level) for three sample sites: a) Karare; b) Dirig Gombo and c) Loiyangalani

[11] The complete set of graphs and plots can be seen in Section 7, Appendix II, p. 52

4.4.3. Borena recall exercise

Figure 22 presents examples of validation graphs for three sites purposely selected to show strong, medium and weak correlations between livestock mortality rate and indemnities as calculated by the three methods (i.e. Figures 21.a; 21.b and 21.c respectively)[12]. In Siku (Figure 20.a), GBI shows the best correspondence with mortality rate with the sole exception of LR2011 where it seems to be under triggered. On the contrary, the other methods (and notably IBLI 1) are over triggered earlier (SRSD 2001 and 2003). In the other two sites (Figures 21.b and 21.c), payments from the three methods tend to be shifted with respect to the mortality event, either advanced (Figure 21.c, SR 2009) or delayed (Figure 21.b, LR 2008).

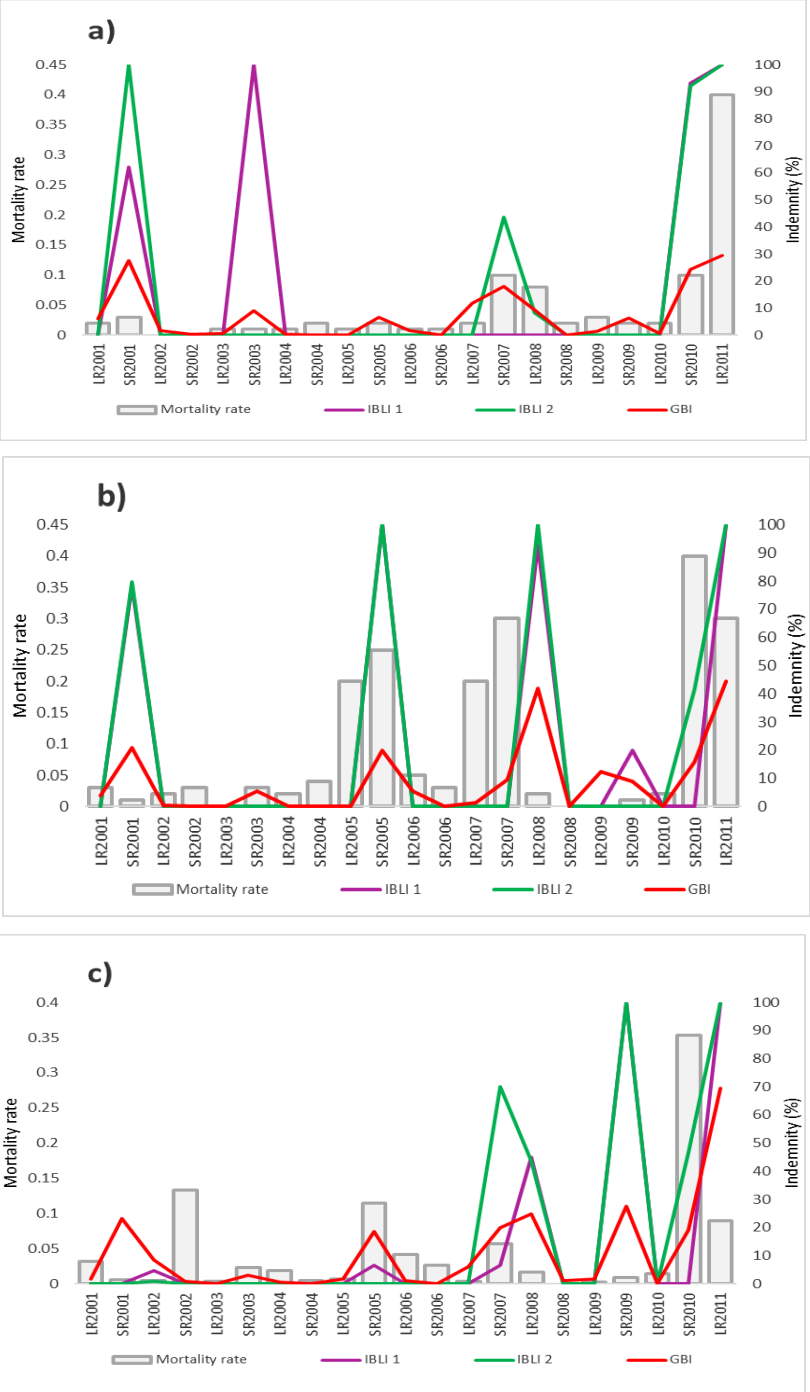

Figure 22. Timelines integrating livestock mortality rate and indemnities as calculated by IBLI 1, IBLI 2 and GBI for three sample sites in Borana: a) Siku, Yabello b) Bakosa, Dire and c) Teso Kallo, Dhas

[12] The complete set of graphs and plots can be seen in Section 7, Appendix III, p. 55

5. DISCUSSION

5.1. On the ecological stratification

Image stratification based on similar temporal behavior of NDVI is a rapid approach to separate ecologically-meaningful units across large areas. While de Bie et al. (2011) presented and applied the approach for the identification of cropping areas, this research attempted to extract meaningful units as they relate to forage availability for livestock. The stratification approach assisted in excluding marginal areas in terms of forage production from the analysis.

Unlike the original application by de Bie et al. (2011), the ISODATA classification has been run here first on a reduced data stack, then on the complete 10-day image stack to compare results. Data reduction was based on the 10, 50 and 90 percentiles. This aimed at grouping pixels together for which the distribution curves of historical readings are similar in terms of mean and tales. Extremely dry or wet periods (reflected in unusually low or high NDVI readings) are normally related to weather events that are not necessarily cyclic. While use of these readings for classifying is interesting and appropriate in the framework of insurance products, it can also be seen as a classification based on outliers, which is somehow contradictory.

Although the outcomes are very similar, some differences exist as it was shown in section 4.1.2. The clusters remain very close in terms of main statistical parameters (i.e. mean, standard deviation, maximum and minimum), but slight differences in the spatial distribution of the classes can be noticed. The extent to which these minor differences affect the final indemnity outcomes is presumably negligible, but remains unknown. The peaks in separability may also be affected and consequently for the full image stack the optimal number of classes to stratify the area could be different. Given the considerations mentioned, it would be of interest to perform the classification procedure again, including the selection of the number of classes, with the full stack of NDVI data.

As explained in section 4.1.1., due to both technical and practical reasons, 35 was retained as the best number of classes to stratify the area. However, as it can be seen in Figure 3, separability is also good considering a larger number of classes. Increasing the number of strata would certainly make the data management more laborious but would presumably result in lower standard deviations per class and therefore help reducing variability within each stratum.

In line with the findings of Vrieling et al. (2016), the main part of the study area correspond to classes presenting a clear bi-modal seasonality (i.e. type 3: 72% of the area). Although 87% of the study area shows stable phenological cycles with limited inter-annual variability (i.e. types 1, 2 and 3), the remaining 13% (i.e. type 4) shows strong year-to-year variations which results in complex phenological patterns. The results obtained by the phenological model can therefore be distorted and may lose accuracy. Defining seasons for this type is a challenge. Consequently, season based analyses may not be the most appropriate approach for classes within this type. This conclusion is also in good agreement with Vrieling et al. (2016), who detected complex seasonality patterns in the same areas (i.e. Turkana and Baringo).

Classes have been stratified here based on pixels values. Higher resolution imagery from Google Earth and pictures have been used as ancillary data to help identifying land cover types. This complementary information was proven to be very useful to get insight on soil types, flood areas, vegetation structure and density and even for identifying dominant species. However, as discussed in Jacobson et al. (2015), Google Earth imagery presents some issues, of which the most important in this framework is the temporal variation

of the data. Even for a small area, the software can display images from a wide range of dates which constitutes an important drawback when seasonal patterns are crucial for the aim of the study. In this regard, other resources could be integrated that may help evaluating the importance of a certain area for forage production: existing land cover maps (Genovese, Vignolles, Nègre, & Passera, 2001; Rojas, Vrieling, & Rembold, 2011), aerial photographs (Louhaichi, Borman, & Johnson, 2001) or medium spatial resolution remotely sensed data like Landsat or Sentinel-2 imagery (Gómez, White, & Wulder, 2016).

For this study, the assessment was oriented towards discarding classes that are not relevant for forage production. Additionally, classes that are identified as relevant forage producers could also be assigned a weight corresponding to their significance. This weight could for example be based on mean NDVI. A more precise weighting could also be performed by analyzing the herbaceous biomass of different classes as done in Egeru et al. (2014). Typical NDVI temporal profiles of main areas used for grazing can also be reconstructed to create a collection of signatures that are representative of relevant areas for forage production. Classes presenting profiles that match these signatures would get higher weights. A more detailed insight on how pastoralist locally manage their herds and a spatial overview of it would also be an useful input for such an exercise (i.e. maps depicting main routes used for carrying the livestock, frequently used grazing areas, etc). In line with the suggestions by Vrieling et al. (2016), this could result in an improved spatial aggregation which integrates only key forage areas within a unit.

5.2. On the GBI design

Index-based insurance products are becoming more and more popular in developing countries as a practical way to insure small farmers where the implementation of standard insurance packages can be problematic in terms of costs and management (Brown et al., 2011). For this kind of products, the effectiveness of the index depends on both the appropriate selection of the proxy to base the payouts on and the way the product is designed (Chantarat et al., 2013). In this study, the same proxy has been used with different designs and therefore different results have been obtained.

The GBI approach enlarges the statistical basis for index calculation and, contrary to the current IBLI approach, postpones the spatial aggregation step to the end. As a result, indemnities are more frequently triggered at the unit level and the amounts are smoothed, at least in the way GBI is conceived now in this thesis. This can be explained by the fact that even when the exit level is reached by a certain number of pixels within a unit during very dry seasons, it will rarely be the case for all the pixels within that unit and therefore, the average payouts per unit are lower. Conversely, during wet seasons, even when the trigger level is not reached for the majority of the pixels within a unit, chances are high that at least a few pixels will trigger payments. For almost every season and unit the payout is always triggered somewhere at least for a few pixels generating a significant number of payouts below 1%.

The desirability of a product that triggers low payments very often but never attains full payment is arguable. Whilst this high frequency of payments seems to serve for covering minor mortality events, it could be impractical in terms of implementation. At the same time, a product that triggers high payments only rarely is not commercially attractive. In this sense, the proposed design for GBI could be complemented with the definition of a minimum payout or a qualifying franchise below which the payment is not disbursed to the policyholder. Similarly, full payouts could be forced by setting a threshold above which the client gets the complete sum insured (e.g. every time that 60% of the pixels attain the exit level, the whole unit receives full payment).

Although this study explored notable modifications on the design that have positively affected the correspondence of the product with survey data on livestock mortality, further innovations could be tested. The logic of using cumulative NDVI is now maintained. As aforementioned, while proven appropriate for areas with clearly defined seasonality, this logic may not work appropriately for Type IV areas. A season independent analysis, based on dekadal information could potentially be a better option for these areas.

Although not fully relevant for forage production assessment, a dekadal based calculation would allow to identify short duration weather events and provide an indication whether there are specific moments within the season when vegetation growth lacks more behind normal. Shorter cumulative periods could better capture short duration events that would be somehow smoothed when considering a longer period as the base for calculation (seasons in either of the three methods are shorter than eight dekads). Appendix 4 presents a collection of maps which allow to visually compare payouts for Borana, Ethiopia as calculated by GIACIS and GBI. The main droughts are captured by both methods. A larger number of anomalies is detected by GIACIS which may be the result of applying a dekadal-based analysis which is seasonally aggregated only in the last step.

Important efforts have been made in order to convert IBLI into an asset protection insurance product which aims at providing the means to maintain livestock alive during critical periods rather than financially compensate the insured for loss of livestock due to mortality. In this direction, Vrieling et al (2016) have explored options to shorten the temporal aggregation step at unit level and demonstrated that payouts can be done earlier by first accurately defining the period when forage is developing, and second by examining if the per-unit interannual variability in CumNDVI can be explained when brining the end of the temporal aggregation window forward in time. In the context of GBI, a similar analysis could be conducted at strata level to evaluate to what extent the duration of the seasons could be shortened to make earlier index calculations and therefore payments possible.

As highlighted in the introduction, several reasons exist to maintain the rationale of aggregating indemnities at unit level. Apart from the practicality in terms of management, the spatial aggregation corrects for average under- or overpaid pixels, as it was shown in section 4.2. However, this study shows that indemnities calculated at larger scales around sample sites correlate better with mortality rates than payouts calculated at unit level. Although based on data from a few sample sites only, this preliminary result draws attention again to the need for critically evaluating the existing spatial units in place now (Vrieling et al, 2014).

5.3. On validation

Validation is an indispensable step to evaluate the performance of an insurance product in terms of basis risk (Vrieling, 2016). In this study two variables retrieved from three different datasets were used to validate results. The quality of the three datasets differ. The Marsabit Household survey was conceived and conducted with the aim of validating outcomes and evaluating the impacts of IBLI on pastoralists. The data on livestock mortality is complete for every seasons for all the sample sites. Unfortunately, the spatial extension of the survey is only limited to part of one county. The NDMA survey in turn, gathers information across a larger part of the study area, but substantial data were lost due to poor organization and storage procedures (Mude et al, 2009) limiting the effective dataset to a collection of sites located in three counties. The abundance of gaps, outliers and inconsistencies in terms of names and codes of the sites have rendered the calculations based on this dataset a very challenging task. In the case of Borana, the information is based on a recall exercise. Although particular care has been taken in reconstructing historical mortality

information, a certain degree of imprecision may be expected due to discrepancies among the participants concerning the dates associated with specific high mortality events (ILRI, 2011).

Two variables have been used in this investigation: livestock mortality and forage availability, although the latter was only plotted in temporal graphs and no statistical relationships were established given that forage availability was only presented as binary information in the surveys (i.e. normal or low forage availability). The use of livestock mortality as a proxy for forage scarcity is debatable. Livestock mortality depends on other variables like disease outbreaks or political conflicts. Moreover, it is a function of the herd size and the carrying capacity of the land (ILRI, 2015). However, even if IBLI contracts are no longer based on modeled livestock mortality, the product aims at protecting the pastoralists' assets. This means covering the efforts of keeping herds alive during the drought rather than paying for the losses after the event. In this context, it still makes sense to use livestock mortality as an indicator for validating insurance payment decisions.

Yet, other sources that provide direct information on forage state could be tested, like long-term field observations of forage availability (Roumiguié et al., 2015) or time-lapse photography of forage condition (Inoue, Nagai, Kobayashi, & Koizumi, 2015). Child nutritional data like the mid-upper arm circumference (MUAC) has also been collected. MUAC can capture short-term fluctuations in nutritional stress and therefore serve as a measure of impact of different shocks on humans (Mude et al., 2009). In combination with other variables it can be used as an indicator of food security crisis. Used in the context of a predictive model like in Mude et al. (2009), it can be also use to validate index predictions.

6. CONCLUSIONS

In this research an alternative design for IBLI was explored. This design accounts for ecological variability within the insurance units while enlarging the statistical basis for indemnity calculations. The statistical basis was enlarged following the GIACIS logic whereby each grid cell is assigned to a group of cells with similar NDVI behaviour in time (i.e., a class or stratum). Using ISODATA clustering of NDVI time series 35 classes were identified that can be divided into 4 main types. Covering 72% of the area, bimodal classes with two clear green-up peaks dominate the territory. Extremely dry areas with very low NDVI variability through the year occupy about 13% of the territory. Another 13% correspond in contrast to classes presenting a very large interannual variability in the seasonal behaviour of NDVI. In such cases, seasonal drought indices that cumulate NDVI over a fixed time period (as in the IBLI and GIACIS-based approaches) may not be an effective approach for insuring pastoralists against drought. About 6% correspond to classes that were judged to be irrelevant in terms of forage production either because they are desert areas or densely forested zones situated at high altitudes or within conservation areas and therefore unusable for grazing purposes.

In comparison with the current IBLI design, GIACIS-based IBLI whereby pay-outs are first determined at the grid cell level before spatial aggregation, results in lower unit-level payments that take place more frequently. Although notable differences exist between methods in terms of both payment decision and indemnity amounts, the temporal correlation of the outcomes remains strong for the majority of the units. GIACIS-based IBLI has a slightly stronger correspondence to available livestock mortality data for selected areas, even if the indemnity series derived from all three approaches can only explain a small fraction of the mortality. Although only tested in a small part of the sample sites, the analysis also suggests that for GIACIS-based IBLI the correlation with livestock mortality becomes slightly stronger when contrasted against pay-outs calculated at a sub-unit level.

These initial results constitute an encouraging step forward towards the integration of two existing methods, which may provide a sound basis for an insurance product with lower basis risk. Further validation efforts remain however needed to better understand the relative performance or to suggest further adaptations to the insurance design.

LIST OF REFERENCES

Abburu, S., & Babu Golla, S. (2015). Satellite image classification methods and techniques: a review. *International Journal of Computer Applications*, *119*(8), 20–25. https://doi.org/10.5120/21088-3779

Barnett, B. J., Barrett, C. B., & Skees, J. R. (2008). Poverty Traps and Index-Based Risk Transfer Products. *World Development*, *36*(10), 1766–1785. https://doi.org/10.1016/j.worlddev.2007.10.016

Brown, M. E., Osgood, D. E., & Carriquiry, M. A. (2011). Science-based insurance. *Nature Geoscience*, *4*(4), 213–214. https://doi.org/10.1038/ngeo1117

Carter, M. R., de Janvry, A., Sadoulet, E., & Sarris, A. (2014). *Index-based weather insurance for developing countries: A review of evidence and a set of propositions for up-scaling*. FERDI. Retrieved September 23, 2016 from http://econpapers.repec.org/RePEc:fdi:wpaper:1799

Central Statistical Agency (CSA). (2007). *Population and Housing Census Report - 2007*. Addis Ababa. Retrieved October 2, 2016 from http://www.csa.gov.et/index.php/2013-02-20-14-51-51/2013-04-01-11-53-00/census-2007

Chantarat, S., Mude, A. G., Barrett, C. B., & Carter, M. R. (2013). Designing Index-Based Livestock Insurance for Managing Asset Risk in Northern Kenya. *Journal of Risk and Insurance*, *80*(1), 205–237. https://doi.org/10.1111/j.1539-6975.2012.01463.x

de Bie, C. A. J. M. (2016). *The 1st Micro-Insurance Product "Seasonal drought" - The risk modelling principles*.

de Bie, C. A. J. M., Khan, M. R., Smakhtin, V. U., Venus, V., Weir, M. J. C., & Smaling, E. M. A. (2011). Analysis of multi-temporal SPOT NDVI images for small-scale land-use mapping. *International Journal of Remote Sensing*, *32*(21), 6673–6693. https://doi.org/10.1080/01431161.2010.512939

de Leeuw, J., Vrieling, A., Shee, A., Atzberger, C., Hadgu, K. M., Biradar, C. M., … Turvey, C. (2014). The potential and uptake of remote sensing in insurance: A review. *Remote Sensing*. Multidisciplinary Digital Publishing Institute. https://doi.org/10.3390/rs61110888

Dror, I., Maheshwari, S., & Mude, A. (2014) Using satellite data to insure camels, cows, sheep and goats: IBLI and the development of the world's first insurance for African pastoralists. Retrieved October 4, 2016 from http://www.iblicasestudy.info

Egeru, A., Wasonga, O., Kyagulanyi, J., Majaliwa, G., MacOpiyo, L., & Mburu, J. (2014). Spatio-temporal dynamics of forage and land cover changes in Karamoja sub-region, Uganda. *Pastoralism: Research, Policy and Practice*, *4*(1), 6. https://doi.org/10.1186/2041-7136-4-6

ESRI. (2015). ArcGIS. Version 10.4.1

ESRI. (2016). World Imagery. Retrieved December 2, 2016 from http://services.arcgisonline.com/ArcGIS/rest/services/World_Imagery/MapServer

Exelis Visual Information Solutions Inc. (2015). IDL. Version 8.5.1

Famine Early Warning System Network (FEWSNET). (2016). Products | Early Warning and Environmental Monitoring Program. Retrieved August 17, 2016, from http://earlywarning.usgs.gov/fews/product/116

Food and Agriculture Organization of the United Nations (FAO) E-learning Centre. (2014). Remotely Sensed Information for Crop Monitoring and Food Security - Techniques and methods for arid and semi-arid areas. Retrieved August 13, 2016, from http://www.fao.org/elearning/#/elc/en/Course/FRS

Genovese, G., Vignolles, C., Nègre, T., & Passera, G. (2001). A methodology for a combined use of normalised difference vegetation index and CORINE land cover data for crop yield monitoring and forecasting. A case study on Spain. *Agronomie*, *21*(1), 91–111. https://doi.org/10.1051/agro:2001111

Gómez, C., White, J. C., & Wulder, M. A. (2016). Optical remotely sensed time series data for land cover classification: A review. *ISPRS Journal of Photogrammetry and Remote Sensing*. https://doi.org/10.1016/j.isprsjprs.2016.03.008

Gommes, R., & Kayitakire, F. (Eds.). (2013). The challenges of index-based insurance for food security in developing countries (pp. 1–284). Luxembourg: European Union. https://doi.org/doi: 10.2788/713

Google Inc. (2017). Google Earth. Version 7.1.8.3036

Hexagon Geospatial. (2016). Erdas Imagine.Version 2016

Hexagon Geospatial. (2017). Documentation Portal. Retrieved February 12, 2017, from https://hexagongeospatial.fluidtopics.net/search#!search;filters=prodname%255C2%2522ERDAS+IMAGINE%2522

Homewood, K. M., Trench, P., & Brockington, D. (2012). Pastoralist livelihoods and wildlife revenues in East Africa: a case for coexistence? *Pastoralism: Research, Policy and Practice*, *2*(1), 19. https://doi.org/10.1186/2041-7136-2-19

Ikegami, M., & Sheahan, M. (2016). Index Based Livestock Insurance (IBLI) Marsabit Household Survey Codebook. Retrieved November 2, 2016 from http://data.ilri.org/portal/dataset/ibli-marsabit-r1/resource/204a5984-ebf9-478a-82bc-729ccbb53f78/request

Inoue, T., Nagai, S., Kobayashi, H., & Koizumi, H. (2015). Utilization of ground-based digital photography for the evaluation of seasonal changes in the aboveground green biomass and foliage phenology in a grassland ecosystem. *Ecological Informatics*, *25*, 1–9. https://doi.org/10.1016/j.ecoinf.2014.09.013

International Livestock Research Institute (ILRI). (2011). *Code book for IBLI Herd Mortality FGDs*.

International Livestock Research Institute (ILRI). (2015). *Internal report on mortality modelling*.

International Livestock Research Institute (ILRI). (2016). Index-Based Livestock Insurance. Retrieved August 12, 2016, from https://ibli.ilri.org/

Jacobson, A., Dhanota, J., Godfrey, J., Jacobson, H., Rossman, Z., Stanish, A., … Riggio, J. (2015). A novel approach to mapping land conversion using Google Earth with an application to East Africa. *Environmental Modelling & Software*, *72*, 1–9. https://doi.org/10.1016/j.envsoft.2015.06.011

Johnson, N., & Wambile, A. (Eds). (2011). *The Impacts of the Arid Lands Resource Management Project (ALRMPII) on Livelihoods and Vulnerability in the Arid and Semi-Arid Lands of Kenya. ILRI Research Report 25*. Nairoby. Retrieved December 2, 2016 from https://cgspace.cgiar.org/bitstream/handle/10568/3416/9291462578_content.pdf?sequence=1

Kenya National Bureau of Statistics (KNBS). (2009). *Kenya Population and Housing Census*. Nairobi. Retrieved November 16, 2016 from http://www.knbs.or.ke/index.php?option=com_content&view=featured&Itemid=435

Louhaichi, M., Borman, M. M., & Johnson, D. E. (2001). Spatially Located Platform and Aerial Photography for Documentation of Grazing Impacts on Wheat. *Geocarto International Geocarto International Centre, G.P.O. Box*, *16*(4122).

Maselli, F., Romanelli, S., Bottai, L., & Zipoli, G. (2003). Use of NOAA-AVHRR NDVI images for the estimation of dynamic fire risk in Mediterranean areas. *Remote Sensing of Environment*, *86*(2), 187–197. https://doi.org/10.1016/S0034-4257(03)00099-3

Meroni, M., Verstraete, M. M., Rembold, F., Urbano, F., & Kayitakire, F. (2014). A phenology-based method to derive biomass production anomalies for food security monitoring in the Horn of Africa. *International Journal of Remote Sensing*, *35*(7), 2472–2492. https://doi.org/10.1080/01431161.2014.883090

Miranda, M. J., & Farrin, K. (2012). Index Insurance for Developing Countries. *Applied Economic Perspectives and Policy*, *34*(3), 391–427. https://doi.org/10.1093/aepp/pps031

Mount, D., Netanyahu, N., & Le Moigne, J. (2007). A fast implementation of the ISODATA clustering algorithm. *IJCGA World Scientific Publishing Company International Journal of Computational Geometry & Applications Proceedings of the IEEE International Geoscience and Remote Sensing Symposium IJCGA*, *17*(171), 71–103.

Mude, A. G., Barrett, C. B., McPeak, J. G., Kaitho, R., & Kristjanson, P. (2009a). Empirical forecasting of slow-onset disasters for improved emergency response: An application to Kenya's arid north. *Food Policy*, *34*(4), 329–339. https://doi.org/10.1016/j.foodpol.2009.05.003

Mude, A. G., Chantarat, S., Barrett, C. B., Carter, M. R., Ikegami, M., & McPeak, J. G. (2010). Insuring Against Drought-Related Livestock Mortality: Piloting Index Based Livestock Insurance in Northern Kenya. *SSRN Electronic Journal*. https://doi.org/10.2139/ssrn.1844745

Netherlands Space Office. (2016). Geodata for Innovative Agricultural Credit Insurance Schemes (GIACIS) | g4aw.spaceoffice.nl. Retrieved August 14, 2016, from http://g4aw.spaceoffice.nl/en/Projects/G4AW-projects/64/Geodata-for-Innovative-Agricultural-Credit-Insurance-Schemes-GIACIS.html

Nkedianye, D., de Leeuw, J., Ogutu, J. O., Said, M. Y., Saidimu, T. L., Kifugo, S. C., … Reid, R. S. (2011). Mobility and livestock mortality in communally used pastoral areas: the impact of the 2005-2006 drought on livestock mortality in Maasailand. *Pastoralism: Research, Policy and Practice*, *1*(1), 17. https://doi.org/10.1186/2041-7136-1-17

Pettorelli, N. (2013). *The normalized difference vegetation index* (1st ed.). Oxford: Oxford University Press.

Pettorelli, N., Vik, J. O., Mysterud, A., Gaillard, J.-M., Tucker, C. J., & Stenseth, N. C. (2005). Using the satellite-derived NDVI to assess ecological responses to environmental change. *Trends in Ecology & Evolution*, *20*(9), 503–510. https://doi.org/10.1016/j.tree.2005.05.011

Rojas, O., Vrieling, A., & Rembold, F. (2011). Assessing drought probability for agricultural areas in Africa with coarse resolution remote sensing imagery. *Remote Sensing of Environment*, *115*(2), 343–352. https://doi.org/10.1016/j.rse.2010.09.006

Roumiguié, A., Jacquin, A., Sigel, G., Poilvé, H., Lepoivre, B., & Hagolle, O. (2015). Development of an index-based insurance product: validation of a forage production index derived from medium spatial resolution fCover time series. *GIScience & Remote Sensing*, *52*(1), 94–113. https://doi.org/10.1080/15481603.2014.993010

Rufino, M. C., Thornton, P. K., Ng'ang'a, S. K., Mutie, I., Jones, P. G., van Wijk, M. T., & Herrero, M. (2013). Transitions in agro-pastoralist systems of East Africa: Impacts on food security and poverty. *Agriculture, Ecosystems and Environment*, *179*, 215–230. https://doi.org/10.1016/j.agee.2013.08.019

Scargle, J. D. (1982). Studies in astronomical time series analysis. II - Statistical aspects of spectral analysis of unevenly spaced data. *The Astrophysical Journal*, *263*, 835–853. https://doi.org/10.1086/160554

Singh, R. P., Roy, S., & Kogan, F. (2003). Vegetation and temperature condition indices from NOAA AVHRR data for drought monitoring over India. *International Journal of Remote Sensing*, *24*(22), 4393–4402. https://doi.org/10.1080/0143116031000084323

Swain, P. H., & Davis, S. M. (1978). *Remote Sensing: The Quantitative Approach. New York* (Vol. 1). Retrieved January 15, 2017 from http://img.kb.dk/tidsskriftdk/pdf/gto/gto_0081-PDF/gto_0081_72217.pdf

Swets, D. L., Reed, B. C., Rowland, J. D., & Marko, S. E. (1999). A Weighted Least-Squares Approach to Temporal NDVI Smoothing. In *Proceedings of the 1999 ASPRS Annual Conference* (pp. 526–536).

The Presidency of the Republic of Kenya. (2015). *DRAFT: National Policy for the Sustainable Development of Northern Kenya and other Arid Lands "Unlocking Our Full Potential for Realization of the Kenya Vision 2030."* Nairobi. Retrieved August 4, 2016 from http://www.devolutionplanning.go.ke/

Tierney, J. E., Ummenhofer, C. C., & DeMenocal, P. B. (2015). Past and future rainfall in the Horn of Africa. *Science Advances*, *1*(9), e1500682–e1500682. https://doi.org/10.1126/sciadv.1500682

Turvey, C. G., & Mclaurin, M. K. (2012). Applicability of the Normalized Difference Vegetation Index (NDVI) in Index-Based Crop Insurance Design. *Weather, Climate, and Society*, *4*(4), 271–284. https://doi.org/10.1175/WCAS-D-11-00059.1

U.S. Geological Survey (2015). eMODIS (EROS Moderate Resolution Imaging Spectroradiometer). Retrieved August 17, 2016, from https://lta.cr.usgs.gov/emodis

Udelhoven, T., van der Linden, S., Waske, B., Stellmes, M., & Hoffmann, L. (2009). Hypertemporal Classification of Large Areas Using Decision Fusion. *IEEE Geoscience and Remote Sensing Letters*, *6*(3), 592–596. https://doi.org/10.1109/LGRS.2009.2021960

Vrieling, A., de Beurs, K. M., & Brown, M. E. (2011). Variability of African farming systems from phenological analysis of NDVI time series. *Climatic Change*, *109*(3–4), 455–477. https://doi.org/10.1007/s10584-011-0049-1

Vrieling, A., Meroni, M., & Mude, A. (2015). Determining optimal seasonal integration times of NDVI series for index-based livestock insurance in East Africa. In *2015 IEEE International Geoscience and Remote Sensing Symposium (IGARSS)* (pp. 169–172). IEEE. https://doi.org/10.1109/IGARSS.2015.7325726

Vrieling, A., Meroni, M., Mude, A. G., Chantarat, S., Ummenhofer, C. C., & Bie, C. A. J. M. de. (2016). Early assessment of seasonal forage availability for mitigating the impact of drought on East African pastoralists. Remote Sensing of Environment, 174, 44–55. https://doi.org/10.1016/j.rse.2015.12.003

Vrieling, A., Meroni, M., Shee, A., Mude, A. G., Woodard, J., de Bie, C. A. J. M. (Kees), & Rembold, F. (2014). Historical extension of operational NDVI products for livestock insurance in Kenya. *International Journal of Applied Earth Observation and Geoinformation*, *28*, 238–251. https://doi.org/10.1016/j.jag.2013.12.010

Wang, J., Rich, P. M., & Price, K. P. (2003). Temporal responses of NDVI to precipitation and temperature in the central Great Plains, USA. *International Journal of Remote Sensing*, *24*(11), 2345–2364. https://doi.org/10.1080/01431160210154812

Woodard, J., Shee, A., & Mude, A. (2013). A Spatial Econometric Approach to Scalable Index Insurance Design against Drought Related Livestock Mortality in Kenya. In *The 9th International Microinsurance Conference*. Jakarta. Retrieved from http://www.munichre-foundation.org/dms/MRS/Documents/Microinsurance/2013_IMC/S8-IMC2013-Presentation-Shee/S8 IMC2013 Presentation Shee.pdf

Yang, W., Seager, R., Cane, M. A., & Lyon, B. (2014). The East African long rains in observations and models. *Journal of Climate*, *27*(19), 7185–7202. https://doi.org/10.1175/JCLI-D-13-00447.1

7. APPENDICES

Appendix I – NDMA

Complete set of timelines integrating livestock mortality, forage availability and indemnities as calculated by the three methods

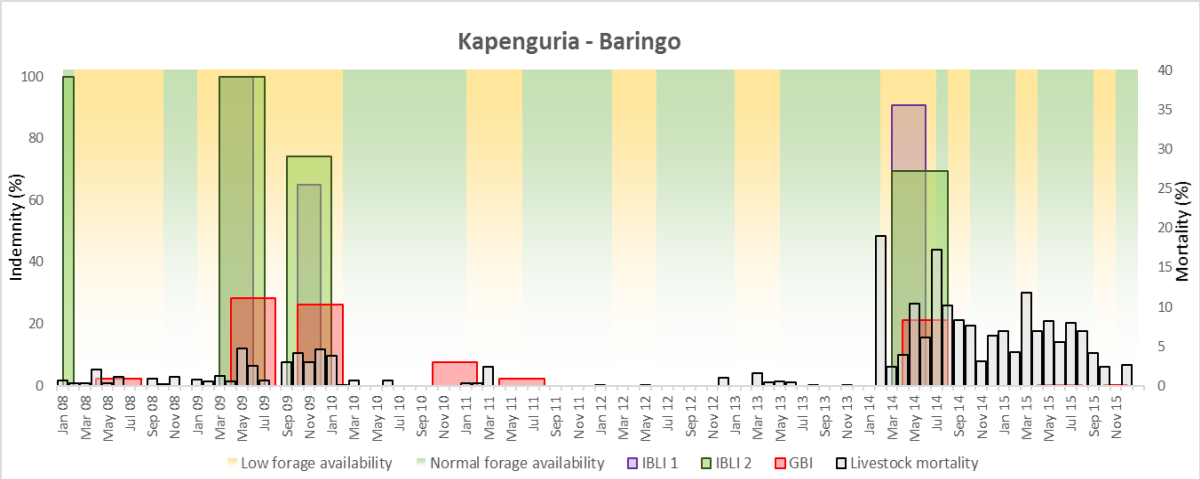

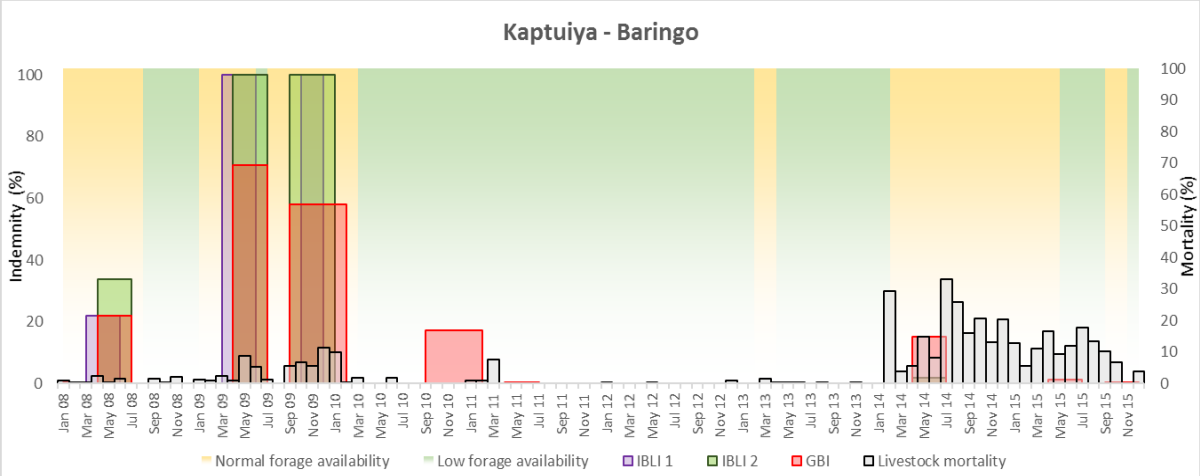

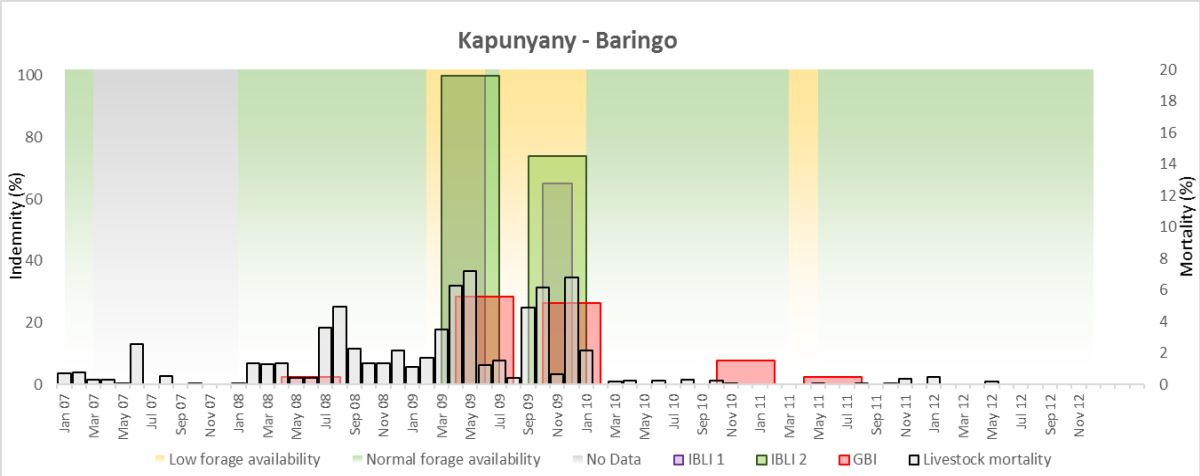

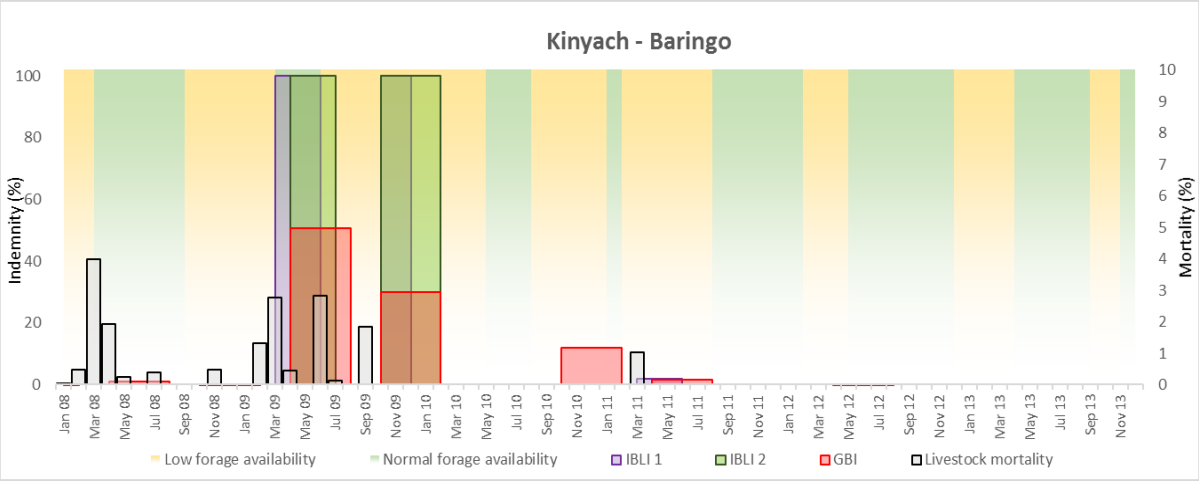
Kinyach - Baringo
Indemnity (%)
Mortality (%)
Low forage availability
Normal forage availability
IBLI 1
IBLI 2
GBI
Livestock mortality

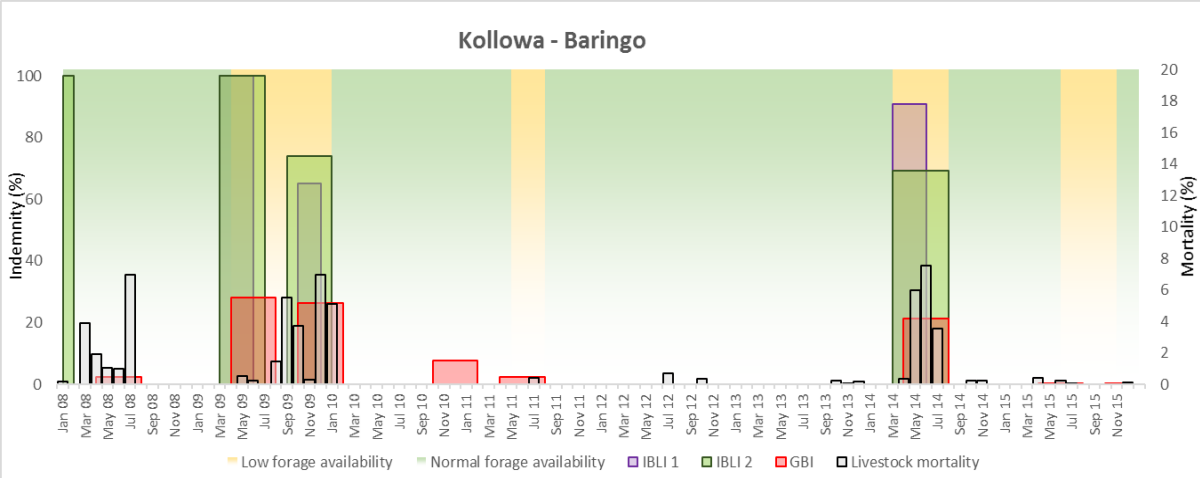
Kollowa - Baringo
Indemnity (%)
Mortality (%)
Low forage availability
Normal forage availability
IBLI 1
IBLI 2
GBI
Livestock mortality

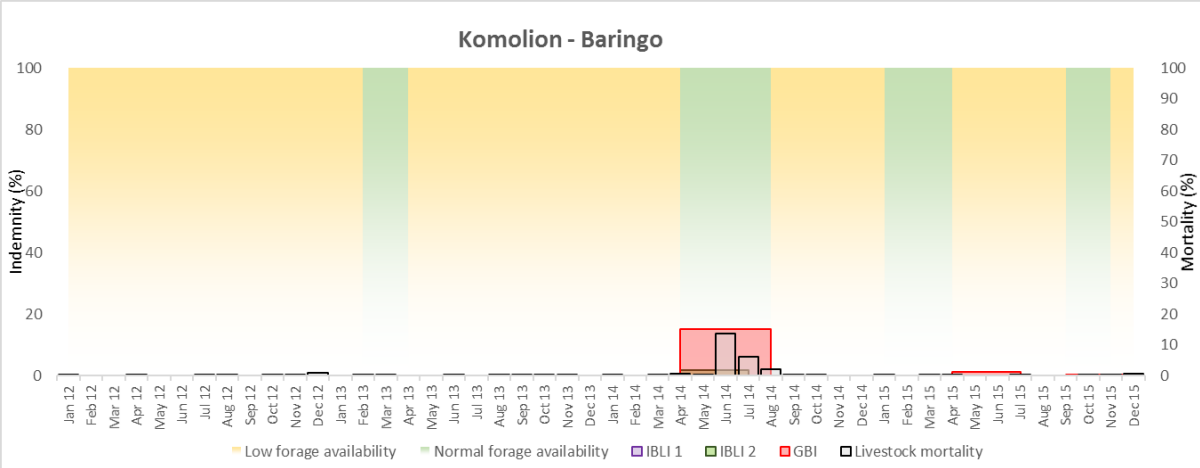
Komolion - Baringo
Indemnity (%)
Mortality (%)
Low forage availability
Normal forage availability
IBLI 1
IBLI 2
GBI
Livestock mortality

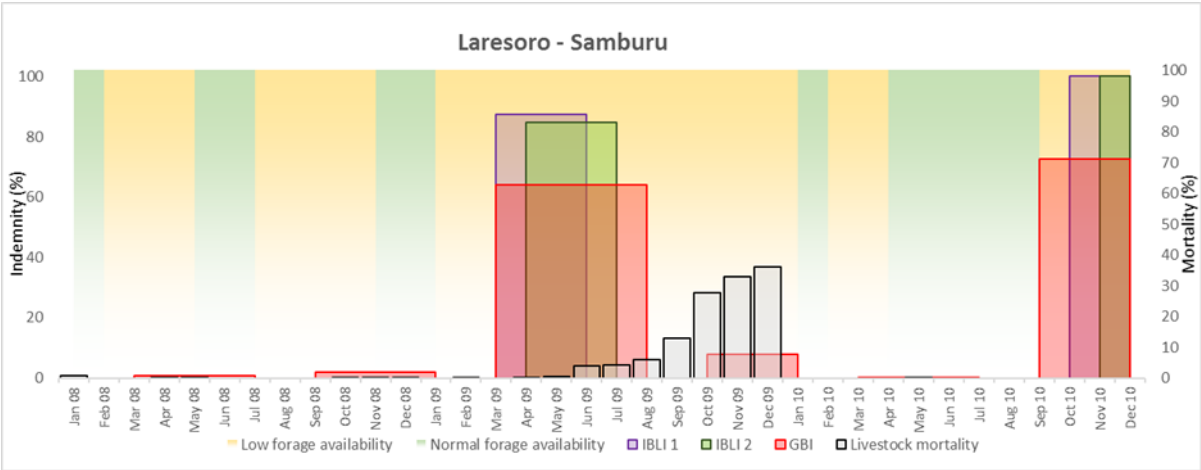
Laresoro - Samburu
Indemnity (%)
Mortality (%)
Low forage availability
Normal forage availability
IBLI 1
IBLI 2
GBI
Livestock mortality

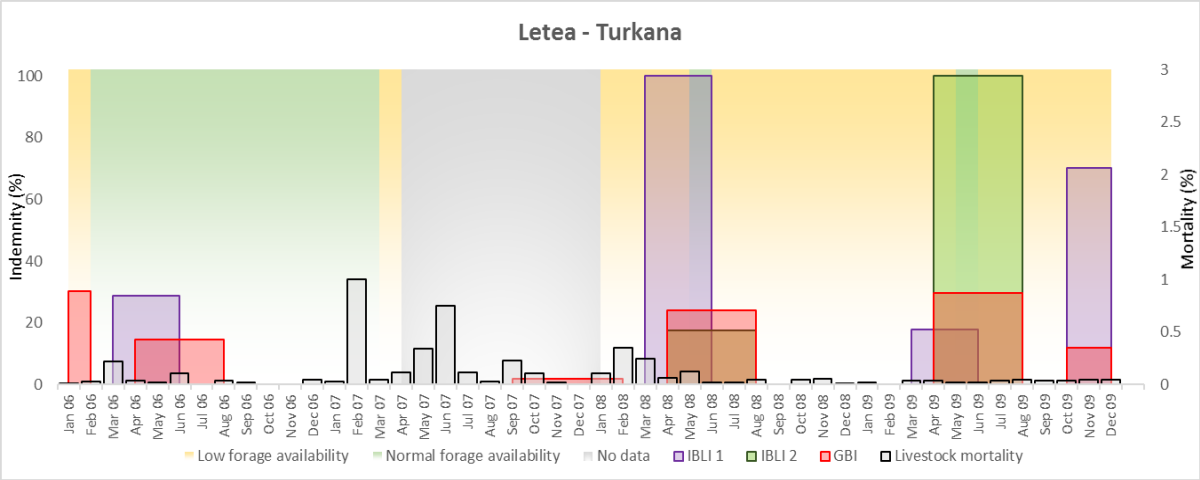
Letea - Turkana
Indemnity (%)
Mortality (%)
Low forage availability
Normal forage availability
No data
IBLI 1
IBLI 2
GBI
Livestock mortality

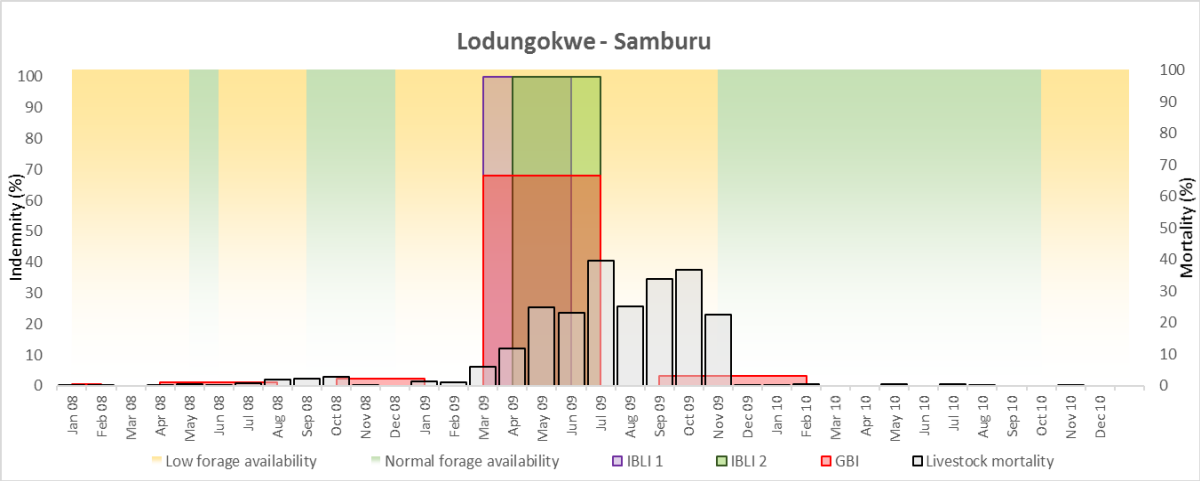
Lodungokwe - Samburu
Indemnity (%)
Mortality (%)
Low forage availability
Normal forage availability
IBLI 1
IBLI 2
GBI
Livestock mortality

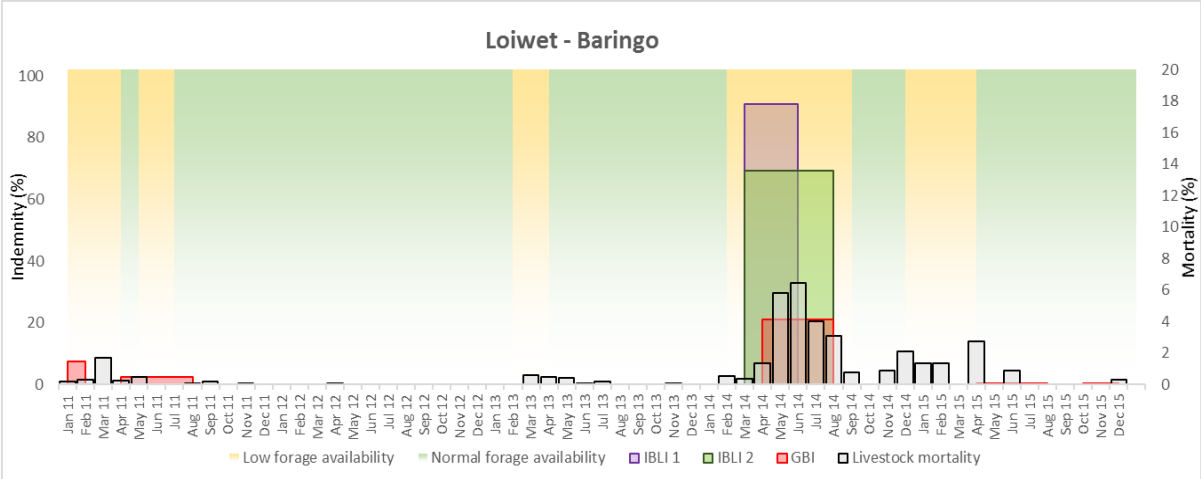
Loiwet - Baringo
Indemnity (%)
Mortality (%)
Low forage availability
Normal forage availability
IBLI 1
IBLI 2
GBI
Livestock mortality

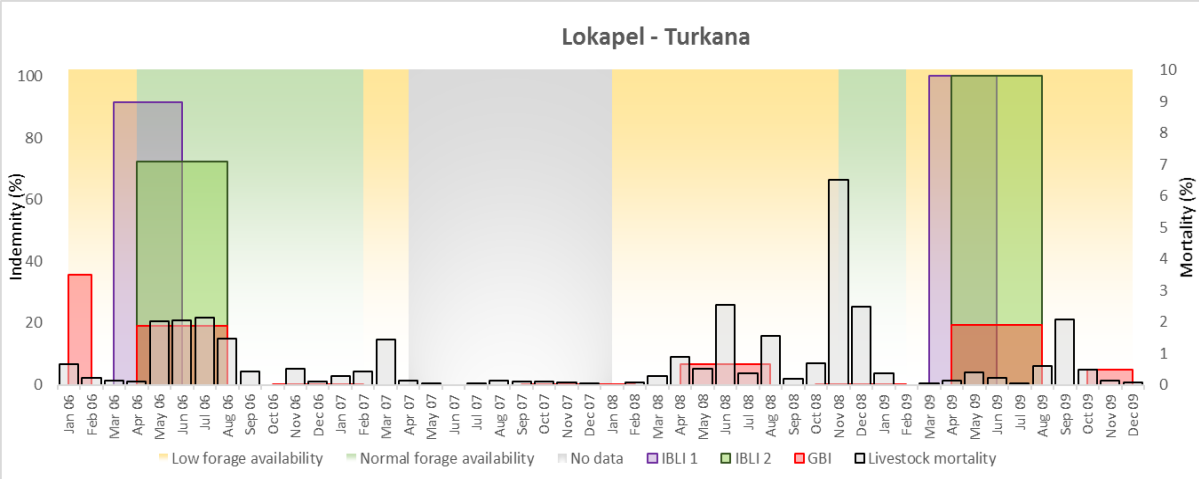
Lokapel - Turkana
Indemnity (%)
Mortality (%)
Low forage availability
Normal forage availability
No data
IBLI 1
IBLI 2
GBI
Livestock mortality

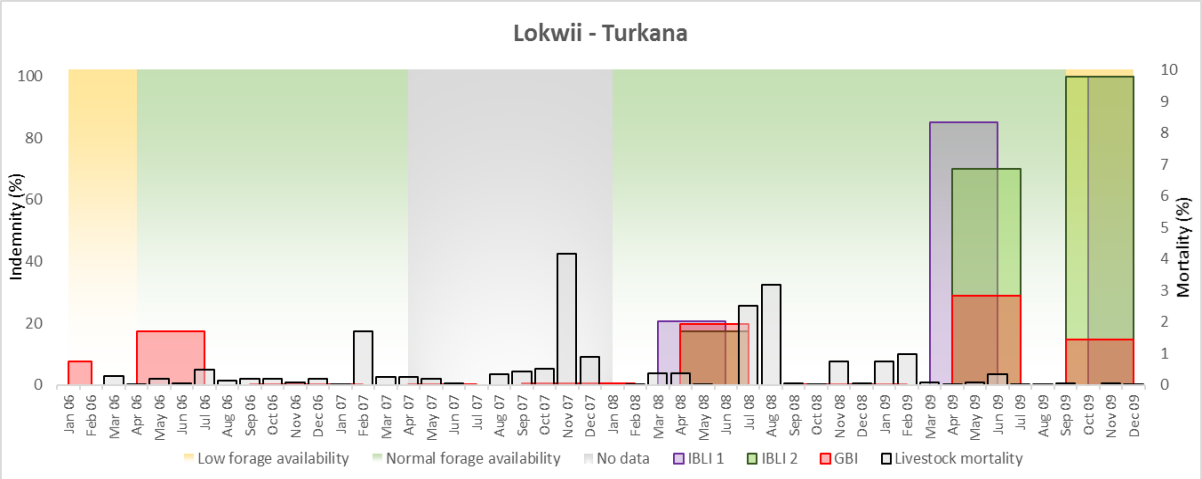
Lokwii - Turkana
Indemnity (%)
Mortality (%)
Low forage availability
Normal forage availability
No data
IBLI 1
IBLI 2
GBI
Livestock mortality

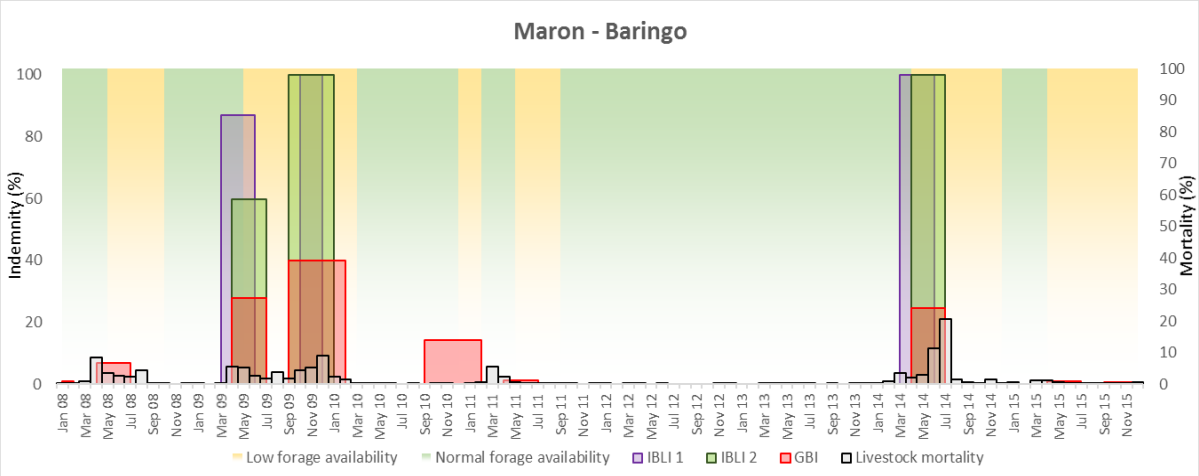
Maron - Baringo
Indemnity (%)
Mortality (%)
Low forage availability
Normal forage availability
IBLI 1
IBLI 2
GBI
Livestock mortality

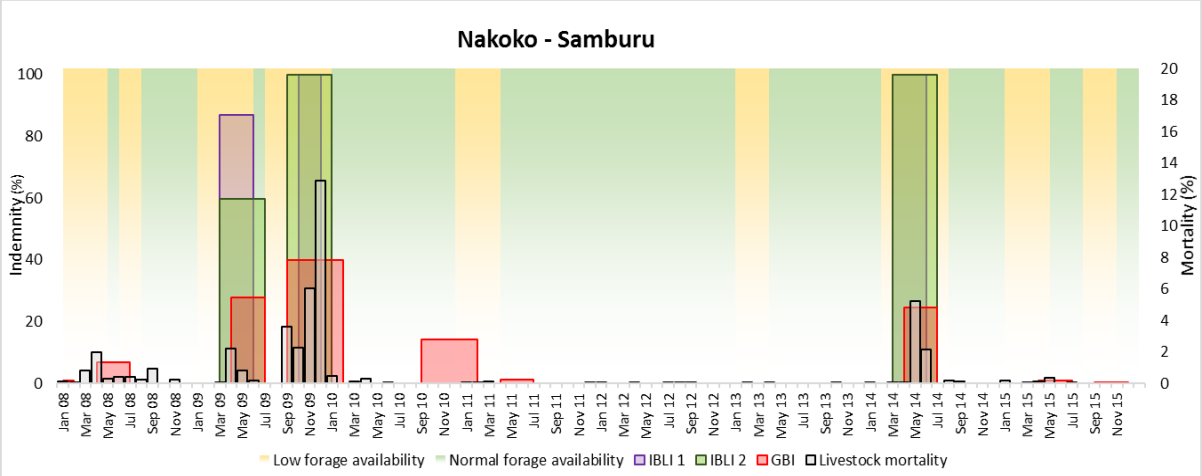
Nakoko - Samburu
Indemnity (%)
Mortality (%)
Low forage availability
Normal forage availability
IBLI 1
IBLI 2
GBI
Livestock mortality

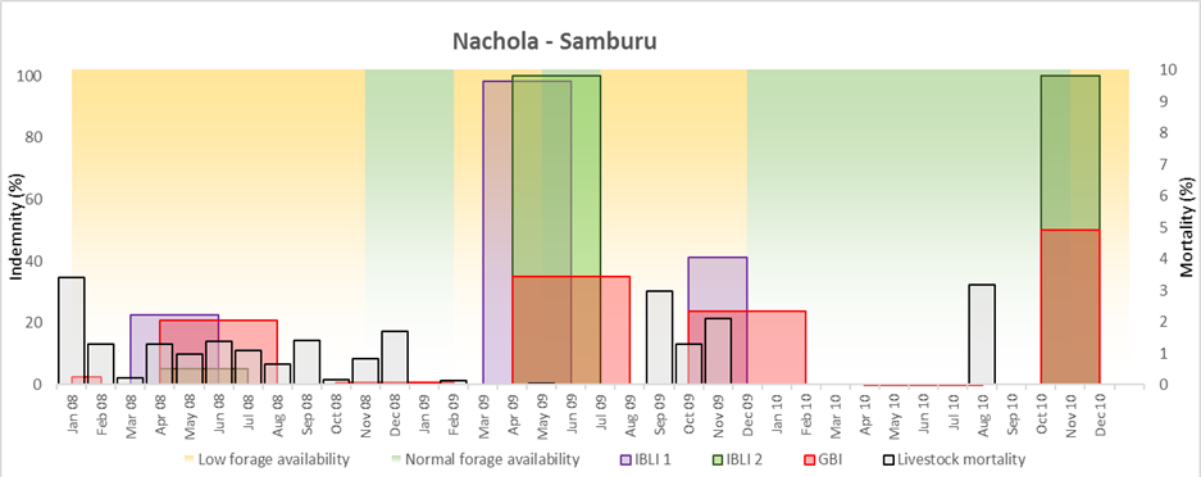
Nachola - Samburu
Indemnity (%)
Mortality (%)
Low forage availability
Normal forage availability
IBLI 1
IBLI 2
GBI
Livestock mortality

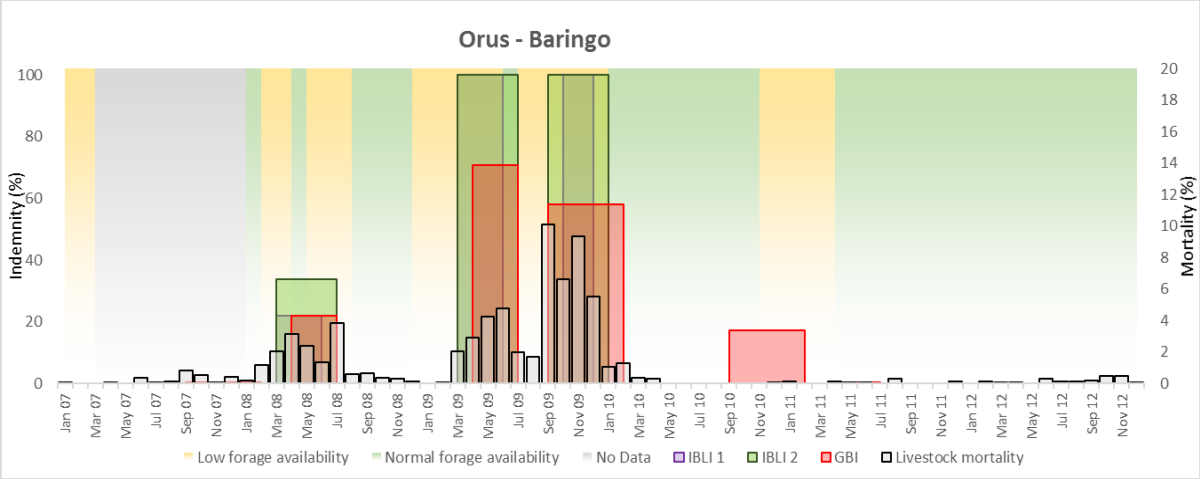
Orus - Baringo
Indemnity (%)
Mortality (%)
Low forage availability
Normal forage availability
No Data
IBLI 1
IBLI 2
GBI
Livestock mortality

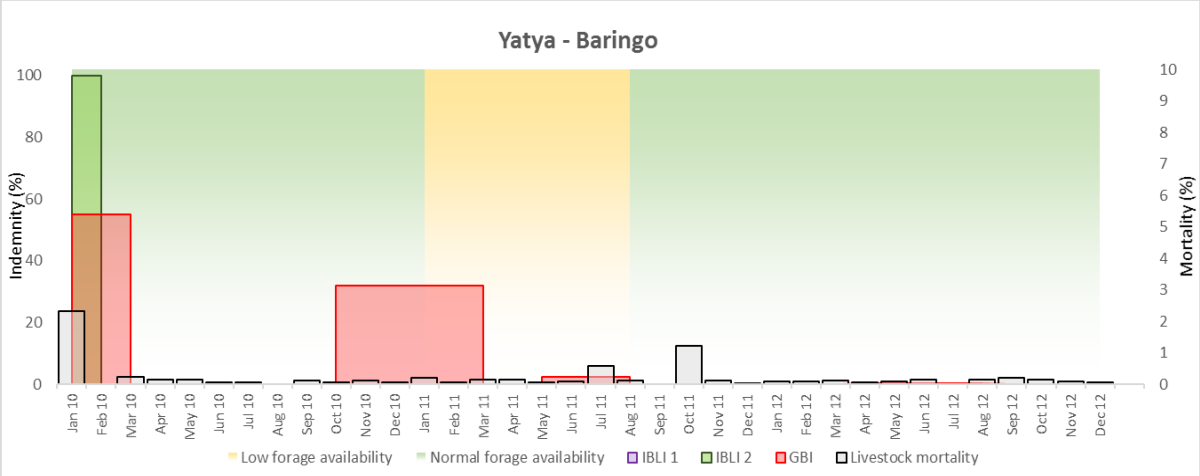
Yatya - Baringo
Indemnity (%)
Mortality (%)
Low forage availability
Normal forage availability
IBLI 1
IBLI 2
GBI
Livestock mortality

Appendix II – IBLI Marsabit Household Survey

Map showing the location of the sample sites and complete set of corresponding timelines integrating livestock mortality, forage availability and indemnities as calculated by the three methods

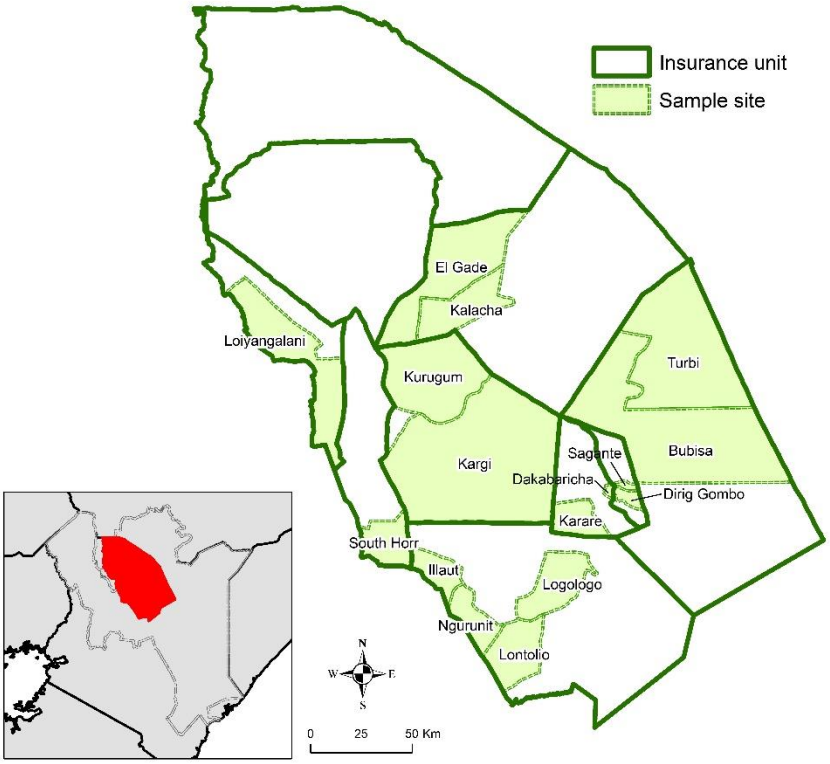

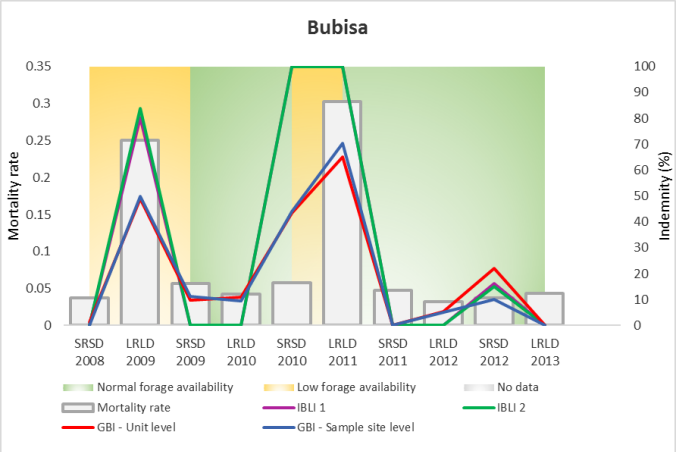

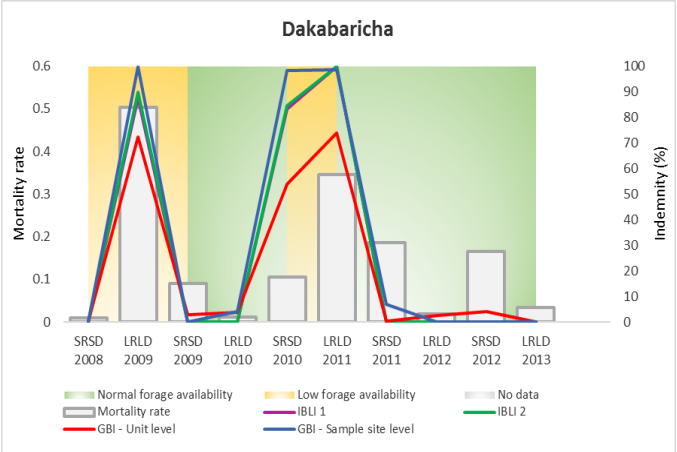

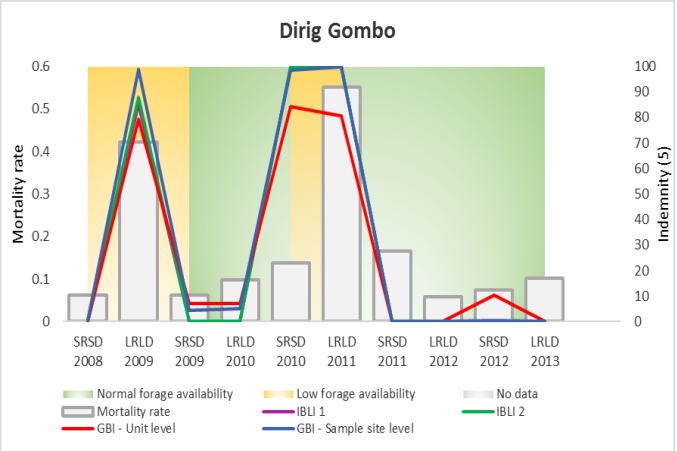

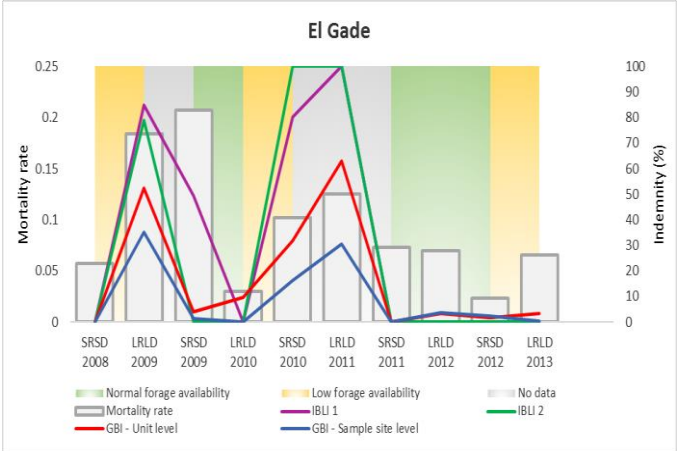

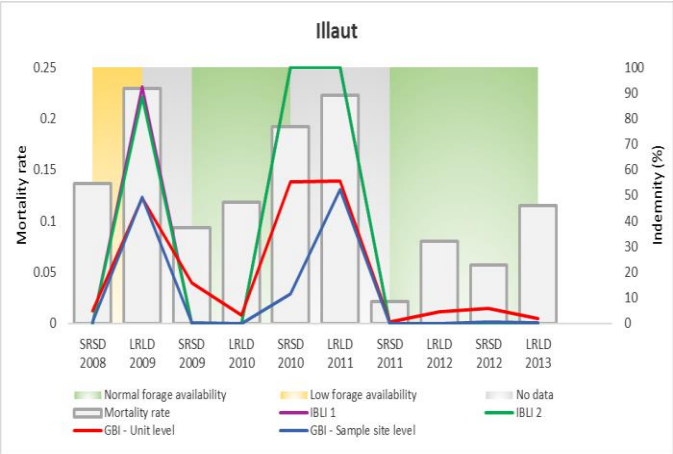
Illaut
Mortality rate
Indemnity (%)
SRSD 2008
LRLD 2009
SRSD 2009
LRLD 2010
SRSD 2010
LRLD 2011
SRSD 2011
LRLD 2012
SRSD 2012
LRLD 2013
Normal forage availability
Low forage availability
No data
Mortality rate
IBLI 1
IBLI 2
GBI - Unit level
GBI - Sample site level

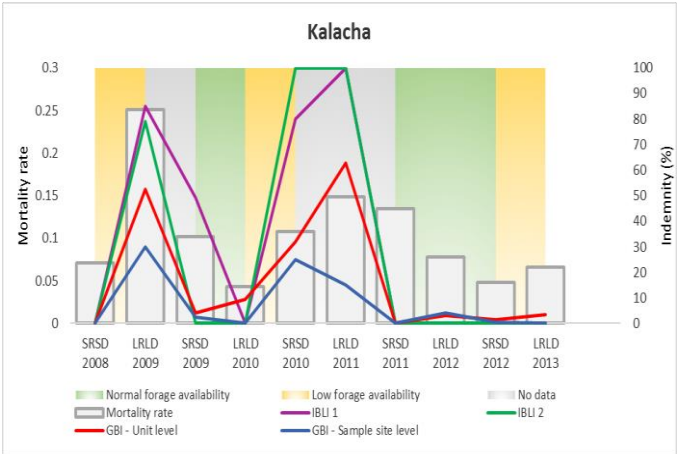
Kalacha
Mortality rate
Indemnity (%)
SRSD 2008
LRLD 2009
SRSD 2009
LRLD 2010
SRSD 2010
LRLD 2011
SRSD 2011
LRLD 2012
SRSD 2012
LRLD 2013
Normal forage availability
Low forage availability
No data
Mortality rate
IBLI 1
IBLI 2
GBI - Unit level
GBI - Sample site level

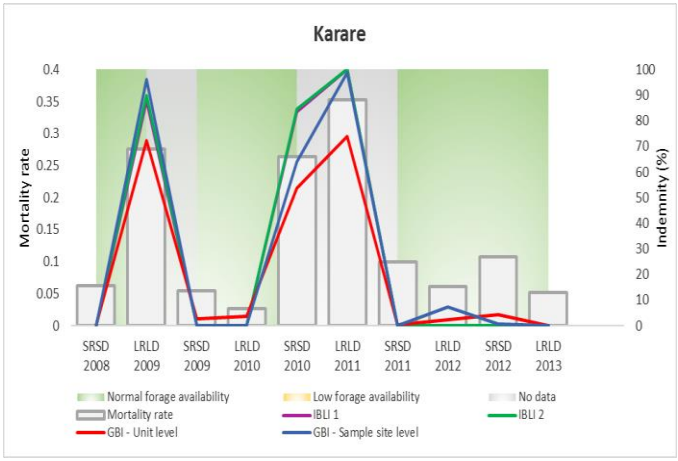
Karare
Mortality rate
Indemnity (%)
SRSD 2008
LRLD 2009
SRSD 2009
LRLD 2010
SRSD 2010
LRLD 2011
SRSD 2011
LRLD 2012
SRSD 2012
LRLD 2013
Normal forage availability
Low forage availability
No data
Mortality rate
IBLI 1
IBLI 2
GBI - Unit level
GBI - Sample site level

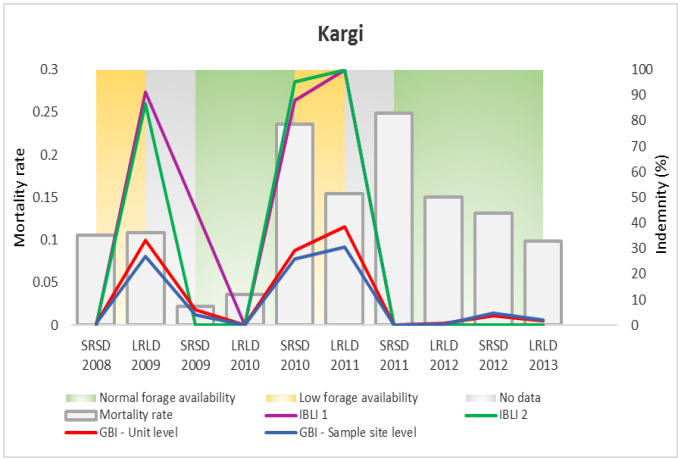
Kargi
Mortality rate
Indemnity (%)
SRSD 2008
LRLD 2009
SRSD 2009
LRLD 2010
SRSD 2010
LRLD 2011
SRSD 2011
LRLD 2012
SRSD 2012
LRLD 2013
Normal forage availability
Low forage availability
No data
Mortality rate
IBLI 1
IBLI 2
GBI - Unit level
GBI - Sample site level

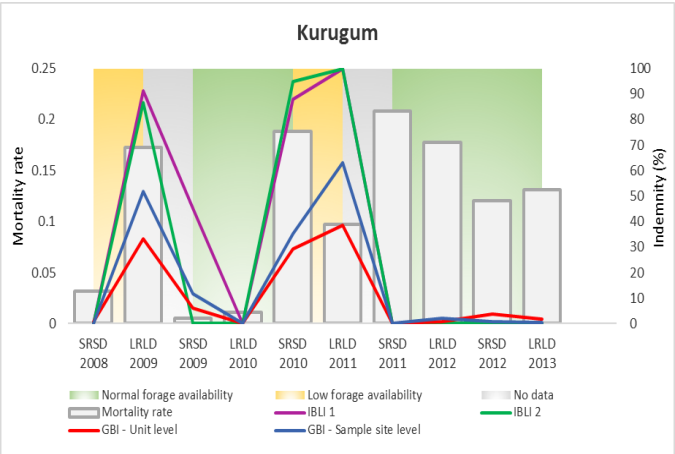
Kurugum
Mortality rate
Indemnity (%)
SRSD 2008
LRLD 2009
SRSD 2009
LRLD 2010
SRSD 2010
LRLD 2011
SRSD 2011
LRLD 2012
SRSD 2012
LRLD 2013
Normal forage availability
Low forage availability
No data
Mortality rate
IBLI 1
IBLI 2
GBI - Unit level
GBI - Sample site level

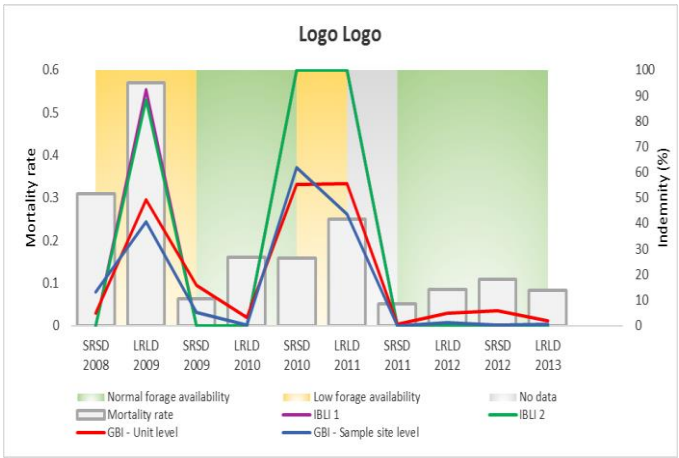
Logo Logo
Mortality rate
Indemnity (%)
SRSD 2008
LRLD 2009
SRSD 2009
LRLD 2010
SRSD 2010
LRLD 2011
SRSD 2011
LRLD 2012
SRSD 2012
LRLD 2013
Normal forage availability
Low forage availability
No data
Mortality rate
IBLI 1
IBLI 2
GBI - Unit level
GBI - Sample site level

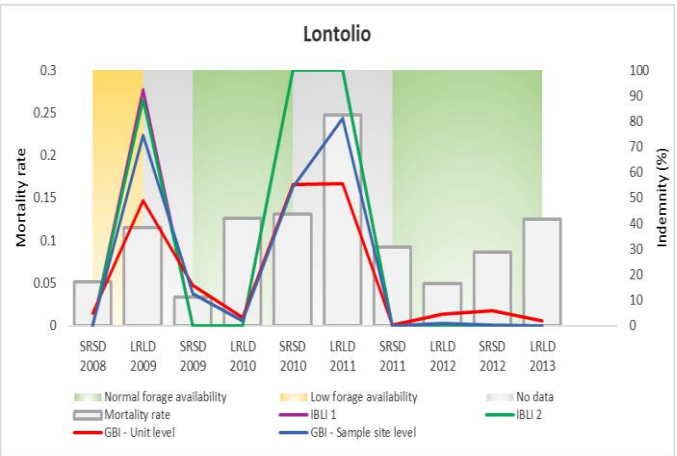
Lontolio
Mortality rate
Indemnity (%)
SRSD 2008
LRLD 2009
SRSD 2009
LRLD 2010
SRSD 2010
LRLD 2011
SRSD 2011
LRLD 2012
SRSD 2012
LRLD 2013
Normal forage availability
Low forage availability
No data
Mortality rate
IBLI 1
IBLI 2
GBI - Unit level
GBI - Sample site level

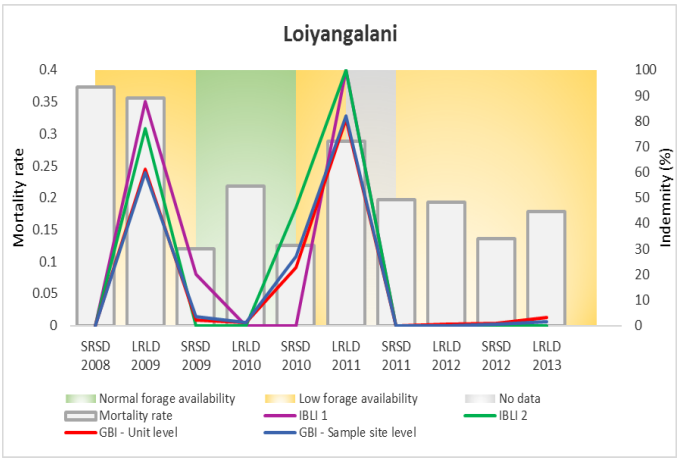
Loiyangalani
Mortality rate
Indemnity (%)
SRSD 2008
LRLD 2009
SRSD 2009
LRLD 2010
SRSD 2010
LRLD 2011
SRSD 2011
LRLD 2012
SRSD 2012
LRLD 2013
Normal forage availability
Low forage availability
No data
Mortality rate
IBLI 1
IBLI 2
GBI - Unit level
GBI - Sample site level

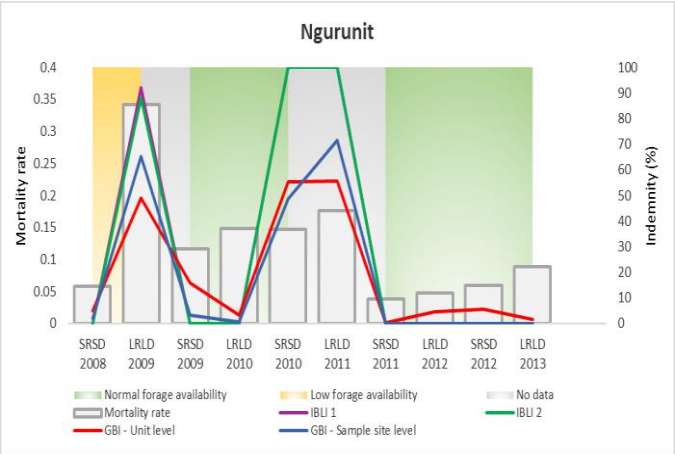
Ngurunit
Mortality rate
Indemnity (%)
SRSD 2008
LRLD 2009
SRSD 2009
LRLD 2010
SRSD 2010
LRLD 2011
SRSD 2011
LRLD 2012
SRSD 2012
LRLD 2013
Normal forage availability
Low forage availability
No data
Mortality rate
IBLI 1
IBLI 2
GBI - Unit level
GBI - Sample site level

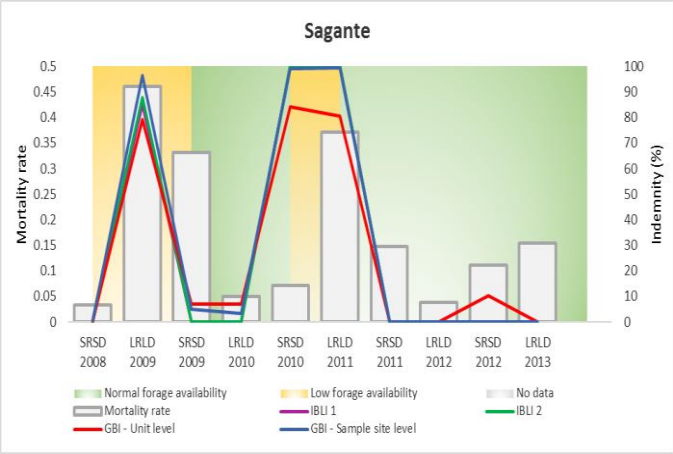
Sagante
Mortality rate
Indemnity (%)
SRSD 2008
LRLD 2009
SRSD 2009
LRLD 2010
SRSD 2010
LRLD 2011
SRSD 2011
LRLD 2012
SRSD 2012
LRLD 2013
Normal forage availability
Low forage availability
No data
Mortality rate
IBLI 1
IBLI 2
GBI - Unit level
GBI - Sample site level

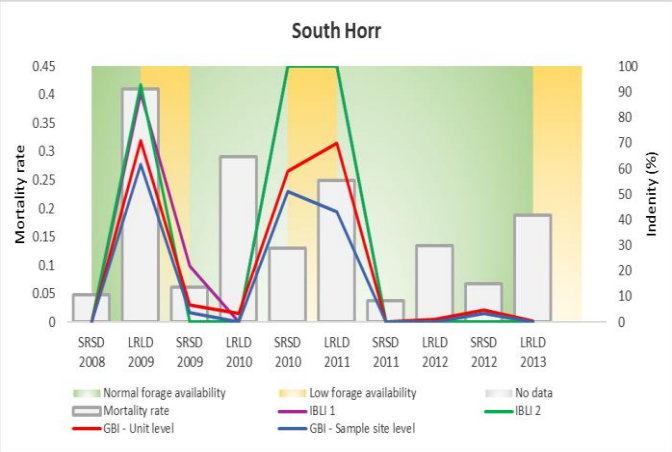
South Horr
Mortality rate
Indemnity (%)
SRSD 2008
LRLD 2009
SRSD 2009
LRLD 2010
SRSD 2010
LRLD 2011
SRSD 2011
LRLD 2012
SRSD 2012
LRLD 2013
Normal forage availability
Low forage availability
No data
Mortality rate
IBLI 1
IBLI 2
GBI - Unit level
GBI - Sample site level

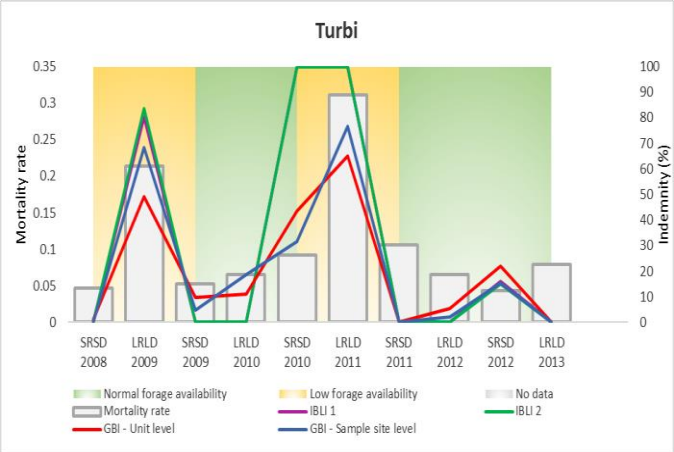
Turbi
Mortality rate
Indemnity (%)
SRSD 2008
LRLD 2009
SRSD 2009
LRLD 2010
SRSD 2010
LRLD 2011
SRSD 2011
LRLD 2012
SRSD 2012
LRLD 2013
Normal forage availability
Low forage availability
No data
Mortality rate
IBLI 1
IBLI 2
GBI - Unit level
GBI - Sample site level

Appendix III – Borana recall exercise

Complete set of timelines integrating livestock mortality rate and indemnities as calculated by the three methods

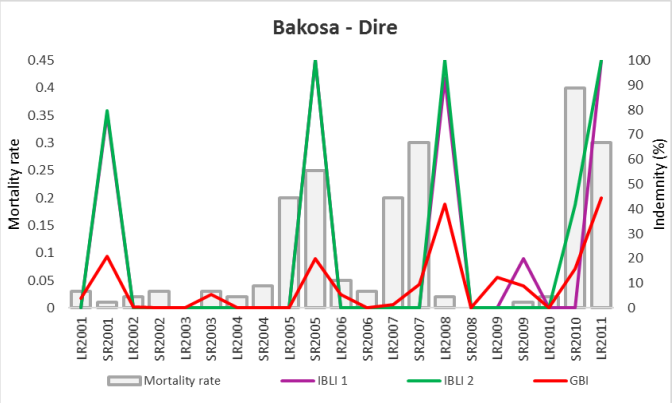

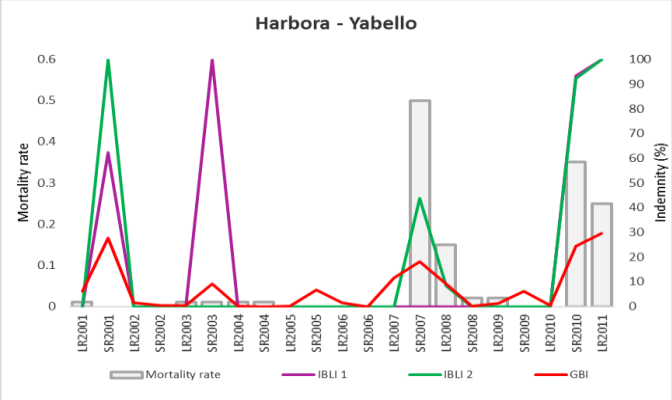

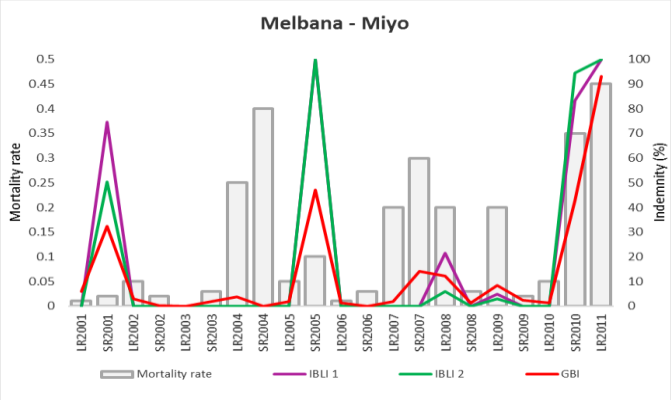

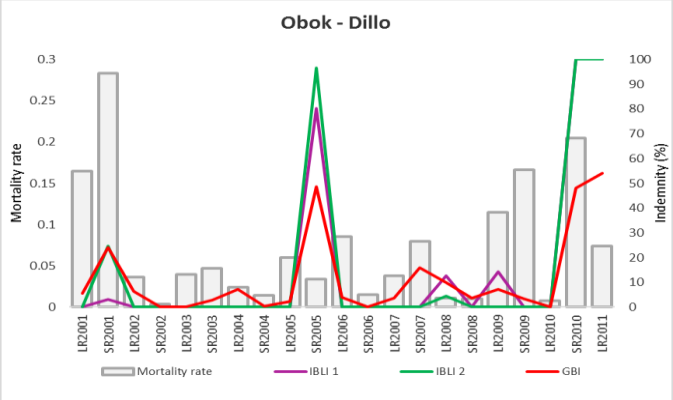

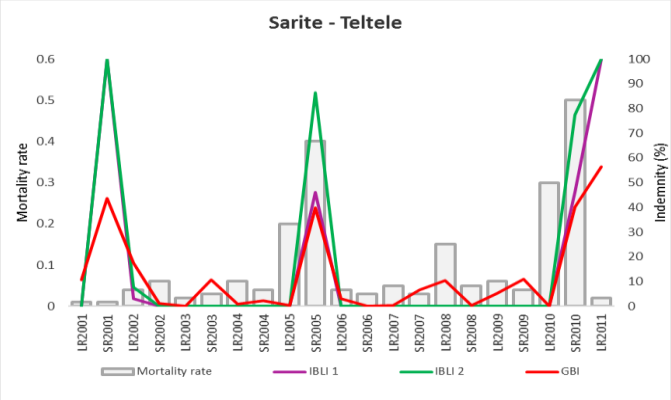

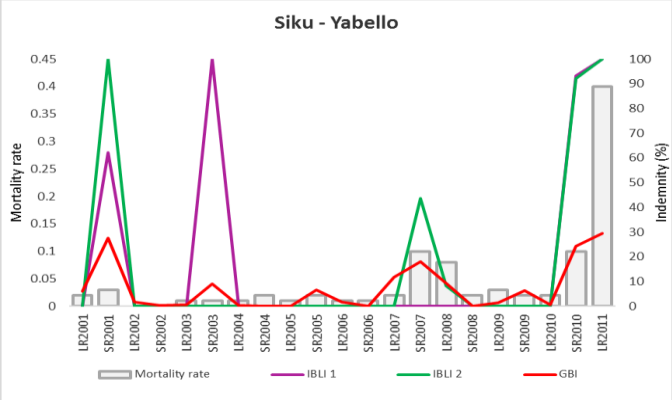

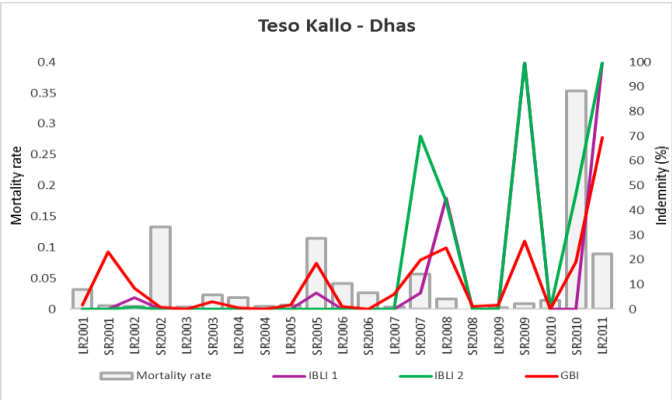

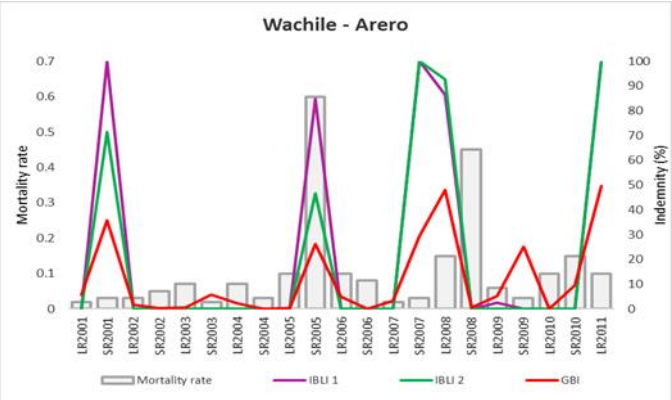

Appendix IV – Indemnities for Borana as calculated by GIACIS and GBI

Indemnities as calculated by GIACIS and GBI for Borana, Ethiopia for the long rain seasons 2002 - 2012[13]

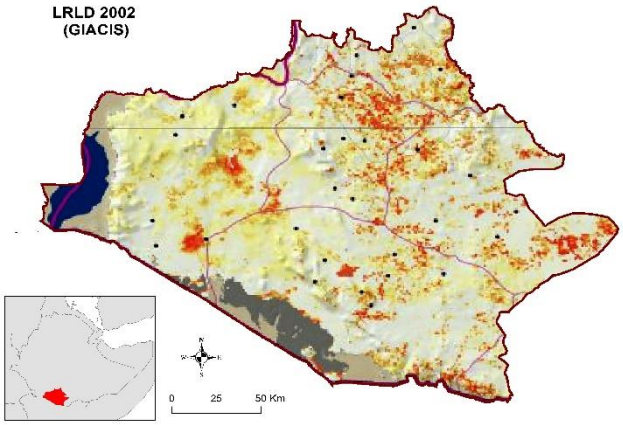

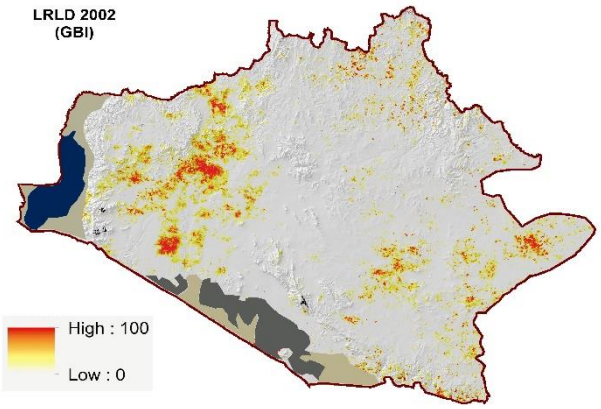

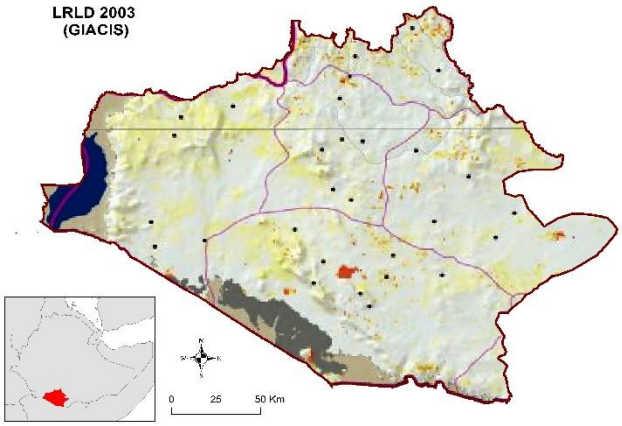

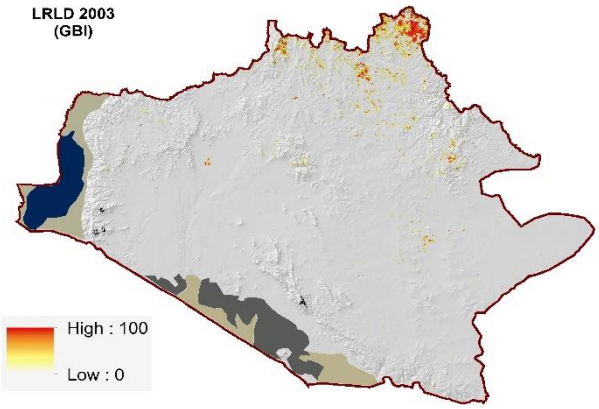

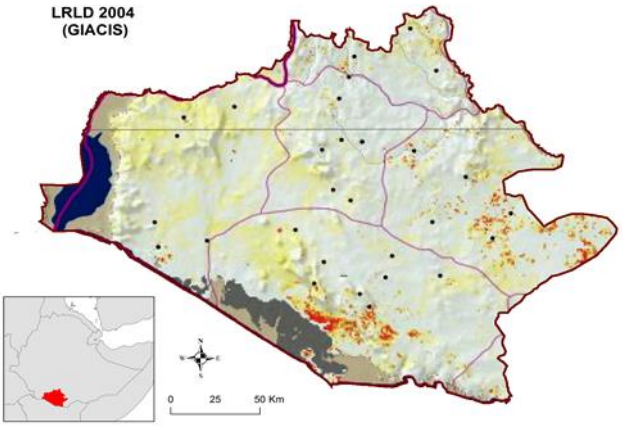

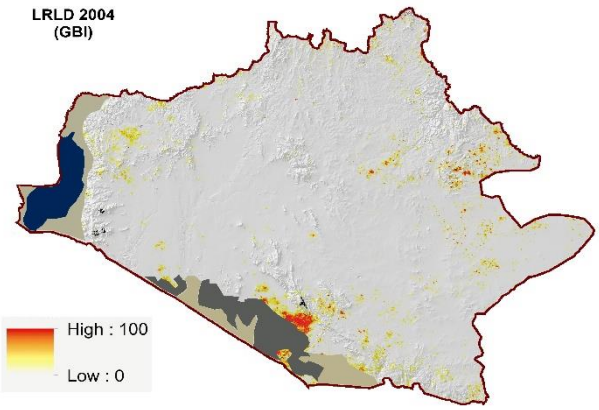

[13]GIACIS maps have been provided by Dr. Kees de Bie

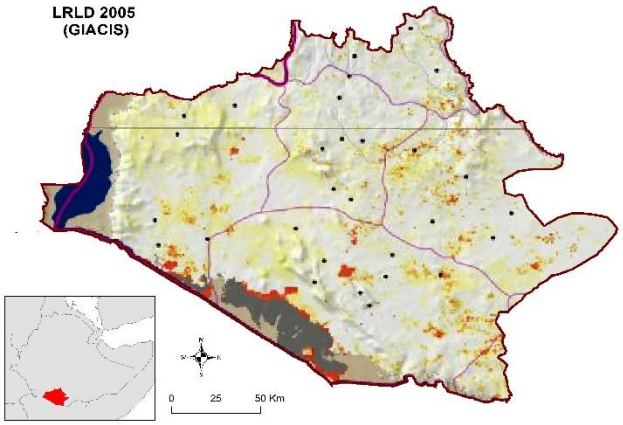
LRLD 2005
(GIACIS)
0 25 50 Km

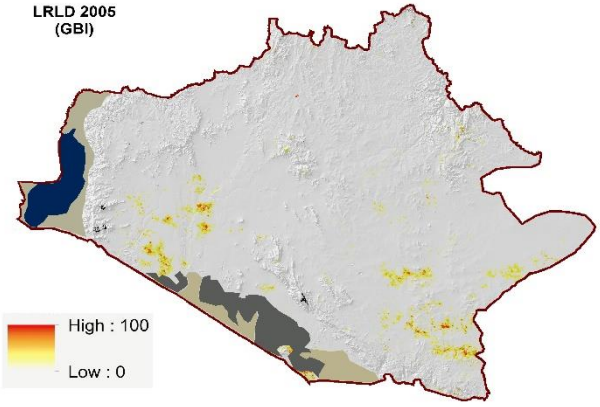
LRLD 2005
(GBI)
High : 100
Low : 0

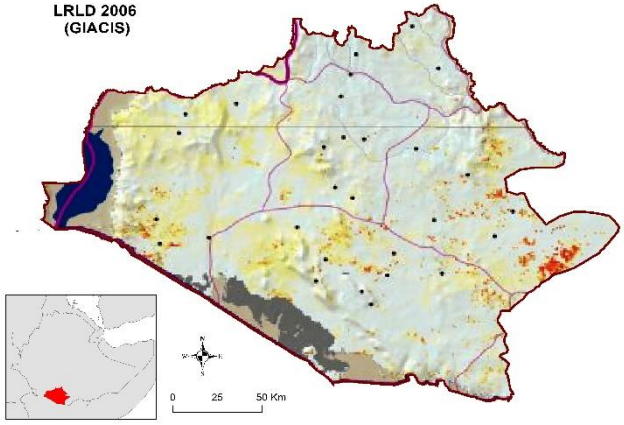
LRLD 2006
(GIACIS)
0 25 50 Km

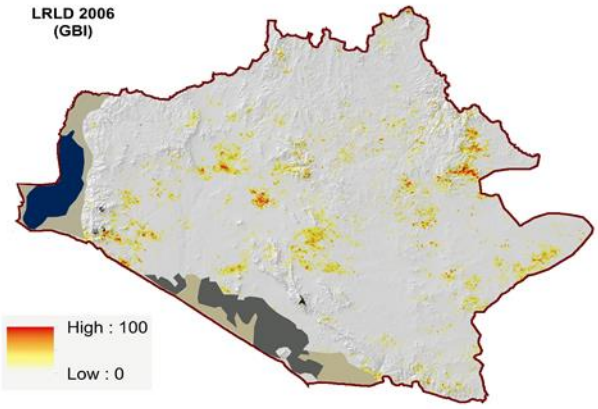
LRLD 2006
(GBI)
High : 100
Low : 0

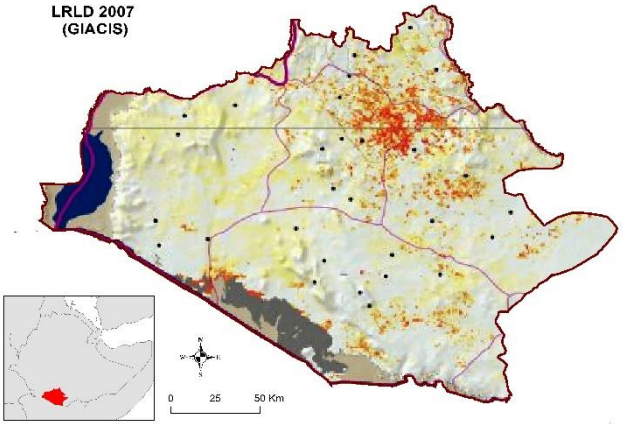
LRLD 2007
(GIACIS)
0 25 50 Km

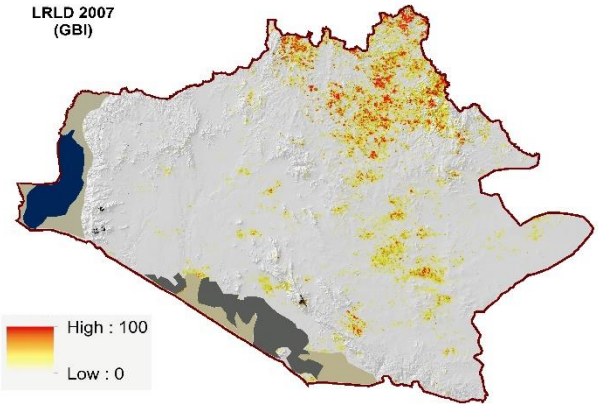
LRLD 2007
(GBI)
High : 100
Low : 0

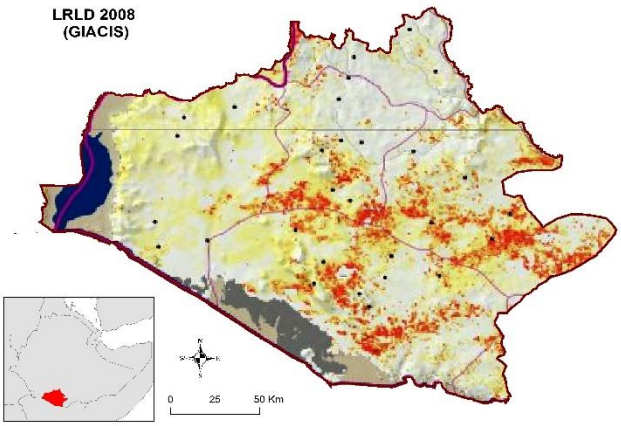
LRLD 2008
(GIACIS)
0 25 50 Km

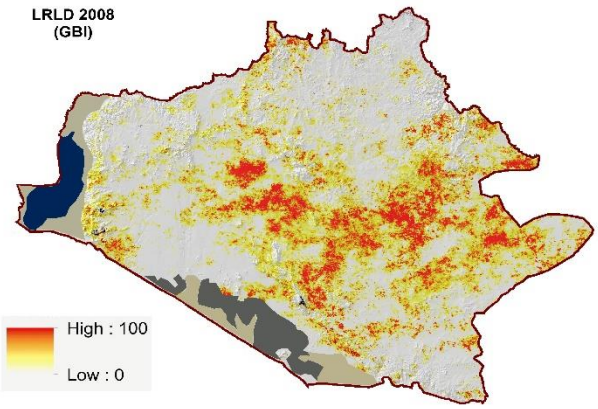
LRLD 2008
(GBI)
High : 100
Low : 0

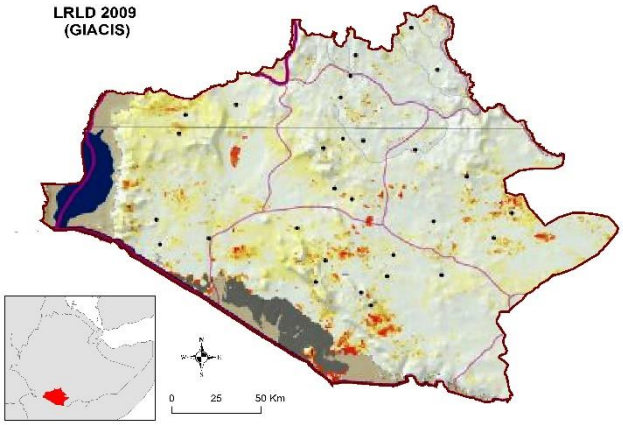
LRLD 2009
(GIACIS)
0 25 50 Km

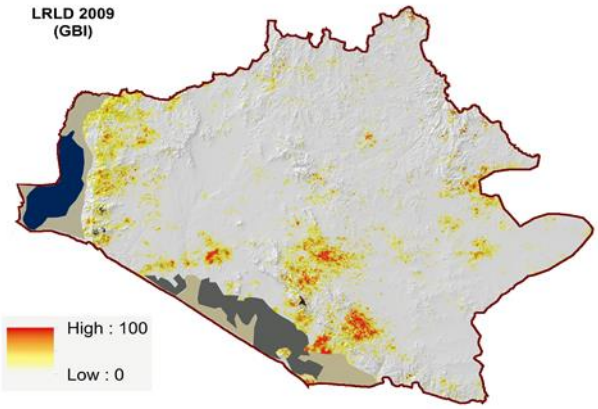
LRLD 2009
(GBI)
High : 100
Low : 0

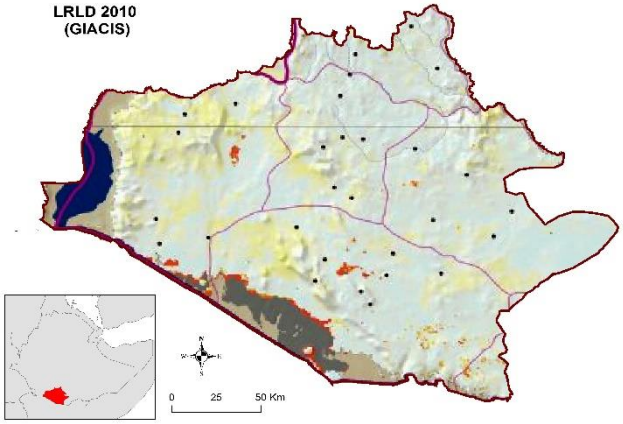
LRLD 2010
(GIACIS)
0 25 50 Km

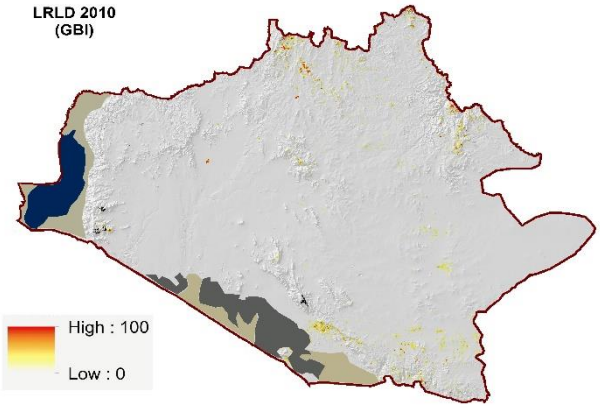
LRLD 2010
(GBI)
High : 100
Low : 0

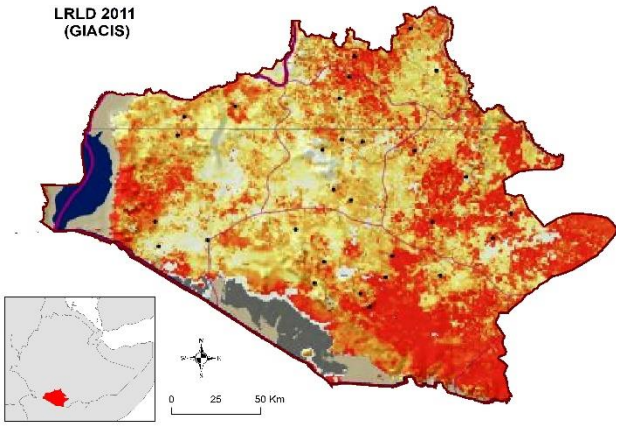
LRLD 2011
(GIACIS)
0 25 50 Km

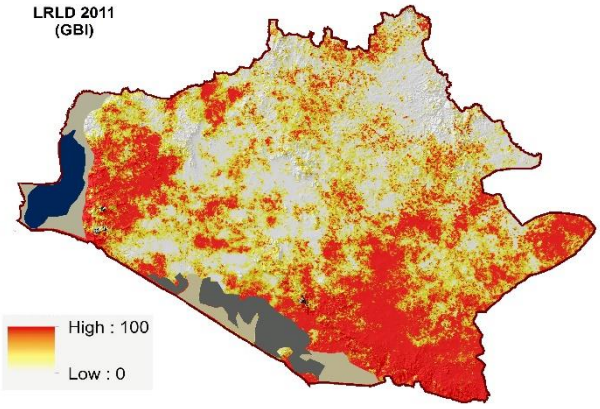
LRLD 2011
(GBI)
High : 100
Low : 0

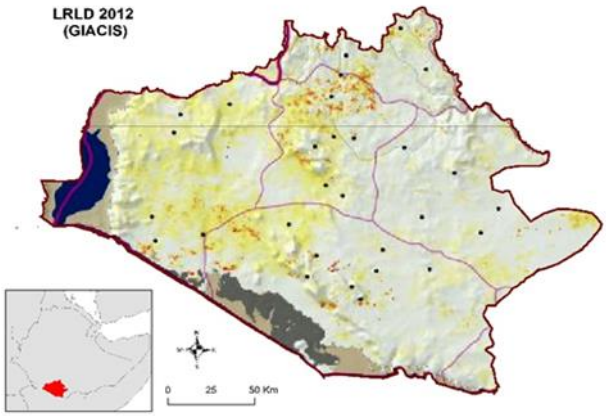
LRLD 2012
(GIACIS)
0 25 50 Km

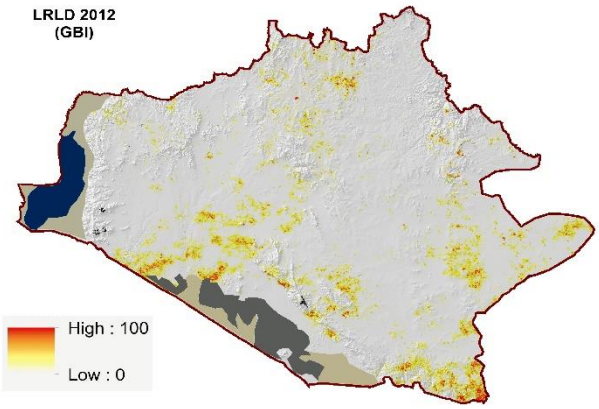
LRLD 2012
(GBI)
High : 100
Low : 0